Tailored SID and Profile Allocation for Amsterdam Airport Schiphol

A Study into Noise Abatement Departure Procedures

B. Ceulemans

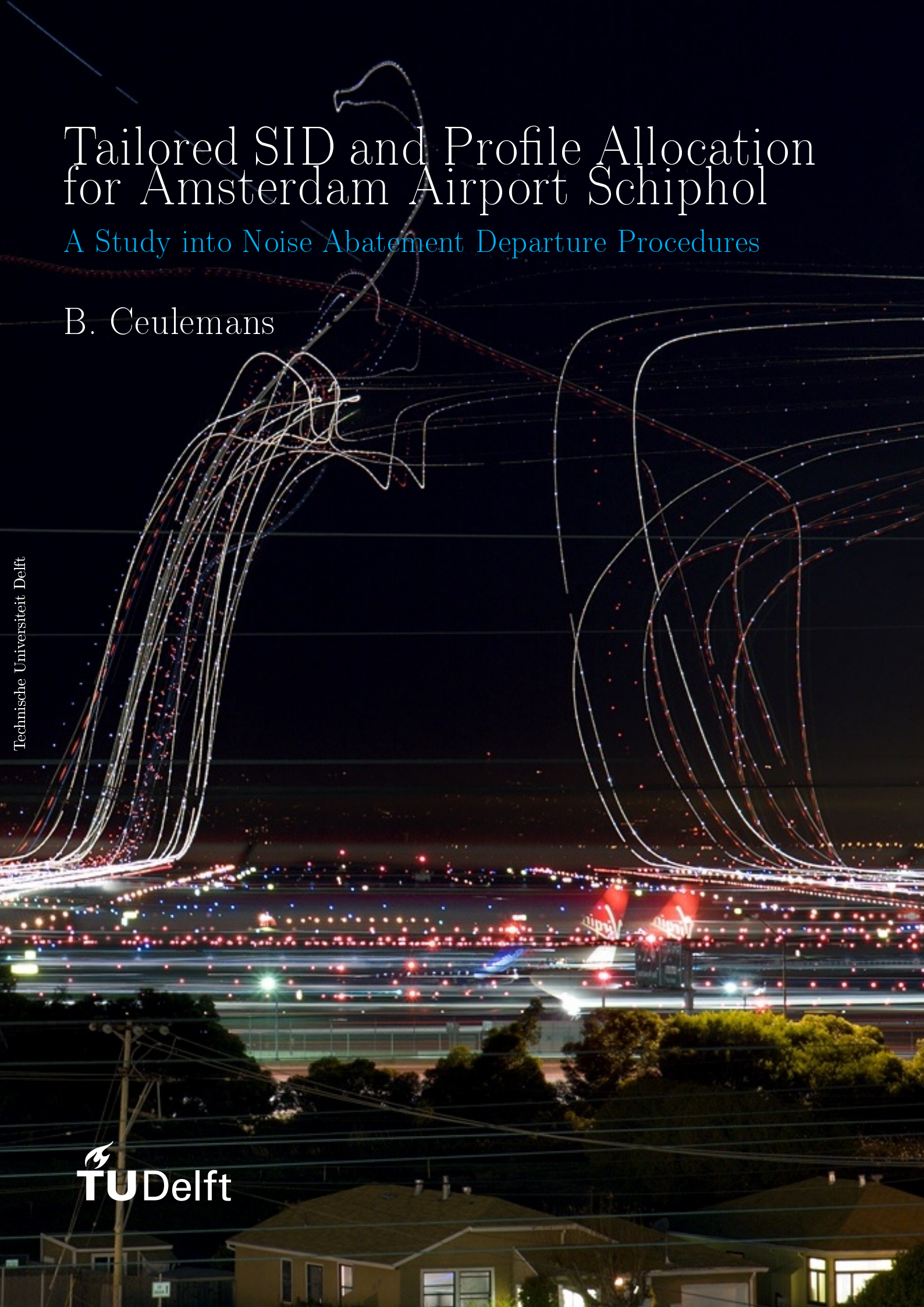

Technische Universiteit Delft

TU Delft

Tailored SID and Profile Allocation for Amsterdam Airport Schiphol

A Study into Noise Abatement Departure Procedures

by

B. Ceulemans

to obtain the degree of Master of Science
at the Delft University of Technology,
to be defended publicly on Tuesday July 5, 2016 at 10:00 AM.

Student number: 1384422

Thesis committee:

Prof. dr. ir. H.G. Visser,	TU Delft, chairman
Ir. P.C. Roling,	TU Delft, supervisor

An electronic version of this thesis is available at `http://repository.tudelft.nl/`.

TU Delft

Executive Summary

Amsterdam Airport Schiphol (AAS) is limited due to noise caused to the surrounding population. If the airport wants to retain its top five position of major European hubs, it will have to increase its capacity. In a crowded country like the Netherlands, this is challenging. In order to cope with future growth, research projects focus on more sustainable operations. Bringing down noise and fuel emissions leaves room for an increasing number of operations before the maximum capacity of AAS is reached. Currently, only one Standard Instrument Departure (SID) track and one flight procedure is used per runway departure fix combination. In contrast to tailored arrivals, the potential benefit of tailored departures has been left relatively undiscovered. This research focuses on the potential benefit of tailored SID and profile allocation as formulated by the following research objective:

Quantify the potential benefit of tailored SID and profile allocation for Amsterdam Airport Schiphol by developing a model that is capable of simulating departure trajectories per runway departure fix and optimize the overall allocation of departing aircraft for noise and fuel consumption.

The aim of this research is to achieve significant noise reduction and fuel savings for departures at AAS. In order to investigate the potential benefit of tailored SID and profile allocation, tailored trajectories need to be available first. For this research, trajectory optimization is used to define the tailored trajectories. Subsequently, these trajectories are used to study the allocation problem by means of mixed integer linear programming (MILP).

This research includes the development of two models. First, the trajectory optimization model is developed to compute a set of tailored trajectories dependent of aircraft type, take-off weight and flight procedure. The trajectory optimization model uses a parametrization technique to simulate departure trajectories. Subsequently, a multi-objective genetic algorithm is used in combination with an aircraft performance model and integrated noise model to perform a multi-objective trajectory optimization. The resulting set of tailored trajectories serves as input data for the second model. The second model is the allocation model. This model is developed to compute the optimal allocation of flights to one of the simulated trajectories in order to optimize for fuel, noise or a trade-off between these two objectives. By writing the problem down into a

linear format the allocation problem is solved. The final results consist of the total fuel burned and the number of people or houses within the noise contour. Additionally, the optimal allocation of flights and populated areas located within the noise contour are graphically represented to the user.

A case study is performed to demonstrate the workings of the model when applied to a real case scenario. The case scenario considered, is the 09 runway ARNEM departure fix combination. Two different aircraft types with three different take-off weights are taken into account, resulting in six different flight categories. For every flight category a set of tailored trajectories for both NADP-1 and NADP-2 flight procedures is simulated using the trajectory optimization model. Ground track parameters that define the actual ground track serve as input to the trajectory optimization model to simulate current trajectories. It is assumed that current departures make use of a NADP-1 flight procedure. Subsequently, the allocation model is used to calculate the impact of current operations with respect to fuel and noise.

Historical flight data is used as input for the case study. Every flight from the flight schedule is represented by one of the six flight categories. Subsequently, the allocation model is used to compute the optimal allocation of flights to one of the simulated tailored trajectories in order to optimize for fuel and noise. By adjusting weighting factor α ($0 \leq \alpha \leq 1$) different weightings are applied to the individual objectives. This allows for investigating different trade-off's. By comparing current departure procedures to results of the allocation model, the potential benefit of tailored SID and profile allocation is investigated. The results of the model are presented on a Pareto front, indicating the potential benefit with respect to the impact of current departure operations.

Four different noise criteria were evaluated. By comparing results of the four different noise criteria, the optimal range for weighting factor α was determined to be $0.14 \leq \alpha \leq 0.66$. Applying the novel approach for the optimal range of α results in solutions that show potential fuel savings and noise reduction for all four noise criteria. The first criteria considers the number of houses located within a noise contour of 58 dB L_{den} and shows potential fuel savings of 6.1% and of 44.2% noise savings. The second criteria considers the number of people located within a noise contour of 48 dB L_{den} and shows potential fuel savings of 7.1% and of 48.5% noise savings. The third criteria considers the number of houses located within a noise contour of 48 dB L_{night} and shows potential fuel savings of 3.6% and of 78.8% noise savings. The fourth criteria considers the number of people located within a noise contour of 40 dB L_{night} and sows potential fuel savings of 5% and of 64.2% noise savings.

Based on these results it is concluded that the potential benefit of tailored SID and profile allocation can be quantified by means of the proposed methodology. Optimizing the allocation for fuel results in assigning all departures to the most fuel efficient trajectories available. Optimizing the allocation for noise results in a distribution of flights over the different tailored trajectories

available. Furthermore, it is concluded that potential fuel savings are within a plausible range. On the other hand, results show extreme values for potential noise savings. It is assumed that these extreme values can be explained by the fact that an extreme scenario is considered for the case study. Not only the runway departure fix combination is sensitive in terms of noise, but the B744 aircraft model representing all wide body aircraft is dominant in terms of noise as well. The fact that an extreme scenario is being considered probably results in an extreme outcome for noise. Furthermore, it is likely that some of the grid points reach cumulative noise levels that are very close, but just below the opposed noise limits. This modelling behaviour is related to the optimization characteristics of MILP.

Preface

This thesis is the result of my research into the potential benefit of tailored departure tracks and profile allocation for Amsterdam Airport Schiphol. It has been an exciting and challenging period in my life, where I have learned a lot about myself and my individual qualities as an aerospace engineer. I am very glad with the topic of my research as it combined two fields of research: trajectory optimization and allocation problems. This allowed me to really dive into the scientific field of air transport and operations (ATO) which enlarged my interest for operational problems in the aviation industry.

This research could never have been conducted without the support of a number of people in my environment. Special thanks to Paul Roling, the principal supervisor of my project. Without the high level brainstorms and discussions we had during our two weekly progress meetings the project would never have been a success. Also thanks to Dries Visser, supervisor and chairman of my assessment committee. Fruitful discussions and the positive attitude of Dries always motivated me to bring the project to a higher level.

Special thanks to Sander Hartjes, who is also active at the ATO department and often shared his knowledge on trajectory optimization problems. Thanks to my good friends Huib Keemink and Jochem Delsen, who supported me in the technical challenges of my research project. I learned a lot from our discussions on programming and the complexity of algorithms. Your support allowed me to improve the quality of my models.

Many thanks to Tom Lemmens, Yannick Janssen, Tom Timmerman, Jochem Delsen, Jelle Reichert and Geert Mulder. Your support formed a huge contribution to the final result of my thesis by either reading my report, actively listening to my presentation or ask challenging questions about the project.

Last, but not least, I want to thank my family Harrie, Carla, Eefje and Ties Ceulemans and my girlfriend Nathalie Meuleman for their love and dedication. Always supporting me in everything I do and in what I am willing to achieve.

Bas Ceulemans

Delft, July 2016

Contents

List of Figures

List of Tables

List of Acronyms

AAS	Amsterdam Airport Schiphol
ACI	Airport Council International
AIP	Aeronautical Information Publication
ATC	Air Traffic Control
ATO	Air Transport and Operations
BB	Branch and Bound
BILP	Binary Integer Linear Programming
CBS	Centraal Bureau Statistiek
CDA	Continuous Descent Approach
DEN	Day Evening Night
FAA	Federal Aviation Administration
FCFS	First Come First Serve
FICAN	Federal Interagency Committee on Aviation Noise
GNSS	Global Navigation Satellite System
IAF	Initial Approach Fix
IATA	International Air Transportation Association
ICAO	International Civil Aviation Organization
ILP	Integer Linear Programming
INM	Integrated Noise Model
LvNL	Luchtverkeersleiding Nederland
LP	Linear Programming
MFW	Maximum Fuel Weight
MILP	Mixed Integer Linear Programming
MTOW	Maximum Take Off Weight
MZFW	Maximum Zero Fuel Weight
NADP	Noise Abatement Departure Procedure
NGO	Non Governmental Organizations
NP	Non-deterministic polynomial
NPD	Noise Power Distance
NSGA	Natural Sorting Genetic Algorithm
RF	Radius to a fix
RNAV	Area Navigation
RPK	Revenue Passenger Kilometer
SEL	Single Event Noise Level
SID	Standard Instrument Departure

TF	Track to a Fix
UDP	Uniforme Daglichtperiode

List of Symbols

Constant	Description	Value	Unit
g_0	standard acceleration of gravity	9.80665	m/s^2

Symbol	Description	Unit
α	weighting factor	-
β	weighting factor	-
γ	flight path angle	deg
γ_n	percentage of max allowable flight path angle	-
$\Delta\chi$	change in heading angle of ground track turn segment	dB(A)
η_n	percentage of max allowable thrust	-
μ	bank angle	deg
ρ	air density	kg/m^3
χ	heading angle	deg
a	acceleration	m/s^2
D	drag force	N
h	altitude	m
h_1	altitude at which acceleration segment is initiated	m
g_d	L_{den} noise penalties	-
L	length of a straight leg ground segment	m
L_{den}	day-evening-night sound level	dB(A)
L_{night}	8 hours night average sound level	dB(A)
M	penalty factor	-
m	number of turn segments in trajectory	-
N_{limit}	noise limit	dB(A)
n	number of straight legs in trajectory	-
n_f	normalization factor for fuel objective	-
n_n	normalization factor for noise objective	-
R	radius of a ground track turn segment	m
T	net thrust force	N

T_0	reference time period	s
t_0	weighted equivalent time index	s
V	true airspeed	m/s
V_2	take off speed	m/s
W	aircraft weight	N
x	x-coordinate	m
y	y-coordinate	m
z	z-coordinate	m
Z	objective function	-

Index	**Description**
a	aircraft type
d	period of the day
f	flight category
p	flight procedure
r	route
w	take-off weight
xy	coordinate

Set	**Description**
A	aircraft
D	periods during the day
F	flights
P	flight procedures
R	routes
W	take-off weights
G	grid coordinates

Decision Variable	**Description**
$x_{a,w,d,p,r}$	flight $f_{a,w,d}$ following route r with profile p
x_{xy}	grid point xy

Cost Function	**Description**
$C^F_{a,w,d,p,r}$	fuel cost of flight $f_{a,w,d}$ following route r with profile p
C^N_{xy}	population of grid coordinate xy
$C^N_{a,w,d,p,r}$	noise impact in dB(A) L_{den} of an occupied flight on grid point xy

1

Introduction

Statistics show it is likely that air travel demand is going to increase in the upcoming years. For instance, a publication of the Airport Council International (ACI) presented an annual growth of 5.7% in revenue passenger kilometer (RPK) [7]. Moreover, according to a forecasting report of the International Air Transportation Association (IATA) airlines expect to see a 31% increase in passenger numbers between 2012 and 2017 [8]. With almost 450,000 aircraft movements a year Amsterdam Airport Schiphol (AAS) is getting near its maximum capacity of 510,000 movements in 2020 [9]. Currently, the airport is one of the five major hubs in Europe. But if AAS wants to hold on to its top five position it will have to make sure that it can deal with a growing number of passengers in the near future. The airport will have to increase its capacity so that it can cope with the growth of its industry.

Improving the airport capacity is easier said than done. The Netherlands has a high population density and the area in the vicinity of AAS is getting more and more crowded, resulting in a growing number of noise complaints. Secondly, sustainable awareness is rising among people which makes aircraft emissions a critical point of discussion in politics. Strict regulations for aircraft noise and emissions have always been present, but a continuously growing pressure from political and social parties forces airports to bring down noise production and aircraft emissions even further. In addition, the airlines have their own interest by aiming for more sustainable operations to lower fuel costs as they struggle with tough competition. The many stakeholders involved have different and often conflicting interests which makes it challenging for AAS to increase its capacity.

In order to cope with future growth, a tremendous amount of research projects is initiated by AAS in cooperation with several research institutes all over the world [10]. One of these insti-

tutes is the Delft University of Technology, where this research is executed. The research projects involve a large variety of targets and goals, but have one thing in common: all research projects anticipate a growth in aviation and an increasing number of sustainable operations.

The aim of this research is to quantify the potential benefit of tailored departure tracks and profile allocation for AAS. By means of a trajectory optimization model a set of alternative, tailored trajectories are defined dependent on aircraft type and take off weight. Also the possibility of flying an alternative departure procedure is taken into account. Subsequently, the set of tailored departure trajectories serves as input for a second optimization model. An allocation model is developed and used to determine the optimal allocation of aircraft departures to the set of tailored departure trajectories. Positive results have lead to promising recommendations for future research on this topic.

A clear report structure is used to describe the full research project. The first two chapters are used to introduce the research objective and familiarize the reader with the research context. Therefore, the project plan is presented in chapter 2 of this report. This chapter starts with a clear problem description to clarify the motivation for this research. Subsequently, chapter 3 provides background information on AAS. After the research objective and its context are introduced, the main research of this project is discussed. In order to achieve the research goal two models are developed. The first model is a trajectory optimization model. The development and working principles of this model are discussed in chapter 4. The trajectory model computes a set of tailored trajectories which serves as input for the second model. The second model computes the optimal allocation of departing aircraft to the available trajectories as generated by the trajectory model. The development and working principles of the allocation model are explained in chapter 5. Subsequently, a case study is carried out to test the model. In chapter 6 several noise criteria are evaluated. Chapter 7 elaborates on the verification and validation of the model. Finally, the conclusions, recommendations and future research proposals are presented in chapter 8 of this report.

2

Project Plan

In order to gain better understanding of the research objective this chapter starts by giving a clear explanation of the motivation for this research in section 2.1. With the problem definition in mind the research objective is formulated and presented in section 2.2 of this chapter. Subsequently, section 2.3 will elaborate on the research methodology. In this section a project plan is presented that is used to structurally work towards the final goal of this research. Finally, this chapter will close with a short conclusion in section 2.4.

2.1 Problem Definition

2.1.1 Introduction to Aircraft Departures at AAS

AAS counts six different runways. Five of the six runways are available for commercial aviation. The sixth runway is located in the east of AAS (Oostbaan) and is mainly used for general aviation. For the year 2015 over 225.000 aircraft departed from AAS. What runway is used for aircraft departures depends on multiple factors, mostly related to weather conditions and noise. AAS uses a preference list that indicates which runway configuration is most preferable considering the situation at hand. After take off an aircraft is guided to one of the five departure sectors in Dutch airspace. The five exits are marked by so called departure fixes. From a departure fix the aircraft enters en route airspace and continues its flight in the desired direction towards its final destination.

A Standard Instrument Departure (SID) is a prescribed set of instructions that defines the ground track to be flown from take-off towards a certain departure fix. Meanwhile, the aircraft

gains height by flying a departure profile, therefore defining the vertical component of a departure trajectory. A departure procedure prescribes thrust versus altitude and speed settings in order to reach a certain altitude on time and specifies when to accelerate towards the desired climb or cruise speed. Although aircraft follow the same procedure, the vertical profile of their trajectories always differs due to differences in aircraft type, take-off weight and atmospheric circumstances. A Noise Abatement Departure Procedure (NADP) is a departure procedure that aims to minimize noise in the vicinity of the airport. Currently there are two different NADP's available. NADP-1 intends to alleviate the noise impact of departing aircraft on communities close to the airport by first climbing towards an altitude of 3000 ft. before it starts accelerating towards its en route climb speed. NADP-2 intends to alleviate the noise impact to communities located further away from the airport by giving priority to accelerating towards the en route climb speed before it climbs towards the desired departure fix altitude.

Looking at current departure operations at AAS, only one SID per runway and departure fix way point is used, as well as only one departure procedure. This means that, independent of aircraft type and weight, each departure flight follows the same ground track and climb procedures in order to leave Dutch air space. One of the reasons to prescribe the SID and departure procedure is because of safety regulations and regulating the complexity of the airspace for air traffic control (ATC). Looking at current arrival procedures research already lead to the application of tailored arrivals, especially in combination with continuous descent approaches (CDA). This means that, dependent of aircraft type and weight, aircraft approaches at AAS follow tailored arrival routes. In chapter 3 the airport operations of AAS will be discussed in more detail.

2.1.2 Noise: A Limiting Factor

AAS is limited in terms of noise caused to the surrounding population. In order to keep aircraft noise to a minimum, authorities have restricted the number of people and houses allowed to experience noise by 48 and 58 dB L_{den} respectively.[1] In the forecasting process, authorities distinguish between day-, evening- and night-time operations. The noise and emissions produced by the aircraft movements around AAS are monitored on a yearly basis. Every year a forecast for the expected amount of noise is done to manage expectations from people living in the vicinity of AAS.

The restrictions to noise and emissions affect the capacity of AAS. In order to comply with the regulations for noise, the number of aircraft movements is limited. It is not possible to increase the number of aircraft operations at AAS, and therefore increase its capacity, unless the current operations are able to be more sustainable and noise efficient. Air travel demand will grow but with a continuously growing pressure from political and social parties to bring down noise levels, it will be challenging to keep the capacity of AAS large enough to handle this growth. Therefore, AAS would benefit from measures that make airport operations more sustainable by improving

[1] L_{den} is a metric for noise that takes the impact of day, evening and night flights into account

the current noise impact and emissions in the vicinity of the airport.

2.1.3 Proposed Solutions

Reducing noise and emissions in the vicinity of the airport can be a way for AAS to comply with future regulations and leave room to increase its capacity. Several noise abatement measures are being researched in order to achieve this goal. One way is by approaching the source of the noise. Research and development teams of aircraft manufacturers work on new technologies to design more sustainable engines and improve the aerodynamics of aircraft. Another noise abatement measure is by protecting the receiver from noise. For aviation this is an infeasible way to reduce noise since one cannot expect people to wear earplugs 24/7 when living in the vicinity of the airport.

Lastly, optimization studies work on more sustainable trajectories and an improved allocation of flights to already existing routes. The Air Transport and Operations (ATO) department of the faculty of Aerospace Engineering at the Delft University of Technology specializes in understanding, modelling and improving the air transport performance in capacity, cost effectiveness, sustainability and safety. This research focusses on the final option to make current operations more sustainable and alleviate noise in the vicinity of the airport. Research on tailored arrivals has resulted in significant noise reduction and fuel savings during the final phase of flight. For departures, research has been done on trajectory optimization of single events or optimal allocation to already existing routes. This leaves room to investigate the potential benefit of allocating aircraft departures to a tailored SID and profile, depending on aircraft type, weight and time of the day.

2.2 Research Objective Statement

Based on an introduction of the topic and a clear description of the problem definition in the previous section, the research objective is formulated as follows:

Quantify the potential benefit of tailored SID and profile allocation for Amsterdam Airport Schiphol by developing a model that is capable of simulating departure trajectories per runway departure fix and optimize the overall allocation of departing aircraft for noise and fuel consumption.

The main reason to execute this research is to achieve significant noise reduction and fuel savings. These two elements are the main drivers for research on tailored arrivals as well, resulting in the CDA. An optimal allocation of aircraft departures might decrease the number of people annoyed due to aircraft noise while also resulting in fuel savings for the airlines. It should be noted that the term *'tailored'* is used to emphasize that the SID's are designed to be dependent of aircraft type and weight.

The use of more sustainable flight procedures reduces the yearly noise and emissions of aircraft movements at AAS. This could also be used for additional airport operations before the limitations on noise and emissions are reached. As a result the airport will be able to handle more passengers. Therefore, the results of this study can contribute in balancing noise, fuel consumptions and airport capacity of AAS in the near future. Overall the findings of this research aim to contribute to research on a more sustainable and environmental friendly way of performing air transport operations at AAS.

Regardless of best practices, the level of detail of the project will have to be limited in order to fit it in a fixed time span of 9 months. To limit the size of the project, the effects of wind are not included in the scope of this project. Capacity and delay dependant constraints are not taken into account. Departure flights for cargo traffic and general aviation are also left out of the project scope, because the number of movements is relatively small with respect to commercial traffic.

2.2.1 Sub-goals

This research investigates the potential benefit of tailored SID and profile allocation. In order to achieve the research objective four sub goals are defined. The sub-goals support in achieving the main research objective and are listed below.

- Define a limited number of departure trajectories dependent on aircraft type and take-off weight per runway and departure fix[2]
- Distinct a limited number of departure procedures
- Calculate the noise of each aircraft type, weight, SID and profile combination
- Optimize the overall allocation for the following objectives:
  - Minimize overall noise
  - Minimize fuel consumption
  - Minimum noise vs. fuel

2.2.2 Hypothesis

The main objective of this research is to quantify the potential benefit of tailored SID and profile allocation for AAS. Before it is possible to investigate the potential benefit of the allocation problem, the tailored trajectories need to be available first. Unless the trajectories can be defined by doing reasonable assumptions or gathered from existing data, trajectory optimization will be required to define the tailored trajectories for this research. These trajectories can then be used for the allocation problem. Therefore, it is expected that two research topics need to be combined in order to achieve the main objective of this research, namely trajectory optimization and trajectory allocation.

[2] tailored SID

Looking at the basic concept of tailored SID and profile allocation it is expected that positive results will be achieved on fuel savings. Although the results are expected to be positive, the outcome of the model will probably show limited fuel savings of around 5% compared to current departure operations at AAS. The model is expected to provide an optimal solution for fuel savings, but this solution is expected not to be compatible with noise restrictions. Chapter 3 provides more information on legal obligation and restrictions that limit the operations of AAS.

Also for noise it is expected that the basic concept of tailored SID and profile allocation will lead to positive results in terms of noise savings. The potential benefit for noise is expected to be a lot higher with respect to fuel savings, probably around 10% compared to current departure operations at AAS. Maximum savings for noise are achieved at the cost of fuel and vice versa. The use of a trajectory optimization model creates the opportunity to design alternative routes that avoid populated areas in the vicinity of the airport. Taking into account that time dependencies, like capacity and delay constraints, are being left out of the scope leaves a lot of potential to improve the noise impact of aircraft departures.

2.3 Research Methodology

The project is carried out at the faculty of Aerospace Engineering of the Delft University of Technology. The research is carried out independently of stakeholders like AAS, Luchtverkeersleiding Nederland (LvNL) or any airline operating at AAS. Nevertheless, information about the airport operations at AAS are conducted by means of interviews with employees of Schiphol Group. In addition, a literature study is conducted to get familiar with relevant topics of the research context. All the information about the research context forms a solid basis to develop a model that is capable of defining a set of tailored SID per runway departure fix and optimize the overall allocation of departing aircraft for noise and fuel consumption. A complete overview of the research methodology can be found in appendix A of this report.

2.3.1 Modelling Framework

A schematic representation of the proposed method in the form of a modelling framework is given by figure 2.1. It shows that the model consists of two sub-models. The first sub-model generates input data for the second sub-model. Since usually research focus either on trajectory optimization or allocation problems, combining these two techniques in one research project is rather unique and an addition to the body of knowledge, especially for the topic on noise abatement departure trajectories. Both sub-models are discussed below.

The first model is the trajectory optimization model. This model is used to compute tailored SID and profiles depending on a specific flight category. A flight category is defined by the aircraft type and take-off weight of a specific flight. The flight trajectory is simulated by a combination of ground track and profile segments. The segments are defined by parameters that form the

decision variables of the optimization model. By means of a multi objective genetic algorithm multiple solutions are computed and presented by a so-called Pareto optimal front. From the Pareto optimal front several solutions for a specific flight category are chosen. In this way the tailored trajectories are computed and used as input for the second sub model. The first sub model is developed using Matlab version 15b in order to achieve the first three sub goals of the main research objective.

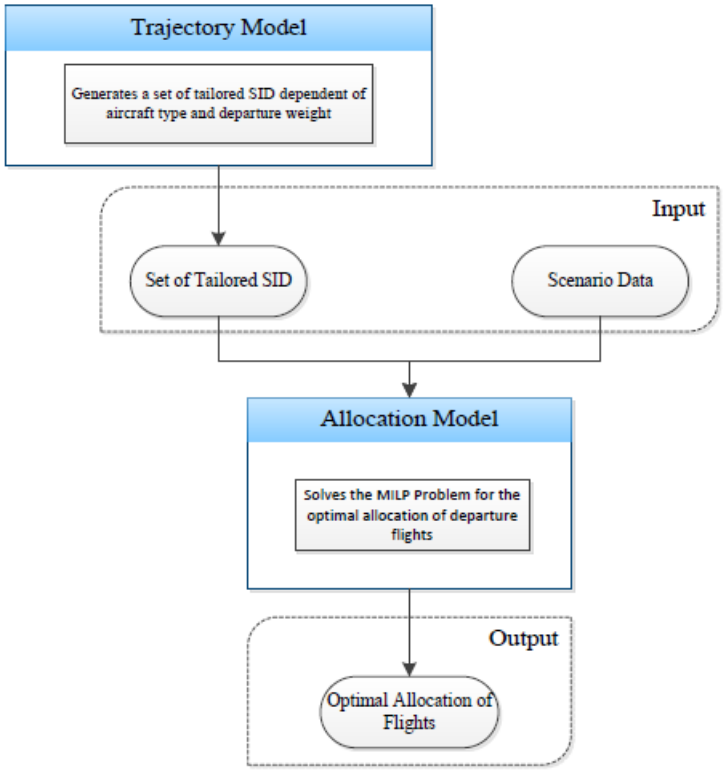

Figure 2.1: Block diagram of the modelling framework, giving a general overview of the model

The second sub-model is the allocation model, which is used to optimally allocate the aircraft to one of the simulated tailored departure tracks. The allocation model aims to optimize the overall allocation with respect to noise and fuel, as indicated in section 2.2.1. The model makes use of a data set generated by the trajectory optimization model to allocate the specific aircraft categories to the most suitable tailored departure trajectories available. This means that the outcome of the allocation model depends on the performance of the trajectory optimization model as well. Again, Matlab will be used to develop the model in order to achieve the final sub goal of the main research objective statement.

It should be noted that figure 2.1 only gives a general overview of the overall model. Both the trajectory optimization model and the allocation model are explained in more detail in chapter

4 and chapter 5 respectively. These chapters will elaborate on the modelling frameworks of each sub-models individually.

2.3.2 Methodologies

The overview of the modelling framework showed that the overall model consists of two sub-models. These models use different methodologies in order to achieve their individual goals. The goal of the first model is to generate a set of tailored trajectories dependent on aircraft type and take-off weight. Therefore, its main task is to perform a trajectory optimization for the different flight categories involved. Several trajectory optimization studies have been done. Chircop et al. used a generic framework for multi-parameter optimization of flight trajectories and Hebly and Visser developed a departure profile optimization model based on a previous tool called NOISHHH [11] [12].

For this study a multi objective genetic algorithm in the Matlab optimization toolbox is used to compute the tailored departure trajectories. The tailored trajectories are optimized for fuel and noise. Fuel flow models and an application of the Integrated Noise Model (INM) are used to calculate the two objectives [13]. The computation methods for noise, fuel and trajectory optimization are brought together in the first model to realize the required set of tailored departure trajectories. The methodologies used by the first model are discussed in more detail in chapter 4.

The goal of the second model is to optimally allocate departure flights to one of the tailored departure tracks. The allocation problem can be translated into a mathematical approximation that aims to minimize an objective function while it is subject to several constraints. For these kind of optimization problems the concept of Mixed Integer Linear Programming (MILP) is frequently used. This method makes use of integer and binary states to identify allocation possibilities. MILP has several methods available to determine an optimal solution. For example, the combination of First Come First Serve (FCFS) with a local Branch and Bound (BB) has proven to be a promising method to determine the optimal solution within reasonable computation times [14]. The concept of MILP is also used by the second model and discussed in more detail in chapter 5.

2.4 Conclusion

In this chapter the main research objected was presented to be:

Quantify the potential benefit of tailored SID and profile allocation for Amsterdam Airport Schiphol by developing a model that is capable of simulating departure trajectories per runway departure fix and optimize the overall allocation of departing aircraft for noise and fuel consumption.

The main reason to execute this research is to achieve significant noise reduction and fuel savings.

These two elements are the main drivers to investigate the potential benefit of tailored departures. Where research on tailored arrivals already lead to the practical implementation of CDA-s, the potential benefit of tailored departures has been left relatively undiscovered yet. The proposed method includes the development of two models. The first model is used to compute tailored SID and profiles depending of aircraft type and take-off weight. This model is used to generate input data for the second model. The second sub-model is the allocation model and used to allocate aircraft departures to one of the simulated tailored departure tracks with the goal to optimize for fuel, noise or a trade-off between these two objectives. The research methodologies give a general overview of the different techniques used to develop the models. Before entering the main research some background information on the airport operations of AAS is provided in the next chapter.

3

Amsterdam Airport Schiphol

Since this study is applied to AAS it is important to be more familiar with the airport and some of its departure operation procedures. This chapter provides the required background knowledge on the airport and its day-to-day operations. The chapter will start with section 3.1. This section gives a description of the AAS runway lay out and a brief explanation of how the different runways are used. In section 3.2 the current departure routes at AAS are discussed. Subsequently, section 3.3 elaborates on different departure procedures. Finally, in section 3.4 the legal obligations that are imposed on AAS are discussed.

3.1 Airport Lay Out and Runway Usage

AAS makes use of six different runways. Five of these runways are used for commercial aviation. These are the 'Polderbaan', the 'Zwanenburgbaan', the 'Kaagbaan', the 'Aalsmeerbaan'and the 'Buitenveldertbaan'. The sixth runway is the 'Oostbaan' which is mainly used for general aviation and sometimes for small commercial aircraft due to the limited length of the runway. Since most research focus on commercial aviation this runway is usually left out of the scope. The reason for this is because the noise impact caused by the general aviation operation can be neglected compared to that of commercial aviation operations.

Figure 3.1 shows the runway configuration of AAS for landing and take-off operations. Every combination of runway and direction has been given a code, as can be seen in the figure as well. The numbers in the code represent the runway direction with respect to the magnetic north. Since three of the five runway are perfectly aligned ('Polderbaan', 'Zwanenburgbaan' and 'Aalsmeerbaan') an extra letter is added to the code to indicate the most left, the most right and the center runway from the pilot's point of view. Finally, it should be noticed that two of

the six runways can only be used in one direction due to populated areas in the vicinity of the airport. The noise sensitive areas are indicated in figure 3.1 by means of a red cross.

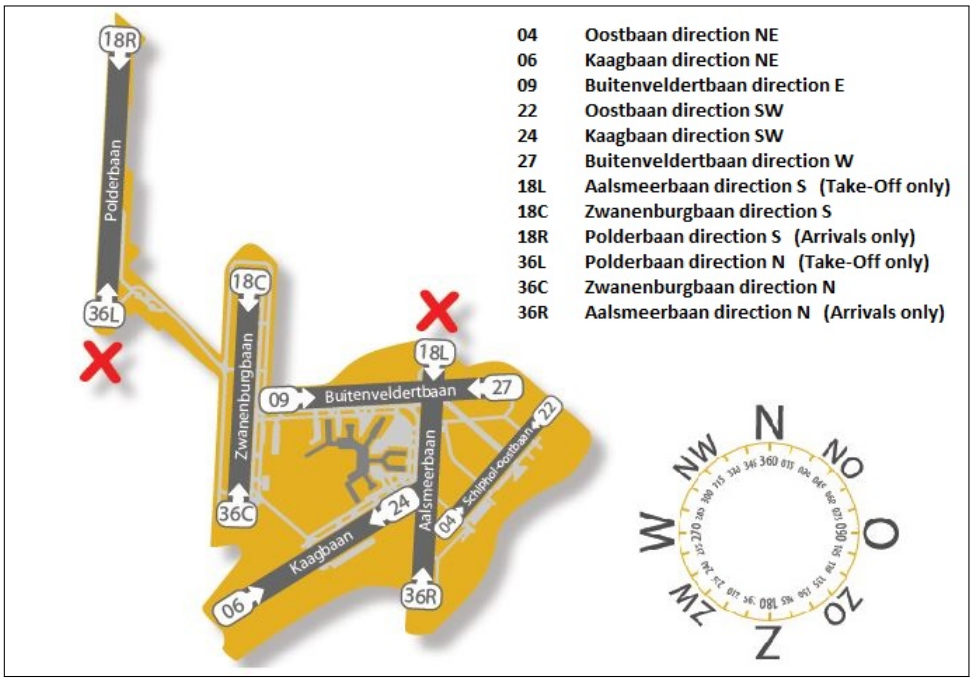

Figure 3.1: Runway lay out of Amsterdam Schiphol airport [1]

Although there are five runways available for commercial aviation, they are never operational at the same time. The main reason for this is because air traffic control always prefers to use the runway combination that imposes the least amount of noise impact on local communities. Secondly, the weather is a dominant factor in determining what runway combination is suitable for use. This has to do with the fact that there should be a minimum amount of cross and tail wind present in order for aircraft to take off and land safely. Another reason is that simultaneous operations may result in crossing flight paths. These runway combinations are not allowed because of safety reasons. Finally, once in a while the runways require maintenance. In that case the runway is closed and not available for use.

It is already mentioned that AAS is an important hub in Europe. Most of the passengers are transfer passengers. In order to make travelling via AAS as comfortable as possible the airport tries to bring down the transfer times to a minimum. This results in peak hours for in- and outbound traffic during the day. Therefore, plenty of aircraft arrive within a small time slot, subsequently all passengers transfer to their connecting flights and all aircraft take-off within a relatively short amount of time again. During these peak hours the capacity needs to be high enough to handle all air traffic. The maximum airport capacity depends on the number and combination of runways available which, in turn, depends on the limiting factors as discussed

before. In between the peak hours it is relatively quiet at the airport and more easy to realize the required capacity. Figure 3.2 shows an example of runway usage during peak and off hours at AAS.

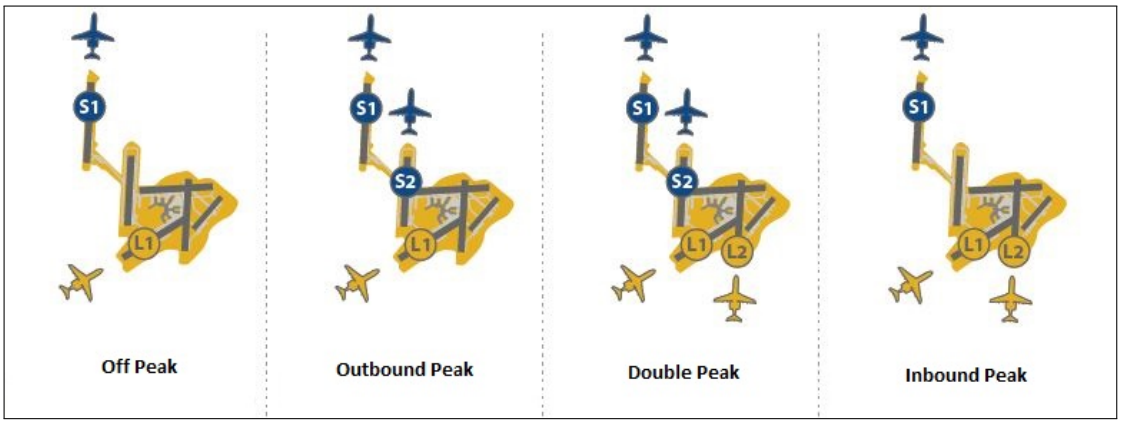

Figure 3.2: Runway usage for different scenario's at Schiphol airport [2]

Concluding, the available airport capacity is mainly determined by weather conditions and safety regulations that avoid interference between simultaneous operations. These factors exclude the use of certain combinations of runways. The runway usage is determined by the required airport capacity at a certain time during the day. High priority goes to runway combinations that avoid noise sensitive areas in the vicinity of the airport. In order to cope with these constraints AAS makes use of a preference list. The preference list ranks combinations of runways that are most preferred by air traffic control. The list is composed with the aim to avoid noise sensitive areas in the first place. Depending on the weather conditions one goes further down the list [15]. Table 3.1 shows the preference list used by AAS for start (S) and landing (L) procedures during day-time operations.

Because AAS distinguishes different periods during the day, a different preference list is used for operations during the night. Due to noise restrictions large penalties are imposed on night time operations. Only a few fixed arrival and departure routes are allowed during the night. The preference list for operations at night time is shown in table 3.2.

3.2 Departure Routes

The previous section explained that only a few combinations of runway directions can be operational at the same time. Still aircraft arrive from and leave in all directions. The different origins and destinations of flights result in a lot of arrival and departure routes through Dutch air space. In order to realize smooth and safe operations all aircraft are directed towards and from the airport in an organized way. Inbound flights arrive via one of the three Initial Approach Fixes (IAF) and outbound flights depart via one of the five outbound sectors. All outbound flights

Table 3.1: Preference list for start (S) and landing (L) between 6:00 - 23:00 in 2015 [1]

Preference	**L1**	**L2**	**S1**	**S2**	**Visibility**
1	06	(36R)	36L	(36C)	**Good:**
2	18R	(18C)	24	(18L)	visibility > 5000 m
3	06	(36R)	09	(36L)	cloud base > 1000 ft
4	27	(18R)	24	(18L)	within UDP
5a	36R	(36C)	36L	(36C)	**Good:**
5b	18R	(18C)	18L	(18C)	visibility > 5000 m
					cloud base > 1000 ft
6a	36R	(36C)	36L	(18C)	**Good or marginal:**
6b	18R	(18C)	18L	(18C)	visibility > 1500 m
					cloud base > 300 ft

Table 3.2: Preference list for start (S) and landing (L) between 23:00 - 6:00 in 2015 [1]

Preference	**L1**	**S1**
1	06	36L
2	18R	24
3	36C	36L
4	18R	18C

are guided to one of these sectors. Each outbound sector is marked by so called departure fixes. From a departure fix the aircraft leaves the controlled Dutch air space and continues its flight in the desired direction towards its final destination. A departure or arrival route define the ground track of a trajectories on the horizontal plane. Figure 3.3 shows the traffic distribution for AAS based on the origin and destination of flights. Since aircraft arrivals are out of scope this section only deals with current departure operations at AAS.

A SID is a fixed routes that guides aircraft from take off at AAS towards a departure fix. Appendix D shows an example of the SID that originate from runway 09. What SID is used depends on the runway configuration and the aircraft's destination. Logically, each runway should have five SID's: one for each exit sector in Dutch air space. However, a SID might not always be available due to the risk of interfering with other flights that operate at the same time. Based on the runway configuration another, more appropriate SID is chosen to direct the outbound flights to their exit sector. Furthermore, it might happen that the amount of departure flights exceeds the capacity of a SID. In that case a second SID is required. All SID are published by the Aeronautical Information Publication (AIP) [6].

Aircraft that follow a SID can make use of Area Navigation (RNAV). This allows aircraft to follow a predefined route very precisely by using ground based beacons and Global Navigation

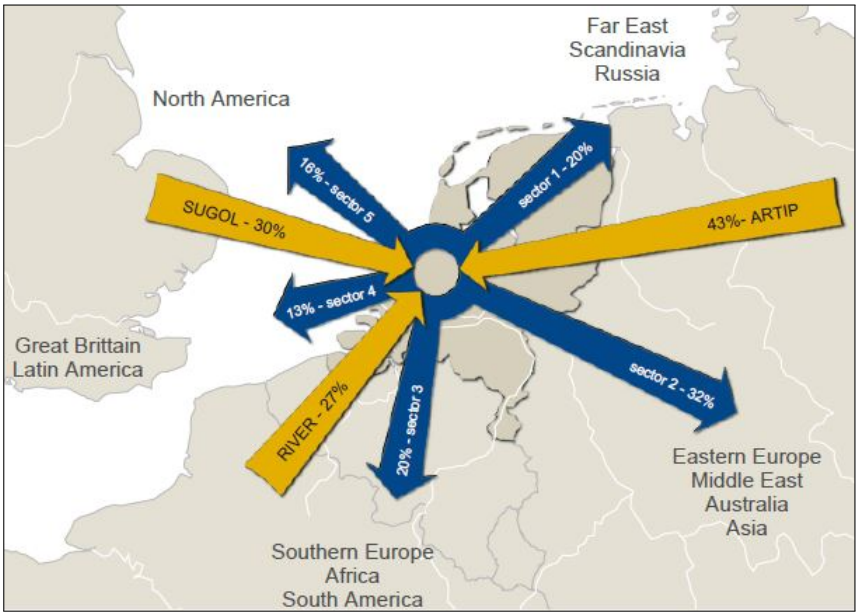

Figure 3.3: Traffic distribution for in- and outbound flights [1]

Satellite Systems (GNSS). RNAV routes consist of fly-by way points that are connected by Track to a Fix (TF) legs and make use of Radius to a Fix (RF) legs in turns. A schematic representation of TF and RF legs is given by figure 3.4.

3.3 Departure Procedures

The departure routes discussed in the previous section define the aircraft's flight path in the horizontal plane. The flight profile defines the flight path of a trajectory in the vertical plane. A departure procedure prescribes thrust versus altitude and speed settings in order to reach a certain altitude on time and specifies when to accelerate towards a desired climb or cruise speed. Although aircraft can follow the same procedure, the vertical profile of their trajectories always differs due to differences in aircraft type, take-off weight and atmospheric circumstances. The Federal Aviation Administration (FAA) and the International Civil Aviation Organization (ICAO) defined noise abatement flight procedures for airports, operators and ATC to manage the air traffic of arrival and departure flights in the US and Europe respectively. Nowadays, these procedures are applied all over the world. In general, there are four noise abatement departure procedures. In 1993, the FAA defined the noise abatement departure procedures 1 and 2, which are denoted as NADP-1 and NADP-2 respectively [16]. In the same year, ICAO promulgated the procedures in its reports, but referred to it as ICAO-A and ICAO-B procedures. For consistency reasons one refers to the departure procedures as NADP-1 and NADP-2 from now on. Both procedures are discussed below.

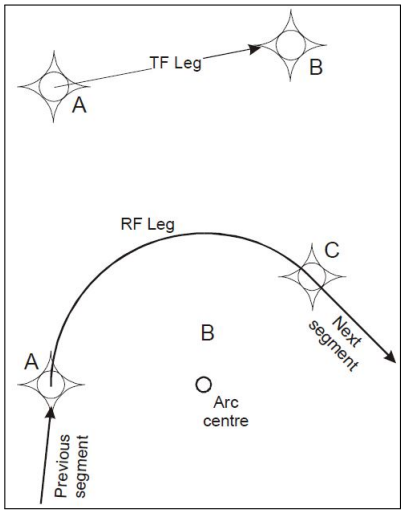

Figure 3.4: Schemetic representation of Track to a Fix (TF) and Radius to a Fix (RF) legs [3]

3.3.1 NADP-1 Procedures

NADP-1 is defined as a close-in procedure because it intends to alleviate the noise impact of departing aircraft on communities close to the airport [17]. Therefore, the procedure involves a thrust reduction at or above an altitude of 3000 ft. The take-off configuration for flaps and slats is maintained until this altitude is reached. Once the prescribed altitude is reached, flaps/slats are retracted on schedule and the aircraft is accelerated while maintaining a positive rate of climb to reach en-route climbing speed. Figure 3.5 shows a schematic representation of the NADP-1 procedure.

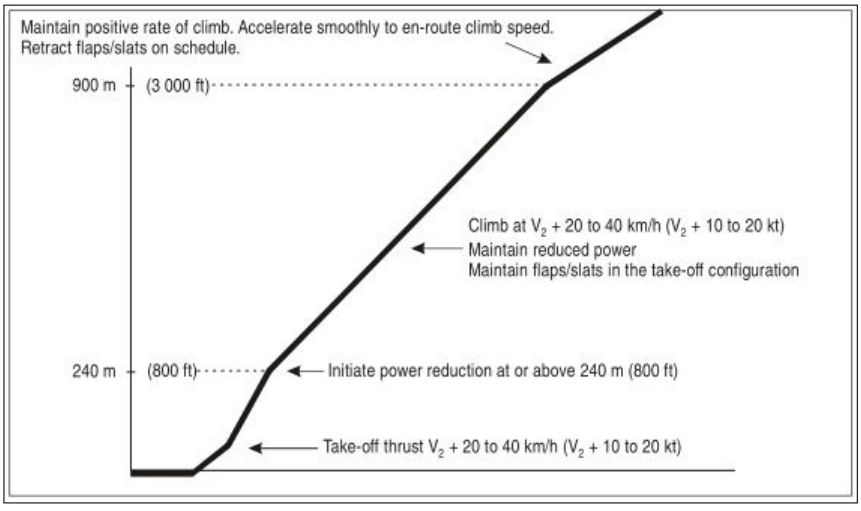

Figure 3.5: NADP-1 procedure [3]

3.3.2 NADP-2 Procedures

NADP-2 is defined as a distant procedure because it intends to alleviate the noise impact to communities located further away from the airport. Therefore, the procedure involves flap and slat retraction at 800 ft. The flaps and slats are retracted according to schedule. As the flaps/slats are retracted, the aircraft reduces thrust at a point along the path that ensures satisfactory acceleration performance. Subsequently, the aircraft starts accelerating while maintaining a positive rate of climb to reach the desired climb speed at an altitude of 3000 ft. Once this altitude is reached the aircraft transmits to en-route climb speed. Figure 3.6 shows a schematic representation of the NADP-2 procedure. The close-in and distant procedures are described in more detail by ICAO [3].

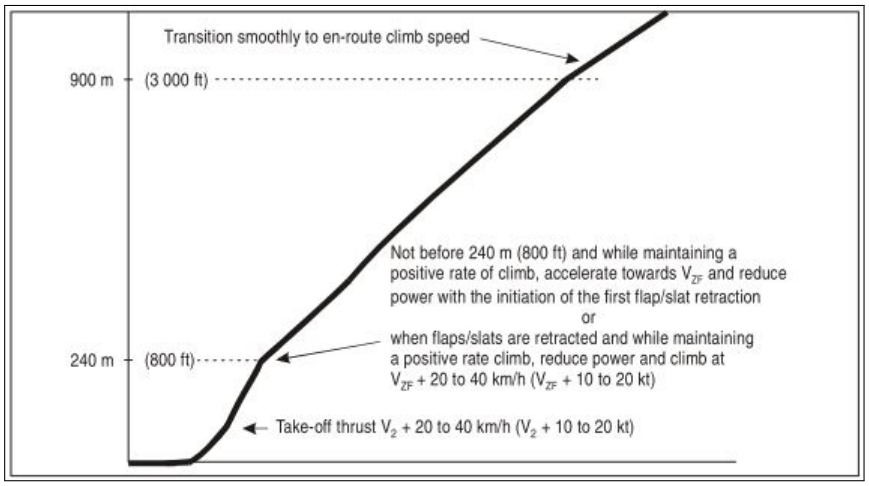

Figure 3.6: NADP-2 procedure [3]

3.4 Restrictions and Obligations

The previous sections explained how AAS is organized and how the air space around it is filled with multiple arrival and departure routes. Naturally, all these trajectories increase the complexity of Dutch air space and simultaneous operations make it challenging for ATC to guarantee safe operations. Therefore, the design of new SID is limited to several constraints. Secondly, AAS is limited to noise. In order to sustain liveability in the vicinity of the airport AAS needs to comply with a number of obligations for noise. Both the operational constraints and legal obligations for noise are discussed in this section.

3.4.1 Operational Constraints

Due to safety reasons all trajectories are subjected to operational constraints. In case of designing a new SID it is necessary to take these constraints into account. First of all, it is important

that aircraft keep sufficient distance to nearby obstacles when taking off. This is why obstacle clearance is a primary safety constraint for departure trajectories. In case of AAS, it is not necessary to account for particular obstacles that might form a risk for aircraft departure. ICAO Doc 8168 provides guidelines to ensure that obstacle clearance is sufficient for every flight from a given runway [3]. This comes down to the fact that aircraft should maintain runway direction until a minimum turn height is reached. It follows that aircraft are not allowed to turn before an altitude of 120 m. is reached [3].

Secondly, assuming that commercial aviation aims for comfortable flights aircraft trajectories are subject to a maximum bank angle in turn phase. Given a certain air speed and turn radius the aircraft will need a specific bank angle to stay on track. Aircraft that follow a turn with a small turn radius in combination with high air speeds will require a large bank angle. This might result in a very steep turn with potential g-forces applied on passengers and crew. Obviously, this is not desirable in commercial aviation. Therefore, a maximum bank angle is applied on current departure operations. The maximum bank angle increases stepwise from 15° to 25° between 125 m. and 915 m. [18].

A third operational constraint is imposed to avoid aircraft collisions between in- and outbound flights in the terminal control area of AAS. Aircraft departures are subject to altitude restrictions in order to keep in- and outbound flights on separate flight altitudes. The current procedure for outbound flights includes a climb until an altitude of 6000 ft. is reached [6]. This altitude is maintained until the outbound flight encounters the borders of Dutch airspace. From there it is allowed to continue climb phase towards cruise altitudes. The altitude restrictions are primarily imposed because of safety reasons. Secondly, it results in a more structured division of in- and outbound flights which makes it easier for ATC to maintain control over Dutch air space.

3.4.2 Legal Obligations

The problem of noise involves many stakeholders like the government, airlines, municipalities and other non-governmental organizations (NGO-s). Since Januari 2015 the 'Omgevingsraad Schiphol' is responsible for advising the government on noise related issues at AAS [19]. Every year the noise restrictions are evaluated and redetermined. Negotiations between all stakeholders result in a set of legal obligations for noise that AAS needs to comply with on a yearly basis. AAS receives a penalty in the from of a fee or a restriction on the number of slots in case it is not able to comply with the legal obligations. A slot contains the right for an airline to make use of the airport once, that is one landing and one departure from AAS.

To guarantee that AAS is able to comply with the obligations Schiphol Group performs a forecast on the number of operations for the upcoming year [1]. The forecast is based on statistical data and probability analysis. Based on historical flight data and statistics on weather conditions a model computes the probability of several air traffic scenario's in combination with certain run-

way configurations. Table 3.3 shows the noise criteria and prospects for the year 2015. As can be seen from the table noise levels are expressed in dB L_{den} and dB L_{night}. These metrics present the average noise load for a 24 hours period or an 8 hours period during night respectively. *den* stands for Day, Evening, Night. For the L_{den} calculation, the noise impact is multiplied by a penalty factor of $\sqrt{10}$ and 10 for aircraft movements during the evening (19:00 - 23:00) and during the night (23:00 - 07:00) respectively [20].

Table 3.3: AAS noise criteria for 2015 [1]

Aspect	**Noise Criteria**	**Prospect for 2015**
Number of aircraft movements	Max. of 510.000 aircraft movements on a yearly basis of which only 32.000 aircraft movements take place between 23:00 and 6:00	450.178 aircraft movements, of which 29.619 operations between 23:00 - 6:00
Noise	- Max. 11.900 homes experience noise of 58 dB(A) L_{den} or more	- 8.600 homes are expected to experience noise of 58 dB(A) L_{den} or more
	- Max. 180.500 inhabitants seriously affect by noise of 48 dB(A) L_{den} or more	- 139.500 inhabitants are expected to experience serious noise impact of 48 dB(A) L_{den} or more
	- Max. 11.000 homes experience noise of 48 dB(A) L_{night} or more	- 6.200 homes are expected to experience noise of 48 dB(A) L_{night} or more
	- Max. 49.000 awakenings because of noise of 40 dB(A) L_{night} or more	- 17.000 expected awakenings because of noise of dB(A) L_{night} or more

The first and third noise criteria are self explaining and can be calculated by counting the number of houses within the noise contour. The second and fourth noise criteria are less straight forward since these criteria require a standard that indicates when people are seriously affected or awakened by aircraft noise. Research is done on people experiencing aircraft noise. Based on statistical analyses so called dose-response relations are formulated. By means of these relations the response is calculated in % of people based on the average noise load. Dose-response relationships for highly annoyed people as a result of aircraft noise are investigated in a publication of Miedema [21]. The dose-response relation for awakenings is also used in a publication of Hartjes and Visser [4].

The obligations for noise will probably become more hypothetical in the near future. The runway configuration is highly dependent on weather conditions. Since this is hard to predict and uncontrollable it is not reasonable to punish AAS for exceeding the noise limits. It is assumed that AAS will always aim to minimize the number of annoyed people and that it will try to avoid

noise sensitive areas as much as possible.

3.5 Conclusion

The previous sections explained more about the functionality of AAS and its current operations. The volume of in- and out-bound air traffic is large enough to make the terminal control area very busy during peak hours. The current movements leave their noise print in the vicinity of AAS. Figure 3.7 shows the expected noise contours as result of aircraft movements on an average day in 2015. The figure clearly shows that AAS tries to avoid populated areas as much as possible. Areas like Hoofddorp, Amstelveen and the western and south-east districts of Amsterdam still fall within a noise contour of 48 dB and some of the areas even experience noise levels of 58 dB.

Concluding, this chapter provided enough background information to understand the complexity of airport operations at AAS. The research context will support in understanding why several decisions or assumptions are made during the project as described in the upcoming chapters. Secondly, the background information supports in understanding the potential of an allocation model that is able to optimally allocate aircraft to tailored departure trajectories. As the research context is now clear, the next chapter will continue with the main research of this MSc. thesis project.

Figure 3.7: Expected noise contours as result of aircraft movements on an average day in 2015 [1]

4

Trajectory Optimization Model

Currently, the number of SID's at AAS is limited. Every runway departure fix combination has at least one SID. What SID's are available for take-off depends on the daily situation. The runway configuration of a particular day is determined by multiple factors, like the wind direction or runway maintenance. All SID's are officially documented by the AIP [6]. In order to investigate the potential benefit of tailored SID and profile allocation for AAS, alternative trajectories need to be available first. Therefore, a trajectory optimization model is developed that is capable of designing novel tailored SID's dependent on aircraft type and take-off weight.

This chapter describes the development and working principles of the trajectory optimization model. In chapter 2 the modelling framework was presented. Figure 4.1 gives a clear indication of the position of the trajectory model with respect to the modelling framework. Section 4.1 starts with a concept description of the trajectory optimization model. Subsequently, the methodology used to model the departure trajectories is discussed in section 4.2. Section 4.3 elaborates on the structure of the trajectory optimization model. In section 4.4 explains how the output data of the trajectory model is processed into input data for the trajectory allocation model. Finally, section 5.4 includes a short summary of this chapter.

4.1 Concept Description

The trajectory optimization model is developed with the goal to generate a set of tailored departure trajectories that can be used as input data for the allocation model. The model is developed in such a way that it is relatively easy to adjust for different flight categories and flight profile procedures.[1] Obviously, the latter is a requirement since the research objective is to investigate

[1] A flight category is defined by a combination of aircraft type and take-off weight.

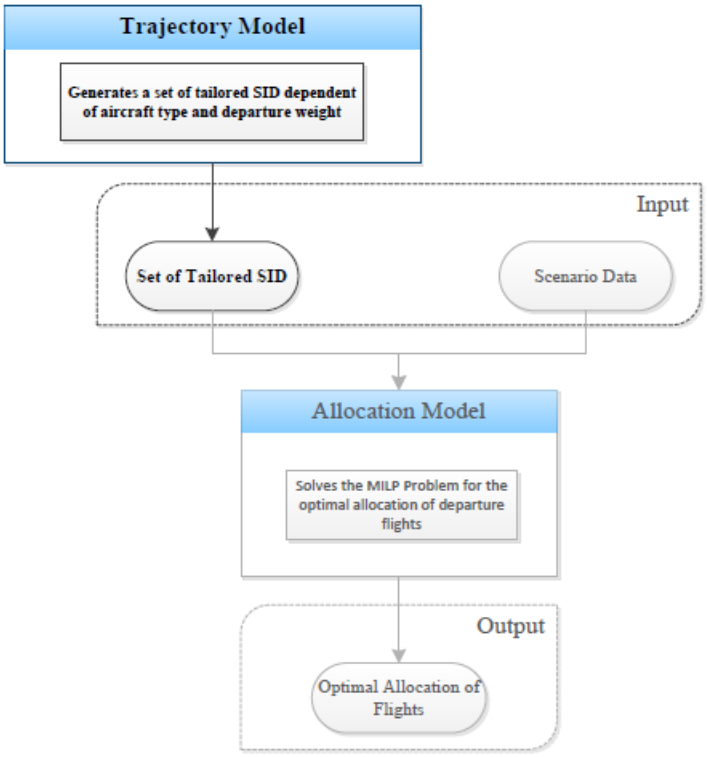

Figure 4.1: Block diagram of the project approach emphasizing the trajectory optimization block

the potential benefit of tailored trajectories. Due to these generic characteristics the model allows to scale up the research by increasing the variety of aircraft within a certain fleet. Developing the model generically is favourable since it might benefit future research on departure trajectory optimization. The remaining part of this section describes the requirements and any assumptions made in developing the model.

4.1.1 Requirements

In order to ensure the functionality of the trajectory optimization model, the following requirements are set:

- The model is capable of performing multi objective optimization (noise vs. fuel)
- Optimized trajectories are dependant of aircraft type and take-off weight
- Trajectories are optimized per runway departure fix
- Optimized trajectories have realistic values for noise and fuel consumption
- Minimum turn height of 120 m. is taken into account
- Maximum bank angle of 25° in turn segments is allowed
- Maximum deviation from departure fix of 50 m. is allowed
- The outcome of the model includes at least two different tailored departure trajectories

(noise optimal & fuel optimal)
- Computation time remains within realistic bounds
- The model can be applied to a wide variety of aircraft types, take-off weights and flight procedures

4.1.2 Assumptions

Some assumptions are made to simplify the development of the aircraft performance model and trajectory optimization model. The most relevant assumptions are listed below.

- The Earth is flat and non-rotating
- No wind vector present
- Aircraft flight performance can be simulated by means of an intermediate point-mass model
- The aircraft performs a coordinated flight
- Altitude restrictions are set to 2000 m (ca. 6000 ft.) in order to prevent conflicts with arrivals
- Departure fix is placed closer to start AAS but in line with original departure fix
- Flight path angle is sufficiently small ($0° < \gamma < 15°$)
- Maximum bank angle remains constant
- Aircraft weight remains constant
- Initial and final coordinates of trajectory are fixed
- Only difference between NADP-1 and NADP-2 is height at which acceleration and flap retraction schedule are initiated
- An average household consists of three people

4.2 Trajectory Parametrization

The optimization model makes use of a parametrization technique to compute the novel tailored trajectories [4]. A trajectory consists of two components: its ground track and vertical profile. By applying the parametrization technique to both components a mathematical approximation of the departure trajectory is made. This allows the model to optimize the parametrized segments for noise and fuel. In this section parametrization of the ground track and vertical profile are explained in more detail. Subsequently, it is explained how parametrization makes optimization by the model possible.

4.2.1 Parametrization of the Ground Track

The trajectory model uses the concept of Track to a Fix (TF) legs and Radius to a Fix (RF) legs in turns to define the ground track. Based on these segment types the lateral trajectory is defined by a combination of straight leg segments and turn segments. It follows that a straight leg segment is defined by one parameter, being length L of the straight leg. A turn segment is defined by two parameters, being turn radius R and heading change $\Delta\chi$ of the fixed radius

turn [4]. The parameters L, R and $\Delta\chi$ are the decision variables for the trajectory optimization model. A schematic representation of the parametrized ground track and corresponding decision variables is given by figure 4.2. By finding optimal numbers for the decision variables the model is able to optimize the ground track of the departure trajectory. By increasing the number of segments the flexibility of the ground track improves, resulting in an increased number of decision variables. This allows the model to define more flexible ground tracks with improved capabilities to avoid noise sensitive areas.

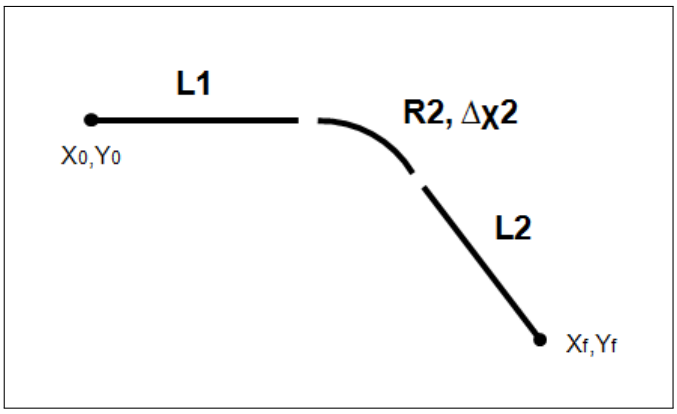

Figure 4.2: Schematic representation of the parametrized ground track and corresponding decision variables

It should be noted that, independent of the number of segments, two decision variables always follow from basic geometry.[2] An example is given in figure 4.3. Here, a basic track is presented consisting of two straight legs and one fixed radius turn, resulting in four decision variables to define the ground track. Assuming that the length of the first segment L_1 and the fixed radius of the second segment R_2 are known, the other two decision variables follow from equation 4.1 and 4.2.

$$\Delta\chi_2 = 180 - \tan^{-1}\left(\frac{\mid x_f - x_0 \mid}{\mid y_f - y_0 \mid - R_2}\right) - cos^{-1}\left(\frac{R_2}{\sqrt{(\mid x_f - x_0 \mid)^2 + (\mid y_f - y_0 \mid - R_2)^2}}\right) \tag{4.1}$$

$$L_3 = \sqrt{(\mid x_f - x_0 \mid)^2 + (\mid y_f - y_0 \mid - R_2)^2 - R_2^2} \tag{4.2}$$

It is concluded that for a ground track that is defined by n straight legs and m radius fixed turns, the optimized ground track can always be determined by means of $(n + 2 * m) - 2$ decision variables. This reduces the number of required optimization parameters significantly which will improve the computation time of the optimization model. In addition, equation 4.3 shows that for a given turn radius and the airspeed known, bank angle μ is no longer required as input to the

[2] Assuming that the initial and final coordinates of the ground track are fixed

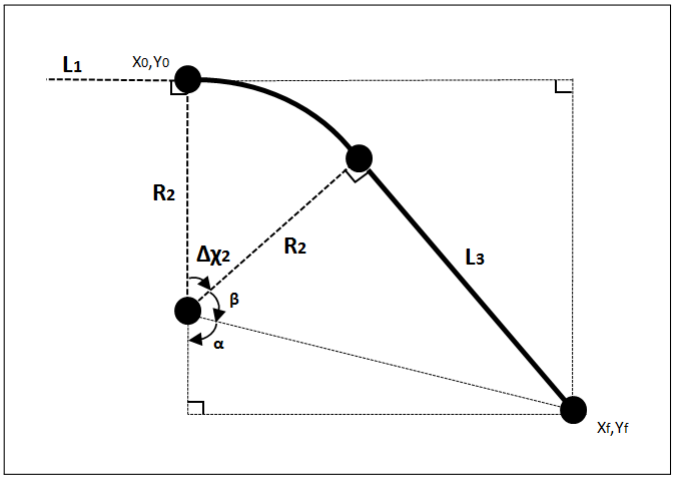

Figure 4.3: Geometric calculation of two unknown ground track parameters

model [4]. It should be noted that equation 4.3 is also used to set a constraint on the minimum turn radius by assuming a maximum bank angle μ_{max}.

$$R_{min} = \frac{V^2}{g_0 \tan(\mu_{max})} \tag{4.3}$$

4.2.2 Parametrization of the Vertical Profile

For this research two different flight procedures are distinguished, namely NADP-1 and NADP-2. It is assumed that the only difference between the two procedures is the height at which acceleration and flap retraction schedule are initiated. This allows for applying the parametrization technique to the vertical profile. Figure 4.4 shows that the vertical procedures can be divided into four separate segments. Each segment is defined by two flight parameters being the flight path angle γ_n and the thrust setting η_n, where n specifies the segment.

It should be noted that γ_n is a percentage of the maximum allowable flight path angle, as shown by equation 4.4 [4]. γ_{max} prevents the aircraft from stalling and is determined by the aircraft performance characteristics. γ_{min} is set to zero to prevent the aircraft from descending again. In a similar way, η_n is a percentage of the difference between the maximum and minimum allowable thrust, as shown by equation 4.5 [4]. The remaining flight parameters follow from the aircraft performance model, which will be discussed in section 4.3.

$$\gamma = (\gamma_{max} - \gamma_{min})\gamma_n \tag{4.4}$$

$$T = (T_{max} - T_{min})\eta_n + T_{min} \tag{4.5}$$

The following assumptions are made to parametrize the vertical profile. Therefore, each

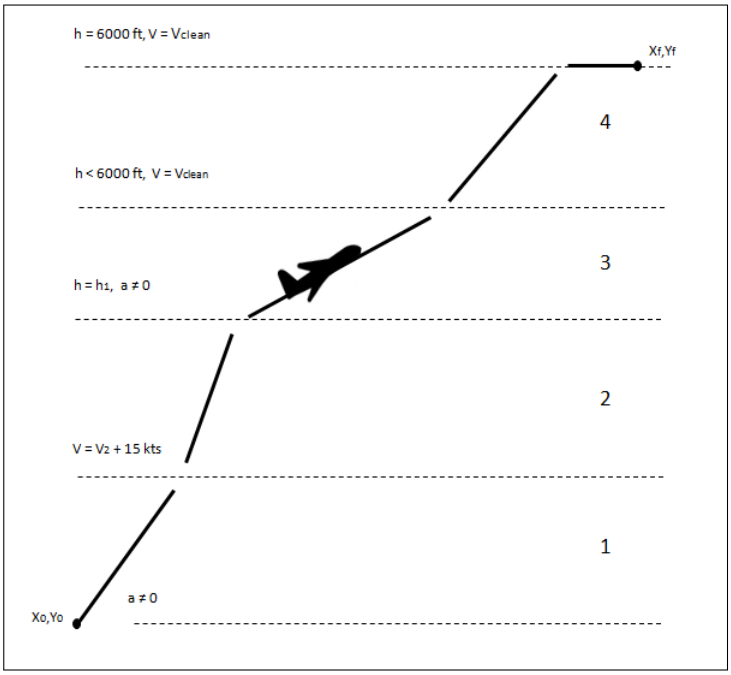

Figure 4.4: Schematic representation of the parametrized vertical profile for four of the five profile segments

segment is discussed separately:

- During the first segment aircraft accelerate from V_2 at take-off towards a speed of $V_2 + 15$ kts. Therefore, γ is left as a decision variable and $\eta = 1$
- During the second segment aircraft climb at constant speed towards height h_1 at which the acceleration segment is initiated. Therefore, γ is left as a decision variable and $\eta = 0$ since γ determines the thrust required to maintain constant airspeed. There is no acceleration present. The value of h_1 depends on what procedure is flown (NADP-1 or NADP-2).
- During the third segment aircraft accelerate towards en-route climb speed and flap retraction schedule is initiated. Both η and γ are left as decision variables.
- During the fourth segment aircraft continue to climb under constant en-route climb speed until the final altitude is reached (altitude restriction). Therefore, γ is left as a decision variable and $\eta = 0$ since γ determines the thrust required to maintain constant airspeed. There is no acceleration present. Once the final altitude is reached the aircraft maintains constant altitude until the final coordinates of the departure trajectory are reached.
- A fifth segment is added for the fixed-radius turn segments. Here, it is assumed that aircraft climb with constant air speed. Therefore, γ is left as a decision variable and $\eta = 0$ since γ determines the thrust required to maintain constant airspeed. There is no acceleration present.

The parametrization of the vertical profile results in six additional decision variables. Again, the number of segments could be expanded. This would allow for further optimization of the vertical profile. Since optimization of the vertical profile falls outside the scope of this research a fixed number of decision variables is taken into account by the trajectory optimization model for defining the vertical profile of tailored departure trajectories.

4.2.3 Sensitivity Analysis

The previous sections explained how the model computes tailored trajectories by optimizing parameters that define the ground track and vertical profile of the trajectory. The number of parameters of the vertical profile is fixed, as explained in section 4.2.2. The number of parameters of the ground track is not fixed because it is desirable that the ground track has enough flexibility to avoid noise sensitive areas.

A sensitivity analysis is done in order to determine the number of ground segments required to guarantee enough flexibility. Therefore, the optimization is done a couple of times. For every simulation the ground track is expanded with one straight segment and a turn, which is equal to adding three decision variables to the optimization model. Increasing the number of decision variables will increase the computation time of the optimization model. The optimal number of ground track segments is reached when the results of the optimization model do not show significant improvements with respect to the previous optimization. As long as the results show significant improvement, the ground track is expanded with another straight segment and a turn.

4.3 Structure of the Model

This section elaborates on the modelling framework of the trajectory optimization model. A schematic representation of the model is given in the form of a block diagram, as shown by figure 4.5. The framework links input, optimizer and output with each other. Use is made of the MATLAB optimization toolbox, an accessible tool for optimization problems in MATLAB [22]. The optimizer of the model makes use of a multi objective genetic algorithm with integrated aircraft performance model, fuel flow model and integrated noise model (INM) [23]. After receiving the input values, the optimizer is able to compute tailored departure trajectories by optimizing the parameters (decision variables) that define the trajectory, as explained in section 4.2. The integrated aircraft performance model and fuel flow model allow to optimize trajectories that are dependent of aircraft type. Subsequently, the output consists of a Pareto front with multiple optimal solutions. In this section the input-, optimizer- and output-blocks are discussed in more detail. The entire model is programmed in MATLAB 2015b.

For the optimizer other applications and algorithms were taken into consideration as well. After some test runs it is concluded that the global search algorithm scores bad on computation times and feasibility due to the fact that it only computes one of multiple solutions in a single run [24].

Furthermore, a MATLAB application of the Natural Sorting Genetic Algorithm II (NSGA-II) is also considered [25]. This application does not show enough variety in its results. Computation times are reasonable and comparable to the genetic algorithm of the MATLAB optimization toolbox.

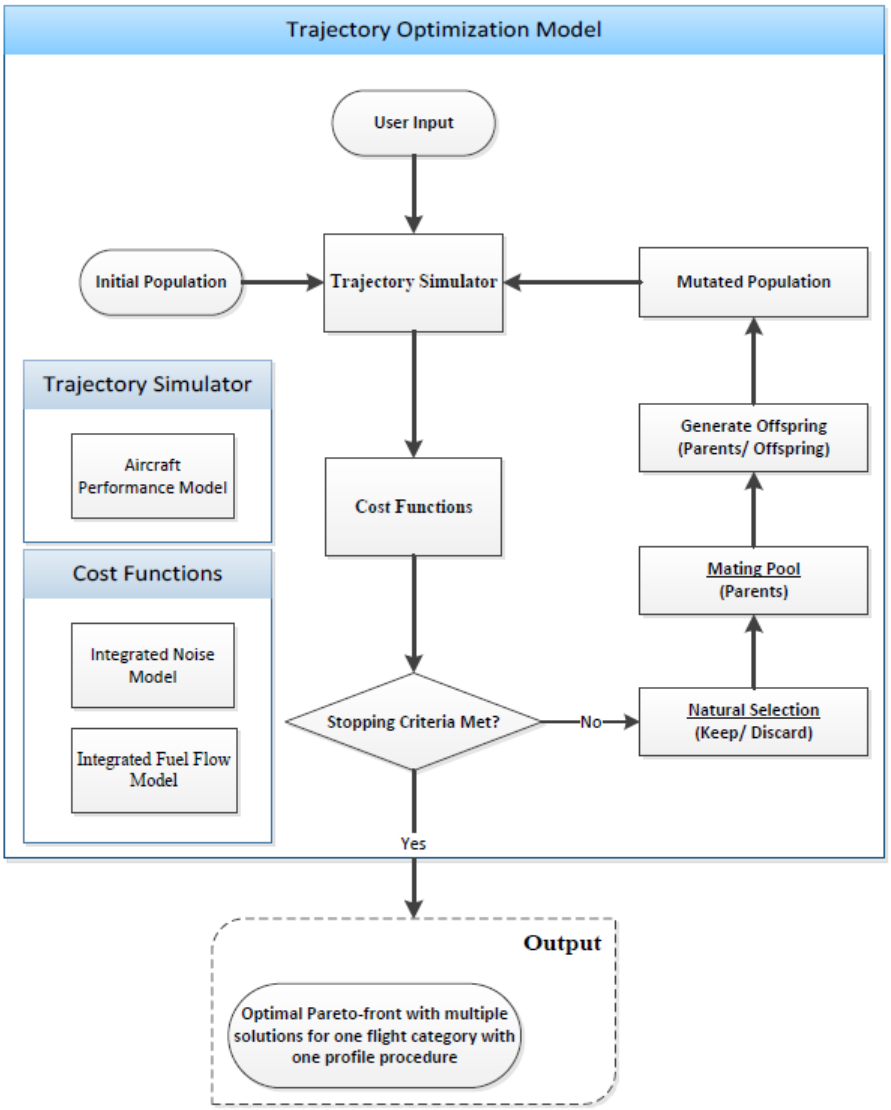

Figure 4.5: Schematic representation of the trajectory optimization model by means of a block diagram

4.3.1 Input

The trajectory optimization model is developed to define tailored departure trajectories dependant of aircraft type and take-off weight. The aircraft type is already taken into account by integrating an aircraft performance model into the optimizer. The only two input parameters left are take-off weight and flight procedure, which are selected by the user. This results in the fact that one simulation performs an optimization for aircraft type, take-off weight and flight procedure. In case of changing aircraft types, another aircraft performance model will need to be integrated in the optimizer.

4.3.2 Optimizer

The trajectory model uses a genetic algorithm for the multi objective optimization. Genetic algorithms are also called evolutionary algorithms because its working principles are inspired by Darwin's principle of natural evolution. Due to this affinity many biological metaphors are used. The different building blocks of the genetic optimization process are shown by the modelling framework in figure 4.5.

Multi Objective Optimization using a Genetic Algorithm

The optimization process starts at the integrated aircraft performance model. The aircraft model receives input parameters from the user and an initial set of candidate solutions (population) for the decision variables that define the trajectory. The aircraft performance model calculates the flight path and cost values by means of the integrated noise and fuel flow model. In each iteration (generation), the better solutions are selected (parents) and used to generate new solutions (offspring). This is done by recombining information of two parents (crossover) or modifying a parent randomly (mutation). Some of the weaker solutions are then replaced by the new offspring solutions [26]. The aircraft performance model calculates the flight path trajectory and cost values for the new population again. From this point onwards the process starts to repeat itself until the stopping criteria are met. By iteratively selecting the solutions that are better and use them to create new candidate solutions, the population "evolves". The solutions become better and better at each generation. Just like Darwin's principles, where individuals become better adapted to their environment through evolution [26].

Since the trajectory model optimizes for both noise and fuel consumption it is not possible to come up with a single optimal solution. A multi objective optimization problem usually results in the fact that optimizing for one objective comes at the cost of the other objective and vice versa. This results in a range of optimal solutions. Therefore, the genetic algorithm is able to search for a representative set of Pareto-optimal solutions, approximating the true Pareto front in one single run. It holds that every optimal solution on the representative Pareto front scores better on either one of the two objectives with respect to all the other solutions. For every iteration the representative set approximates the true Pareto front more and more [26].

Figure 4.5 clearly shows how the aircraft performance model, fuel flow model and noise model are integrated in the optimizer. All three are shortly discussed below. Also a brief description of the MATLAB optimization toolbox is given.

The Aircraft Performance Model

Based on the assumptions made in section 4.1 the equations of motion of the aircraft performance model can be simplified. The equations of motion are given by equation 4.6 [4].

$$\begin{aligned} \dot{x} &= V\cos(\gamma)\sin(\chi) \\ \dot{y} &= V\cos(\gamma)\cos(\chi) \\ \dot{z} &= V\sin(\gamma) \\ \dot{\chi} &= \frac{g_0\tan(\mu)}{V} \end{aligned} \tag{4.6}$$

Where $\dot{x}$, $\dot{y}$ and $\dot{z}$ are the aircraft velocity components in $x-$, $y-$ and $z-$direction respectively and $\dot{\chi}$ is the change in heading angle.

The aircraft performance model is controlled by the control parameters. Using the parametrized control functions as input, the system dynamics propagate forward. The control parameters for this performance model are the flight path angle γ_n and throttle setting η_n, as already defined by equation 4.4 and equation 4.5 respectively. The latter equation shows that the throttle setting determines the amount of thrust used to accelerate the aircraft model while preserving the minimum thrust. Bank angle μ is no longer a control parameter for the model, as it follows from equation 4.3.

The acceleration is determined by using equation 4.7. At constant air speed this equation equals zero and can be rewritten into equation 4.8 and allows for calculating the maximum flight path angle for a given air speed. Here, the maximum thrust is a function of airspeed V and altitude h as shown by equation 4.9. The function for maximum thrust is unique for every aircraft type being considered and follows from the aircraft performance model. Now that γ_{max} is known the actual flight path angle γ follows from equation 4.4 when decision variable γ_n is given. Equation 4.7 can be rewritten one more time into equation 4.10 to calculate the actual thrust for a given airspeed and a given value for decision variable γ_n. It should be noted that it is assumed that T equals T_{min} in order to maintain constant air speed.

$$a = \frac{1}{2\rho}\frac{\delta\rho}{\delta h}V^2\sin(\gamma) + g_0(\frac{T-D}{W} - \sin(\gamma)) = 0 \tag{4.7}$$

$$\gamma_{max} = sin^{-1}(\frac{-2\rho g_0(T_{max}-D)}{W(\frac{\delta\rho}{\delta h}V^2 - 2\rho g_0)}) \tag{4.8}$$

$$T_{max} = f(M, h) \tag{4.9}$$

$$T = \frac{W}{g_0}(g_0 sin(\gamma) - \frac{1}{2\rho}\frac{\delta\rho}{\delta h}V^2 sin(\gamma)) + D \tag{4.10}$$

For the acceleration segment the same steps are followed as when $a = 0$. For a given air speed V, that increases at every time step, the same calculations are done. Only now, the throttle setting η_n (decision variable) is also given. This results in the fact that $T > T_{min}$. Therefore, the aircraft accelerates and for every time step it holds that $V_t > V_{(t-1)}$.

The Fuel Flow Model

One of the objectives of the trajectory optimization model is fuel consumption. From a commercial point of view this is of economical interest to the airlines. An integrated engine model allows for fuel flow assessment of the tailored trajectories. Equation 4.11 shows that the fuel flow is a function of air speed, altitude and thrust. The function is aircraft dependent, which proves that the effect of aircraft performance on the fuel consumption is taken into account.

$$\sigma = f(M, h, T) \tag{4.11}$$

Compared to other optimization studies, often assumptions are made for the cost of fuel. In this case, the thrust and fuel flow settings have direct effect on the aircraft performance, which has its effect on the noise impact. Noise as a result of different aircraft types is an important cost for this research. Therefore, it is decided to integrate the aircraft dependent fuel flow models into the trajectory optimization model.

Integrated Noise Model

The other objective of the trajectory optimization model is noise. In order to assess the individual departure trajectories on community noise impact, it is necessary to know the population density in the vicinity of the airport. The optimization model makes use of population data from 'het Centraal Bureau van de Statistiek' (CBS) containing population density information of the Netherlands for a particular grid-size. The data gives the population density per xy-coordinate of a 2D-grid with an accuracy of 500 m^2. Concluding, to determine the noise cost of a trajectory both the noise impact and population for each xy-coordinate of a 2D-grid need to be known.

The trajectory optimization model uses a replication of the in-flight noise model that is incorporated in INM [23]. This replication is called INMTM [13]. INMTM allows for performing noise assessments for the majority of modern commercial aircraft. The integrated model provides a number of noise metrics that are based on empirically determined Noise-Power-Distance (NPD) tables from INM. These tables are interpolated for the thrust level and the distance between observer and flight segment, assuming that the observer is standing directly below an aircraft

passing along a straight, infinite flight segment, at a given reference speed. Subsequently, INMTM calculates the Single Event Noise Level (SEL) per grid-coordinate.

Using the replication of INM has two benefits. First, it is relatively easy to integrate INMTM into the optimizer of the model. Secondly, it is not necessary to use INM as a whole which saves computation power. The integrated noise model requires two inputs. The first input includes the specifications of the grid. The second input consists of flight data. In order to calculate a SEL value for each individual point on the 2D-grid INMTM requires the following flight parameters:

- x-, y- and z-coordinates
- Air speed V
- Thrust T

As INMTM computes the SEL value per grid-coordinate it is now possible to determine the noise cost of a particular trajectory. A dose-response relationship is used to determine the percentage awakenings per grid-coordinate as result of a single fly over. The dose-response relationship is given by equation 4.12 and yields an upper limit to the percentage of expected awakenings due to a single flyover at night time. This relationship is based on a research done by the Federal Interagency Committee on Aviation Noise (FICAN) in 1997 [3]. An example of the relationship is given by figure 4.6.

$$\%\text{Awakenings} = 0.0087 \cdot (SEL_{indoor} - 30)^{1.79} \tag{4.12}$$

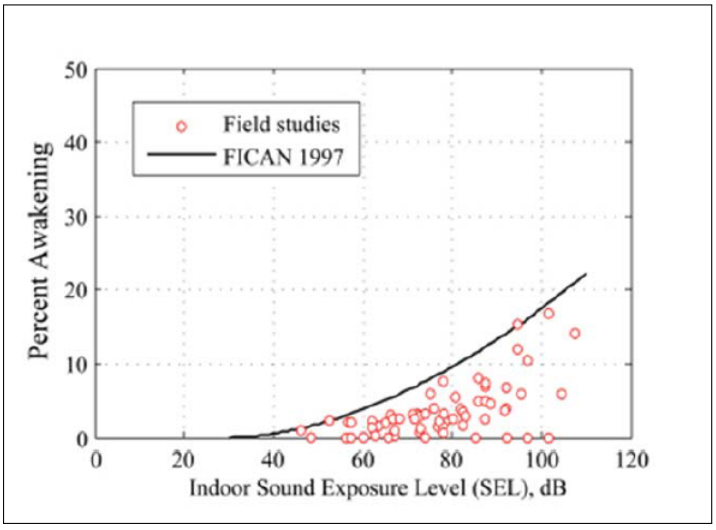

Figure 4.6: FICAN dose-response relationship [4]

By multiplying the number of people living on each grid point with the expected percentage of awakenings, the maximum number of expected awakenings per grid point is calculated. The noise cost of a trajectory is determined by calculating the total number of expected awakenings. A

correction of 20.5 dB on the INMTM SEL-values is applied to account for the sound absorption of an average house [27]. Furthermore, it is assumed that the number of houses per grid-coordinate equals $\frac{1}{3}$ of the population data.

MATLAB Optimization Toolbox

The MATLAB optimization toolbox allows for accessible use of the genetic algorithm [22]. By means of the optimization application the preferred algorithm can be selected. In this case a multi objective optimization is done by means of a genetic algorithm. Therefore, the *gamultiobj* solver is selected. Subsequently, one can recall the fitness function, set lower and upper bounds to the decision variables and add additional constraints. Furthermore, it is possible to set the population size and stopping criteria manually. It is also possible to adjust the mutation settings for the mating process. The optimization settings for the multi objective genetic algorithm are given below.

- Population size: 60
- Selection method: tournament
- Crossover fraction: 0.8
- Crossover function: intermediate
- Mutation function: constraint dependant
- Pareto front population fraction: 0.7
- Generation size: 150

Furthermore, the optimization problem is subjected to several constraints. The first constraint requires the trajectory to end within 50 m from the fixed final coordinates. The second constraint sets a minimum turn height of 120 m. Additionally, for every turn segment a constraint is included to limit the maximum bank angle to 25°. Finally, lower and upper bounds are imposed on the decision variables that define the horizontal ground track and vertical profile of the trajectory. The lower and upper bounds are included in table 4.1. The upper bound of straight leg segments varies as it depends on the specific ground segment n.

Table 4.1: Lower and upper bounds of decision variables

Description	Symbol	Lower Bound	Upper Bound
Strait leg	L	1000 m	varies
Heading change	$\Delta\chi$	1°	90°
Fixed radius	R	1000 m	9000 m
Flight path angle	γ_n	0	1
Throttle setting	η_n	0	1

4.3.3 Output

Since the trajectory model optimizes for both noise and fuel consumption it is not possible to come up with a single optimal solution. In trajectory optimization studies optimizing for noise

usually comes at the cost of fuel consumption and vice versa. This results in a range of optimal solutions presented by the optimal Pareto front. An example of the output of the trajectory optimization model is given by figure 4.7. For every solution on the Pareto front it holds that it always scores better on either one of the two objectives with respect to all other solutions. Otherwise it would not be one of the optimal solutions. Furthermore, every solution on the optimal Pareto front has its unique combination of decision variables that define the departure trajectory.

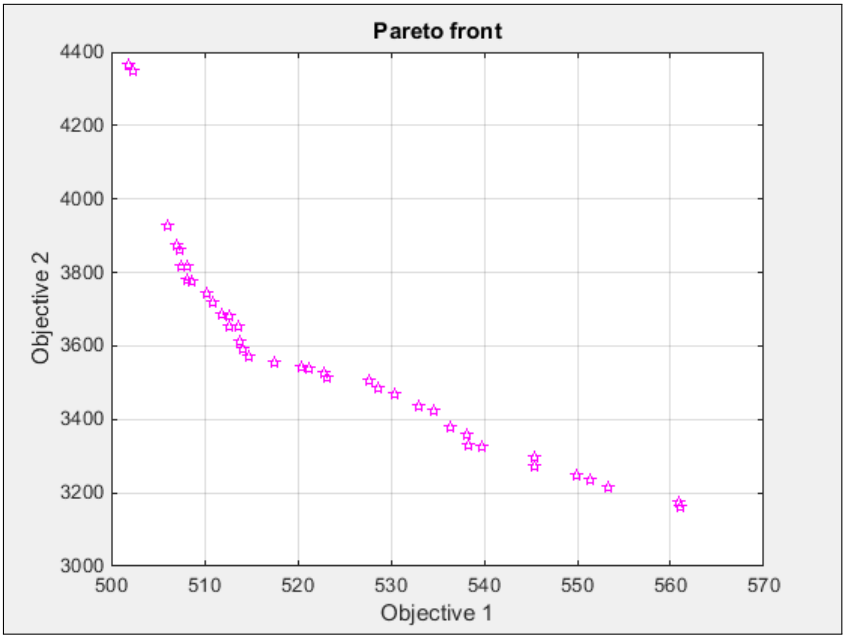

Figure 4.7: Example of model output by means of optimal Pareto front

4.3.4 Computation Times

From the requirements it follows that computation times should stay within realistic bounds. Genetic algorithms are meta-heuristic. In general, there is no analysis available to compute the computation time of genetic algorithms. It is more common to analyse the convergence time when analysing the complexity of genetic algorithms. However, one can note that the computation time of one iteration (generation) depends on its inner operations (e.g. selection, crossover, mutation). The settings of inner operations are problem dependent and easy to adjust by means of the MATLAB optimization toolbox. Furthermore, the computation time of genetic algorithms also depends on the number of iterations required to converge to a set of optimal solutions. Research is done on probabilistic analyses and several other techniques to find the average convergence time of genetic algorithms [28][29].

For this research, an average computation time of 2 hours is observed in order to execute a single

run. One single run generates an optimal Pareto front with multiple solutions (tailored departure trajectories) for one particular flight category following one flight procedure. The set of optimal solutions is then presented by means of an Optimal pareto front. A computation time of 2 hours is considered to be acceptable for this research.

4.4 From Optimization Output to Allocation Input

The objective of the trajectory optimization model is to generate a set of tailored departure trajectories that can serve as input data for the allocation model. The previous sections explained how the model is capable of doing this. One single run generates an optimal Pareto front with multiple solutions for one particular flight category following one flight procedure. All solutions represent tailored departure trajectories with unique cost for noise and fuel. Therefore, all solutions could be used as input for the allocation model. In that case, the number of alternative departures for a particular flight category would equal the total number of optimal solutions on the Pareto front.

Due to limited computational power of the allocation model it is not feasible to use all optimal solutions from the trajectory model output. Taking all solutions into account for every flight category and two different profile procedures would result in a tremendous amount of input data for the allocation model. Secondly, many of the solutions show only minor differences in their cost values. These solutions can be grouped and represented by a single solution. Concluding, it is preferred to select a limited number of tailored trajectories from the optimal Pareto front that can serve as input for the allocation model.

The Derivative Method

To investigate the optimal allocation for noise and fuel it is desirable to take the fuel optimal and noise optimal solutions from the Pareto front into account. These are the two outer lying solutions on the optimal Pareto front and the first two tailored trajectories that will serve as input for the allocation model. A third solution is selected to also analyse the intermediate behaviour of the allocation model. In order to select the third solution the remaining solutions on the Pareto front are analysed by means of the derivative method.

For multi objective optimization problems a set of multiple solutions is generated. One should note that it is not possible to come up with a single optimal solution since the trajectory model optimizes for both noise and fuel consumption. This makes it difficult for the decision maker to select a third optimal solution from the Pareto front. Research is done on computing the most significant solutions from a Pareto front in multi objective problems [30]. Comparison of different methods in multi objective decision making is also investigated [31]. It is concluded that research on this topic has one thing in common. All focus on developing techniques that select the most suitable solutions from the optimal Pareto front. Since it is not possible to identify one

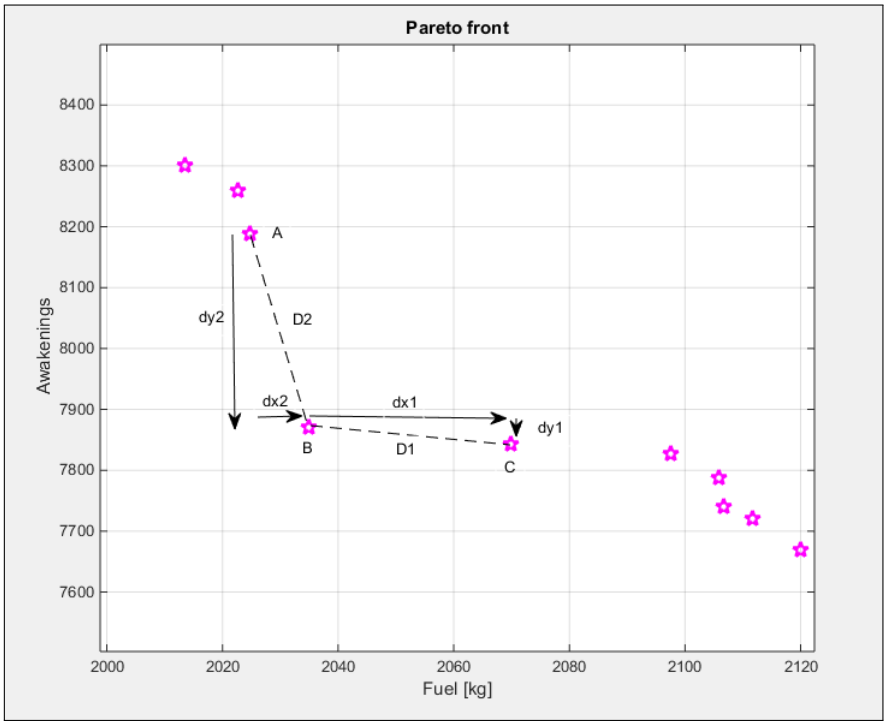

Figure 4.8: Part of an optimal Pareto front showing selection of the third optimal solution for the allocation model

single optimal solution, research focus on developing selection methods resulting in a set of most suitable solutions.

Investigating the different methods would be rather time consuming and out of the scope of this research. Therefore, the derivative method is used to select a third optimal solution from the optimal Pareto front. This method allows for analysing the position of each solution with respect to its neighbouring solutions on the optimal Pareto front. By means of the derivative method a selection of the most suitable solutions is made. Based on additional criteria a third trajectory is selected for the allocation problem.

Figure 4.8 shows a part of the optimal Pareto front. It is preferable to choose a solution like point B. Compared to point C, solution B can save a sufficient amount of fuel while keeping additional costs for noise relatively low. Comparing point A to point B, fuel savings are relatively small and associated with a significant cost increase for noise. In order for a point to comply with these conditions the difference between derivatives D_1 and D_2 should result in a large and positive number. Equations 4.13 and 4.14 define the derivatives between point B and C, and point A and B respectively. For a candidate solution point it holds that $D_1 - D_2$ is a large positive number.[3]

[3]For a particular point B from figure 4.8 D_1 will be a small negative number and D_2 will be a large negative number

The derivative method makes a selection of all points that comply with the desired characteristics of point B in figure 4.8. This are all points on the Pareto curve for which $D_1 - D_2$ is a large positive number. The downside of this method is that points lying in the upper left part of the Pareto front are quickly selected as well because of the steepness of the Pareto curve. Therefore, an additional criteria is applied to select the third optimal solution. It holds that it is desirable that the third solution lies half way the Pareto front to guarantee enough improvement in terms of fuel or noise with respect to the other two trajectories. By calculating the derivatives for every solution on the optimal Pareto front and applying the additional criteria, a third tailored trajectory is selected.

$$D_1 = \frac{dy_1}{dx_1} \tag{4.13}$$

$$D_2 = \frac{dy_2}{dx_2} \tag{4.14}$$

Once the three optimal solutions are selected the following data of the tailored departure trajectories is required as input for the allocation model:

- Fuel cost
- Noise impact per grid-coordinate

4.5 Conclusion

In the previous sections the development and working principles of the trajectory optimization model were explained. The model is developed with the goal to generate a set of tailored departure trajectories dependent on aircraft type and take-off weight. By means of a parametrization technique the model is capable of simulating the departure trajectories. Subsequently, a multi objectives genetic algorithm is used in combination with an integrated aircraft fuel flow model and integrated noise model to perform a multi objective trajectory optimization. Results of the trajectory optimization model are presented by means of an optimal Pareto front. By applying the derivative method a limited number of optimal solutions per flight category is chosen. Running the model for different flight categories will result in a sufficient amount of trajectories with enough variety in flight category. The entire set of tailored trajectories is used by the trajectory allocation model to investigate the potential benefit of tailored SID and profile allocation. The working principles of the allocation model are discussed in the next chapter.

5

Allocation Model

The previous chapter showed how new alternative departure tracks were designed by means of a trajectory optimization model. By running the trajectory model for different flight categories with different profile procedure a set of tailored SID is generated that are dependent of aircraft type, departure weight and profile procedure. The complete set serves as input for the allocation model. Figure 5.1 gives a clear indication of the position of the trajectory model with respect to the modelling framework.

This chapter describes the development and the working principles of the trajectory allocation model. Section 5.1 starts with a concept description of the model. Subsequently, section 5.2 elaborates on the concept of linear programming which is used by the model to solve the allocation problem. In section 5.3 the structure of the trajectory allocation model is discussed. Finally, section 5.4 provides a short summary of this chapter.

5.1 Concept Description

The trajectory allocation model developed for this research is able to assign aircraft to novel tailored departure trajectories based on an optimization trade-off between fuel consumption and noise impact on the environment. The model allows for testing different departure flight schedules and analyse the results on potential noise and fuel savings. In this way, the potential benefit of tailored SID and profile allocation is quantified. The allocation model is developed in MATLAB. A generic set-up is used to allow for scaling the model to different problem sizes. This allows for adding tailored departure trajectories for the same or for different runway departure fix combinations to the model. Due to the generic characteristics the model can even be applied to other airports. This could be beneficial for future research on this topic. The remaining

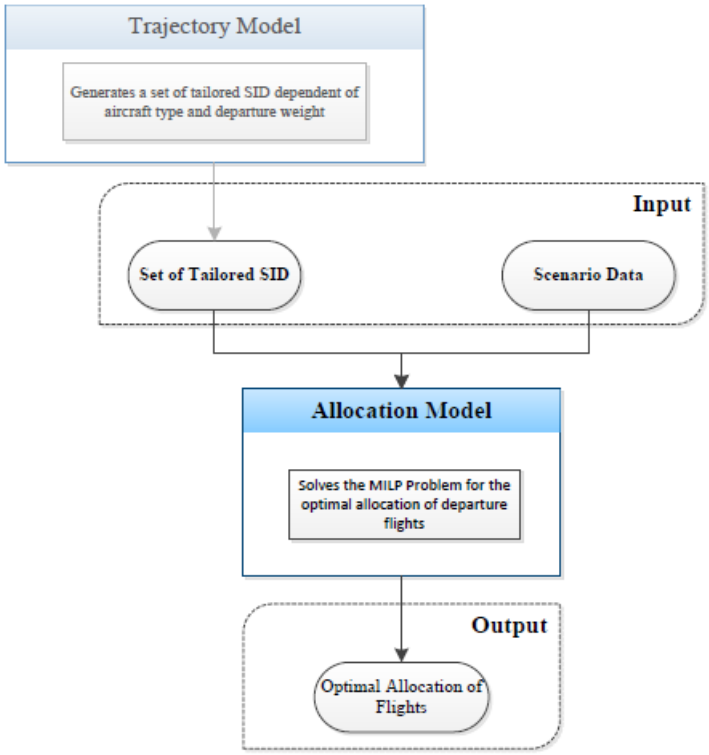

Figure 5.1: Block diagram of the project approach emphasizing the blocks that are involve in with the allocation model

subsections describe the requirements and any important assumptions made for the development of the trajectory allocation model.

5.1.1 Requirements

In order to ensure the functionality of the trajectory allocation model, the following requirements are set:

- For every flight category the allocation model has the option to assign aircraft to at least two alternative departure trajectories with at least one departure profile procedure
- All flights from the departure schedule are assigned to a trajectory
- The allocation model is able to find the optimal allocation of flights for minimum noise impact
- The allocation model is able to find the optimal allocation of flights for minimum fuel consumption
- The allocation model is able to find the optimal allocation of flights for different weightings to noise and fuel consumption
- The allocation model is able to find the optimal allocation of flights for different aircraft

types with different take-off weights
- The allocation model takes the noise impact of day-, evening- and night-time operations into account
- Use is made of a realistic departure flight schedule
- The allocation model is applicable to AAS
- Results of the allocation model are presented to the user in a visual way
- Computation time has to stay within acceptable bounds

5.1.2 Assumptions

Some assumptions are made to simplify the development of the trajectory allocation model. The most relevant assumptions are listed below.

- All flights from the departure flight schedule do take off
- Aircraft grouping can be used to take a wide range of aircraft types into account
- Separation of flights does not affect the optimal allocation of departure flights
- There is no wind vector present that can influence the optimal allocation of departure flights
- Visibility does not affect the optimal allocation of departure flights
- Complexity of the air space does not limit the optimal allocation of departure flights
- The legal obligations discussed in chapter 3 can be used as reference values for the noise contour limits

5.2 Linear Programming

The allocation model uses Mixed Integer Linear Programming (MILP) to solve the optimization problem. After discussing the concept of MILP the trajectory allocation problem will be written out according to linear programming standards. All parameters and variables are written down in a structured way. Also the objective function, cost coefficients and constraints are presented in this section. In this way, an overview is given of the optimization problem as to be solved by the trajectory allocation model. The goal of the allocation model is to minimize the objective function for the cost coefficients representing fuel consumption and noise respectively.

5.2.1 Mixed Integer Linear Programming

Linear Programming is a mathematical method used to find the optimal solution of a problem. The method includes the minimization or maximization of a linear function that is subject to linear constraints. Linear programming is used in various fields of research. The method gained a lot of popularity among operations research in the field of business and economics and has proven its value for engineering studies and other fields of research [32]. For aviation linear programming is often applied to complex linear optimization problems like aircraft planning,

routing and scheduling problems.

Equation 5.1 gives a canonical formulation of a standard linear problem [14]. With linear programming a single objective function $C^T x$ is optimized (maximization or minimization). Here, x represents a vector with all decision variables. C represents another vector containing all cost coefficients of each decision variable in x. The objective function is subject to a set of equality constraints, inequality constraints or a combination of both ($Ax \leq b$ and $x \geq 0$). Here, a pre-established matrix A contains several linear relations between the decision variables that are subject to a corresponding value in vector b.

$$\begin{aligned} Minimize \quad & C^T x \\ Subject\ to \quad & Ax \leq b \\ & x \geq 0 \end{aligned} \tag{5.1}$$

Just like other mathematical methods there are some variations possible on the basic concept of linear programming. One refers to Integer Linear Programming (ILP) when all decision variables are restricted to be integers. For ILP equation 5.2 is added to the canonical formulation of the problem. Here, $\mathbb{Z}^n$ represents a set of integer values. When the decision variables of the problem are allowed to be either integers or continuous variables one refers to the problem as Mixed-Integer Linear Programming (MILP).

$$\forall x \in \mathbb{Z}^n \tag{5.2}$$

Finally, one refers to Binary Integer Linear Programming (BILP) when all decision variables are restricted to be binary integers [33]. For the optimal solution of problems with a binary nature the decision variables are either 1 or 0. For BILP equation 5.3 is added to the canonical formulation. Linear programming for multi-objective optimizations is also possible. In that case the different objectives need to be normalized by normalization factors, as becomes clear in the following sections of this chapter. The trajectory allocation model uses a combination of ILP and BILP to solve the multi-objective optimization problem and is therefore considered to be a form of MILP as well.

$$\forall x \in [0, 1] \tag{5.3}$$

5.2.2 Sets and Indices

The following sets are used for the problem:

- A_a = set of aircraft types
- W_w = set of aircraft departure weights
- D_d = set of different periods of the day
- P_P = set of profiles

- R_r = set of routes
- G_{xy} = set of x-, y-coordinates (Grid)

The following indices are used for the problem:

- a = aircraft type index
- w = aircraft departure weight index
- d = period of the day index
- p = profile index
- r = routing index
- xy = coordinate index

An additional set F_f includes the complete set of departure flights consisting of all different flight categories included in the problem. The additional set is used to simplify reporting of the linear problem. F_f is composed by three different flight characteristics. Each departure flight can be categorized by aircraft type ($a \in A_a$), departure weight ($w \in W_w$) and the period of the day at which the operation takes place ($d \in D_d$). This means that the size of set F_f equals the sum of all combinations of $a \in A_a, w \in W_w$ and $d \in D_d$.

For all f in F_f the trajectory optimization model calculated a set of alternative tailored trajectories. The trajectories are defined by the lateral ground track (routing) and vertical procedure (profile). The diversity between different tailored trajectories for one specific flight category results from the option to fly different flight profiles (either NADP-1 or NADP-2) or to fly different ground tracks. The trajectory optimization model was able to compute several tailored SID by means of a genetic algoritm, as explained in chapter 4.

5.2.3 Objective Function

The trajectory allocation model minimizes a multi objective function shown by equation 5.4.

$$Z = \alpha \cdot n_f \sum_{a \in A} \sum_{w \in W} \sum_{d \in D} \sum_{p \in P} \sum_{r \in R} C^F_{a,w,d,p,r} \cdot x_{a,w,d,p,r} + \beta \cdot n_n \sum_{xy \in G} C^N_{xy} \cdot x_{xy} \tag{5.4}$$

The right hand side of the objective function consists of two objectives. The first summation on the right hand side of the equation represents the objective for fuel consumption Z^F. The second summation on the right hand side of the equation represents the objective for noise Z^N. By means of this objective function the model aims to find the optimal allocation of departure flights while minimizing fuel consumption and noise impact. Below, decision variables $x_{a,w,d,p,r}$ and x_{xy} and cost functions $C^F_{a,w,d,p,r}$ and C^N_{xy} are explained in more detail. After discussing the problem's constraints in section 5.2.4, weighting factors α and β and normalization factors n_f are n_n discussed in section 5.2.5.

Decision Variables

Decision variable $x_{a,w,d,p,r}$ represents a number of flights of a specific flight category $f_{a,w,d}$ that follows a trajectory with route r and profile p. It holds that $x_{a,w,d,p,r}$ is a positive integer if route r with profile p for a number of flights $f_{a,w,d}$ is selected ($x_{a,w,d,p,r} > 0$), otherwise $x_{a,w,d,p,r} = 0$. Therefore, $\forall x_{a,w,d,p,r} \in \mathbb{Z}^+$.

$$x_{a,w,d,p,r} \tag{5.5}$$

Second decision variable x_{xy} represents a grid point of total grid size G. It holds that $x_{xy} = 1$ if grid point xy of grid G falls within the noise contour with a predefined noise limit, otherwise $x_{xy} = 0$. Therefore, $\forall x_{xy} \in [0, 1]$.

$$x_{xy} \tag{5.6}$$

Cost Coefficients

The cost coefficients represent the cost of a flight category $f_{a,w,d}$ that follows route r and profile p. The cost is expressed in terms of noise and fuel burn respectively. Both cost functions are discussed below.

The cost for fuel of a flight $f_{a,w,d}$ that follows route r and profile p is given by $C^F_{a,w,d,p,r}$. The cost coeffeicient can be expressed in kilograms, pounds or price. Since the fuel consumption of a specific tailored SID is already specified in kilograms by the trajectory optimization model, this unit is also used for the allocation problem. It holds that the cost for fuel is independent of d. The period of the day of the particular operation does not affect the fuel consumption for a specific flight category f.

$$\text{Fuel cost coefficient}: \quad C^F_{a,w,d,p,r} \tag{5.7}$$

The cost for noise of flight $f_{a,w,d}$ following a trajectory with route r and profile p is given by C^N_{xy}. The cost for noise can be expressed in number of people living within a contour of 40 dB L_{night} or 48 dB L_{den} and the number of houses within a contour of 48 dB L_{night} or 58 dB L_{den}. It holds that the cost for noise is evaluate per xy-coordinate of a specified grid size G. The grid size G covers the area of interest around AAS. Unlike the cost coefficient for fuel, the period of the day does affect the cost coefficient for noise. Period of the day is taken into account by including L_{den} penalties in one of the constraints.

$$\text{Noise cost coefficient}: \quad C^N_{xy} \tag{5.8}$$

5.2.4 Constraints

The objective function is subject to several constraints. The different constraints are discussed below.

Equality constraints

To guarantee that all departure flights of a specific category are assigned to a tailored SID and flight procedure the conservation constrain is applied. The conservation constraint is defined by equation 5.9. It holds that the sum of allocated flights of a specific fight category should equal the total number of departure flights of that specific category.

$$\text{Conservation constraint}: \quad \sum_{p\in P}\sum_{r\in R} x_{a,w,d,p,r} = N_{a,w,d}\ ; \quad \begin{matrix} \forall a \in A \\ \forall w \in W \\ \forall d \in D \end{matrix} \tag{5.9}$$

The decision variables $x_{a,w,d,p,r}$ are restricted to be either a positive integer or zero. This depends on how many flights $f_{a,w,d}$ of a particular flight schedule are assigned to a trajectory with route r and profile procedure p.

$$\forall x_{a,w,d,p,r} \in \mathbb{Z}^{+} \tag{5.10}$$

The decision variable x_{xy} is restricted to binary lower and upper bounds. This means that the noise limit for a xy-coordinate within grid G is either reached or not and thus,

$$\forall x_{xy} \in [0,1] \tag{5.11}$$

Inequality constraints

The cost for noise in the objective function of equation 5.4 is expressed in number of people living within a contour of 40 dB L_{night} or 48 dB L_{den} and the number of houses within a contour of 48 dB L_{night} or 58 dB L_{den}. In order to determine whether a coordinate lies within the noise contour, each xy-coordinate of grid G is evaluated individually. By applying the inequality constraint of equation 5.12 to each xy-coordinate in G it is possible to assess the noise impact of the overall allocation of departure flights and determine weather a specific coordinate lies within the noise contour or not.

$$\text{Noise constraint}: \quad \sum_{a\in A}\sum_{w\in W}\sum_{d\in D}\sum_{p\in P}\sum_{r\in R} C^{N}_{a,w,d,p,r,xy} \cdot x_{a,w,d,p,r,} - M \cdot x_{xy} \leq N_{limit} \tag{5.12}$$

$$; \quad \forall xy \in G$$

Here, $C^{N}_{a,w,d,p,r,xy}$ represents the noise impact in dB L_{den} or dB L_{night} of an occupied flight ($x_{a,w,d,p,r}$>0) on a specific xy-coordinate of grid G. The penalty factor M represents a large number that prevents the inequality constraint from reaching its noise limit N_{limit}. When the summation of allocated flights reaches the noise limit x_{xy} is forced to become one in order to comply with this constraint. As a result, the optimal solution for the allocation problem will always

comply with the noise constraint. The fact that x_{xy} is also included in the objective function allows for optimizing the number of grid points, or the number of people/ houses, located within the noise contour (when $x_{xy} = 1$). Equation 5.12 is called a *soft* constraint, where M serves as a switching function that decides whether a specific grid point falls within the noise contour or not.

Finally, it is important to note that initially $C^N_{a,w,d,p,r,xy}$ is served as input to the model in SEL (dB). Since this metric is of a logarithmic scale it can not simple be add up in the summation of equation 5.12. By using equation 5.13 the SEL values are converted to dB L_{den} [20]. Subsequently, by bringing all terms in front of the summation to the right hand side of the equation, the left hand side of the constraint is left with a summation of the acoustic energy which overcomes the problem of the logarithmic scale. The soft constraint for noise can be rewritten into equation 5.14.

$$L_{den} = 10 \cdot log[\frac{t_0}{T_0} \sum_{a \in A} \sum_{w \in W} \sum_{d \in D} \sum_{p \in P} \sum_{r \in R} g_d \cdot 10^{\frac{SEL}{10}}] \tag{5.13}$$

$$\sum_{a \in A} \sum_{w \in W} \sum_{d \in D} \sum_{p \in P} \sum_{r \in R} g_d \cdot 10^{\frac{SEL}{10}} \cdot x_{a,w,d,p,r} - 10^{\frac{M \cdot x_{xy}}{10}} \cdot \frac{T_0}{t_0} \leq 10^{\frac{N_{limit}}{10}} \cdot \frac{T_0}{t_0} \tag{5.14}$$

Where g_d represents the noise penalties for flights during day, evening and night which are 1, 3.162 and 10 respectively. The summation is performed over all aircraft noise events that occur during the specified reference time period T_0 which is 86400 seconds for a 24 hour time frame. $t_0 = 1$ is a reference time to determine the weighted equivalent sound level in L_{den} for SEL values.

In a similar way, SEL values are converted to dB L_{night} [20]. It is not necessary to use noise penalties for different periods of the day, since only night flights are taken into account. Therefore, $g_d = 1$. The summation is performed over all aircraft noise events that occur during the night which means that $T_0 = 28800$ seconds (8 hours) and $t_0 = 1$ to determine the weighted equivalent sound level in L_{night} for SEL values.

5.2.5 Normalization Methods

Weighted Sum Method

The weighted sum method allows to write the multi-objective optimization problem as a single objective function [34]. Looking at equation 5.4 each objective of the multi-objective optimization problem is multiplied by a coefficient (α or β). To correctly apply this method the sum of these coefficients equals one. Therefore, β always follows from α as shown by equation 5.15. By means of coefficients α and β different weightings are applied to the two objectives of the multi-objective optimization problem. The weighting can be adjusted to find the fuel optimal solution, the noise optimal solution or any trade-off in between.

$$\beta = 1 - \alpha \tag{5.15}$$

Normalization Factors

Since the two objectives have different dimensions, it is required to normalize the multi-objective function. The coefficients n_f and n_n from equation 5.4 represent the normalization factors. The normalization is done by optimizing each of the objectives individually first. Subsequently, each objective is divided by its individual range. That will say, the difference between the objective optimum value and the objective value corresponding to the individual optimization of the counter objective. Equations 5.16 and 5.17 give the normalization factors for fuel and noise respectively. The objective function now consist of dimensionless, normalized terms and both objectives can be equally compared.

$$n_f = \frac{1}{\mid Z^F_{noiseoptimum} - Z^F_{fueloptimum} \mid} \tag{5.16}$$

$$n_n = \frac{1}{\mid Z^N_{fueloptimum} - Z^N_{noiseoptimum} \mid} \tag{5.17}$$

Optimal Pareto-front

By applying different weightings to the multi-objective function the trajectory allocation model is able to find different optimal solutions. The optimal solutions form a second optimal Pareto-set containing the optimal distribution of flights for different values of α and β [35]. Just like with the trajectory optimization model, the solutions that correspond to the optimal Pareto-set are called Pareto optimal solutions. By connecting these solution a second optimal Pareto-front is formed. By including a reference scenario into the optimal Pareto-front figure a clear indication of potential savings for different optimal solutions is given. As shown by figure 5.2 optimal solutions A and B can easily be compared to reference case D, which is marked by a red dot. Solutions C, E, F and G fall in the feasible search area but are not considered to be optimal solutions since the points are not located on the optimal Pareto-front.

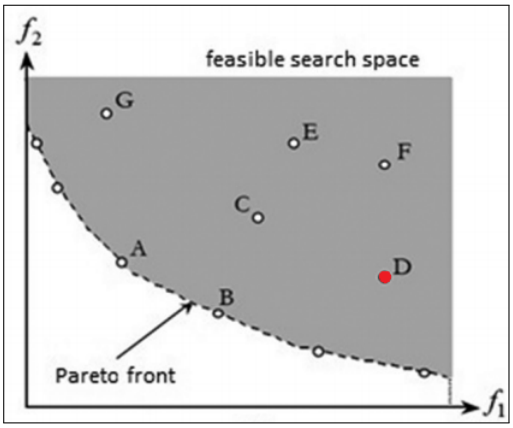

Figure 5.2: Example of the optimal Pareto-front resulting from different values of α, including optimal solutions A and B, feasible solutions C, E, F and G, and reference case D [5]

5.3 Structure of the Model

This section will elaborate on the modelling framework for the allocation problem. A schematic representation of the model is given in the form of a block diagram, as shown by figure 5.3. The model consists of different building blocks which will be discussed in this section separately. The entire model is programmed in MATLAB.

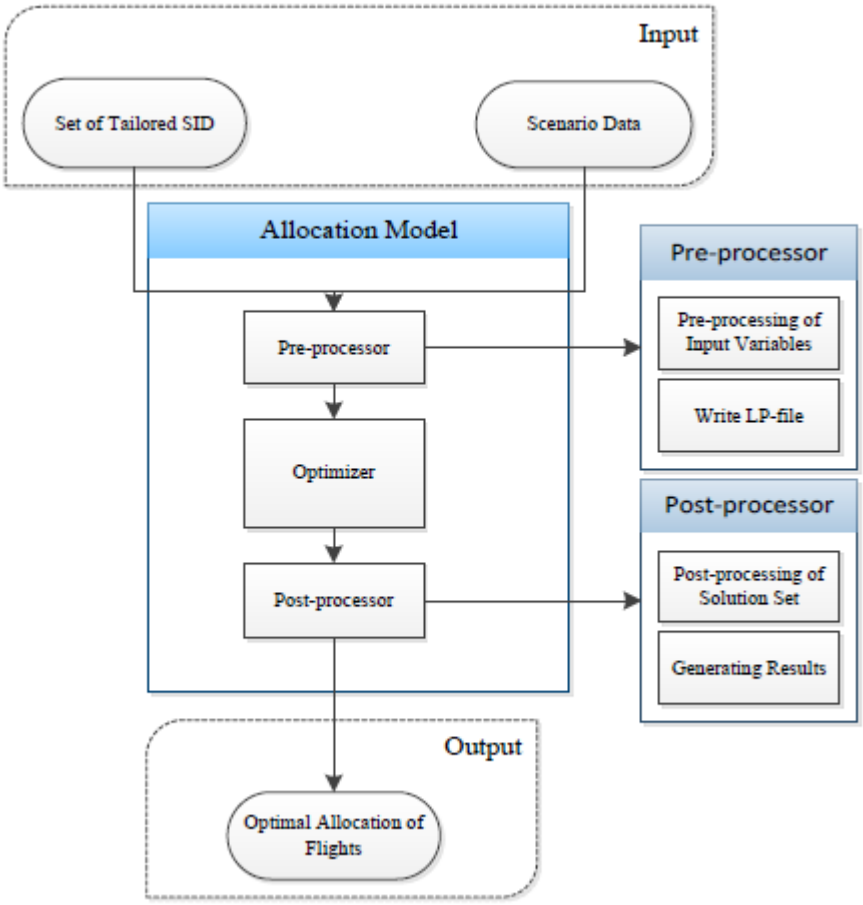

Figure 5.3: Schematical representation of the allocation model by means of a block diagram

5.3.1 Input

The allocation model uses two resources to get its input from. Part of the input comes from the tailored SID trajectory model, which is discussed in the previous chapter. The trajectory model designed several alternative departure trajectories dependent of aircraft type and departure weight. For each alternative SID the fuel consumption and noise impact for a pre-specified grid were calculated. The latter two define the cost for a SID and are therefore necessary input

parameters to the model.

The second resource used by the allocation model includes raw input data. This includes scenario dependent data that should be taken into account for the optimization of specific scenario's. The raw input data includes grid-coordinates, population data and information about the departure flight schedule. An overview of all necessary inputs is given below.

Tailored SID trajectory model:

- Fuel consumption data
- Noise impact grid

Raw input data:

- Grid coordinates
- Population data
- Departure flight schedule

5.3.2 Pre-processor

The main objective of the pre-processor is to write a linear programming file (LP-file) for the optimizer of the model. In order for the optimizer to solve the optimization problem it has to be fed with an LP-file. The first task of the pre-processor is to transform all complex details from the input block into manageable sets of variables. These sets can then be used by the pre-processor to easily generate an LP-file. When the LP-file is constructed it is handed over to the optimizer of the allocation model.

A second task of the pre-processor is to reduce the computational process time of the optimizer. This can be realized by filtering the input data in the transformation process of the pre-processor. The variables that will not have any effect on the outcome of the optimization problem are filtered out beforehand and will not be taken into by the optimizer at all. In this way the manageable sets of variables only include variables of interest.

The output of the pre-processor consists of an LP-file that includes the objective function and its constraints. The decision variables and their bounds are also defined in the LP-file.

5.3.3 Optimizer

The allocation model makes use of the IBM ILOG CPLEX Optimization Studio 12.6 optimizer. The cplex optimizer works as a black box. It needs an LP-file with the MILP problem as input. The MILP problem will then be solved by the optimizer and its solution is returned as an output. Subsequently, the output is passed on to the post-processor. The working principles of the optimizer will not be discussed in more detail since it is not relevant for the working of the optimization model.

5.3.4 Post-processor

The post-processor receives the set of solutions as input from the optimizer. The main objective of the post-processor is to transform the solution set of the optimizer into a manageable set of variables that can easily be used for the visual and graphical representation of results. After transforming the MILP solutions into a manageable set of variables a graphical representation of the optimal solution is generated. The post-processor is responsible for translating the optimal solution of the model into a graphical representation of modelling results. In this way the output is interpretable to the user as shown by the block diagram in figure 5.3.

5.3.5 Output

The output of the model, as generated by the post-processor, provides the following information to the user:

- Distribution of allocated flights
- Noise grid indicating populated areas and populated areas that fall within a specified noise contour
- Total fuel burn
- Total number of people and houses within a specified noise contour

5.3.6 Computation Times

For all variations on linear programming the problem is NP-hard (non-deterministic polynomial time). NP-hard finds its meaning in computational complexity theory and represents a class of problems for which solutions can be found within polynomial time by a non-deterministic Turing machine. The time required to solve these kind of problems increases rapidly as the problem size grows [36]. The trajectory allocation model uses a combination of ILP and BILP to solve the multi-objective optimization problem and is therefore considered to be a form of MILP as well. Since this allocation problem remains limited in its size the computational time of the model is not expected to become an issue.

5.4 Conclusion

In the previous sections the development and working principles of the allocation model were explained. The model is developed with the goal to compute the optimal allocation of flights for fuel, noise and a trade-off between these two objectives. In order to do so, the allocation model makes use of the tailored departure trajectories described in the previous chapter. It was explained that the model consist of several modelling blocks, being the pre-processor, the optimizer and the post-processor. The pre-processor of the model writes the problem down in a linear format. In this way, the allocation model can make use of mixed integer linear programming to solve the problem. Subsequently, Matlab is able to solve the linear problem by

making use of the CPLEX Optimization Studio 12.6 optimizer. Finally, results are past on to the post-processor to process results in the right format. This is necessary in order to present results in a clear and understandable way. By means of the allocation model the optimal allocation for an actual departure flight schedule can now be computed. In the next chapter a case study is carried in which this is done.

6

A Case Study for Amsterdam Airport Schiphol

This chapter describes the work of a case study. The models discussed in chapter 4 and chapter 5 are applied to a specified scenario at Amsterdam Airport Schiphol. The case study is performed to demonstrate the workings of the model when applied to a real case scenario. The goal of the case study is to compare the use of current departure routes to the use of the novel tailored trajectory allocation method, as discussed in previous chapters. Historical flight data is used as input to the model. Fuel and noise calculations are done to compute tailored departure trajectories for different aircraft types with different take-off weights. Subsequently, the optimal allocation of flights is determined by means of the trajectory allocation model. The model output is compared to actual airport operations, which serves as reference data for the case study. In this way, the potential benefit of tailored SID and profile allocation is quantified for AAS. In section 6.1 the case is described in more detail. Section 6.2 explains how the reference data is obtained. Final results of the model are compared to current operations and discussed in section 6.3.

6.1 Experimental Set-up

In this section a clear description of the case study is given. The experimental set-up consists of a case scenario to be evaluated. Subsequently, this has implications on the developed model and its input parameters. Both elements are discussed below.

6.1.1 Scenario Description

Ideally, the complete airport configuration is taken into account so that the model can be applied for a full operational day. Unfortunately, this would require a number of trajectory optimizations for the computation of tailored trajectories that would exceed the limited time period of a MSc thesis project of nine months. Therefore, the model is applied to one runway departure fix combination only. Considering a full operational day means that the current case scenario needs to be scaled up to include all runway departure fix combinations. Furthermore, the number of flight categories needs to be increased to take the complete departure flight scheme into account. Both interventions would require an increased amount of trajectory optimizations resulting in a similar but much larger data set. This does not affect the core working principles of the model. Therefore, the current experimental set-up is assumed to allow for sufficient analysis of the developed model.

As the model is tested for a real case, it is preferred to use a suitable scenario. It is expected that the use of the model will be most beneficial in high populated and therefore noise sensitive areas in the vicinity of AAS. The trajectory optimization model allows for computing tailored trajectories that pave their way through the populated areas, while the allocation model will try to reduce the overall noise impact by computing the optimal distribution of flights. In chapter 3 several noise sensitive areas in the vicinity of AAS were addressed, like Hoofddorp, Aalsmeer and Amstelveen. For this case study the ARNEM departure from runway 09 is analysed. The current SID crosses high populated areas like Aalsmeer and the south east of Amsterdam. The 09 runway of AAS is known for its noisy characteristics and is therefore a suitable candidate scenario for the case study. Figure 6.1 shows the case scenario.

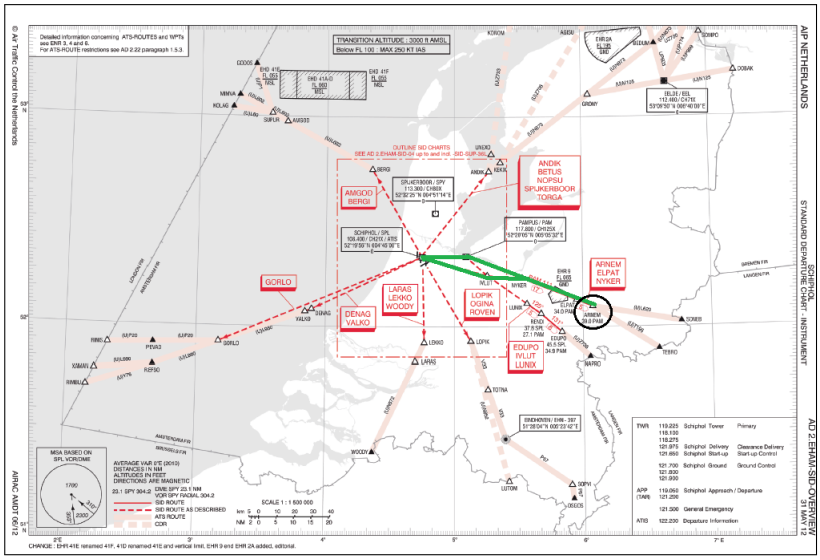

Figure 6.1: Case scenario ARNEM departure from runway 09, marked by a green color [6]

The runway departure fix combination chosen for this case study is not often used by AAS due to the fact that wind directions most of the time originate from the south west. Although this runway departure fix combination is not often used, its noisy characteristics do provide a suitable extreme for the case study. As already mentioned, the goal of the case study is to compare the use of current SID with the use of the novel tailored trajectory allocation model. Therefore, a suitable scenario like the ARNEM departure from runway 09 is preferable.

6.1.2 Model Input

In chapter 4 it was explained that take-off weight and flight profile procedure are the only two input parameters defined by the user. For the case study a specific scenario is considered. Several assumptions are made to simulate a real case scenario with the developed model. This results in some implications on the model. Below, the assumptions made are presented after which further implications on the model are explained in more detail.

Assumptions

It is important to note that several assumptions are made to simulate a real case scenario with the developed model. The most relevant assumptions are listed below.

- No wind vector present
- The B733 aircraft can be used to represent all narrow body aircraft
- The B744 aircaft model can be used to represent all wide body aircraft
- Aircraft types can be categorized by three different take-off weights
- Aircraft weight remains constant during departure flight
- Fuel flow calculations are aircraft type dependent
- Noise calculations are aircraft type dependent
- Noise evaluated area can be limited to a 40 x 21 km grid around AAS
- Flight schedule is based on actual data from AAS
- Population density is based on historical data from CBS
- Tailored trajectories are optimized between fixed initial and final coordinates
- Final coordinates of trajectory (ARNEM departure fix) are set to be 52.13854 latitude, 5.59067 longitude (Barneveld)

Flight Categories

Use is made of two aircraft models to take different aircraft types into account for this research. A B733 aircraft model is used to represent all narrow body aircraft [37]. A B744 aircraft model is used to represent all wide body aircraft from the flight schedule [38]. Each aircraft performance model is integrated separately in de trajectory optimization model and has direct impact on the aircraft's flight performance, fuel consumption and noise impact.

Furthermore, three different weight classes are considered to take different take-off weight classes into account for this researched. The different aircraft types are categorized for low, medium and heavy take-off weights respectively. Obviously, the weight classes differ per aircraft type. The different weights are quantified by calculating the maximum fuel weight (MFW) which is the difference between the maximum take off weight (MTOW) and the maximum zero fuel weight (MZFW). The low and medium weight class follow from adding $\frac{1}{3}$ and $\frac{2}{3}$ of the MFW to the MZFW. The heavy weight class equals to the MTOW. The mathematical formulation for calculating the different weight classes are given by equation 6.1. The quantified take-off weight is given as user input to the model.

$$\begin{aligned} W_L &= MZFW + \frac{1}{3}(MTOW - MZFW) \\ W_M &= MZFW + \frac{2}{3}(MTOW - MZFW) \\ W_H &= MTOW \end{aligned} \tag{6.1}$$

Considering three different weight classes for two different aircraft types eventually results in six different flight categories. The different flight categories are listed in table 6.1. For every flight category the trajectory optimization model runs two times in order to compute tailored departure trajectories for both NADP-1 and NADP-2 flight procedures.

Fuel

Fuel calculations are done according to the fuel flow equations provided by the aircraft performance models. As explained in chapter 4 the integrated fuel flow models, thrust equations and flap retraction schedules are based on the aircraft performance models as well. This allows the trajectory optimization model to compute tailored trajectories that are dependent of aircraft type. By means of the fuel flow model the total fuel consumption for a trajectory is calculated. Once the tailored trajectories of a specific flight category are selected the values for fuel are used as cost values for the allocation model.

Noise

Both the trajectory model and the allocation model optimize for noise. The impact of noise on the environment is largest in the vicinity of the airport. As the aircraft gain height, noise will reduce to a minimum and will not be considered as an issue to the surrounding communities any more. Therefore, it is not necessary to assess the total length of the trajectories on noise. Considering the current case scenario, only a limited area in the vicinity of AAS is selected to optimize the trajectories and allocation for noise. The selected area covers a large part of the area in which the optimizations are done. The area being assessed for noise is marked in figure 6.2 by a red box. Furthermore, the allocation model defines noise according to AAS standards. Therefore, the the allocation model optimizes the number of people or houses within a specified contour as explained in chapter 3.

Runway - Departure Fix Coordinates

The trajectories are optimized between fixed initial and final coordinates. The initial coordinates correspond to $\frac{2}{3}$ of the 09 Buitenveldertbaan. Final coordinates of the departure trajectory correspond to the ARNEM departure fix. Since the ARNEM departure fix is located near the German border, this will result in low noise impact for the final phase of flight. The noise impact will be too low to have any influence on the optimization. Therefore, the departure fix for the case study is replaced and set closer to AAS. The temporary departure fix is placed near the city of Barneveld, in line with the 09 runway and the original ARNEM departure. Figure 6.2 marks the points between which the tailored trajectories are computed. The blue dot marks the point of take-off, whereas the red dot marks the departure-fix for the case scenario.

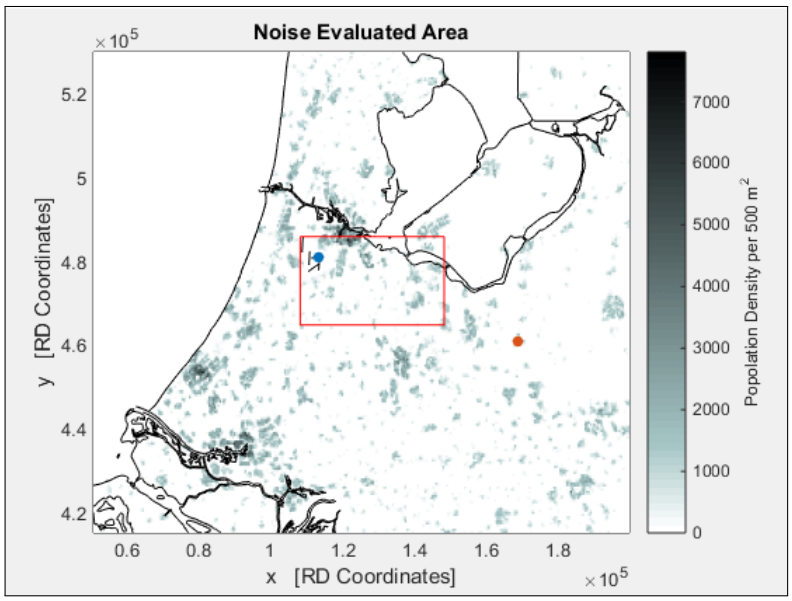

Figure 6.2: Noise evaluated area (red box), point of take-off (blue dot) and final point of tailored trajectory (red dot)

Sensitivity Analysis of the Tailored Trajectory

For this specific case study a sensitivity analysis is done on the number of ground track segments of the departure trajectories. As explained in section 4.2 of this report, a sensitivity analysis is done to assure sufficient flexibility of the ground track while optimizing for tailored trajectories. Furthermore, a B737-300 model with medium take-off weight is considered. It is assumed that this model is representable for all other flight categories as well. It should be noted that a new sensitivity analysis is required for a different case scenario because the required flexibility is dependent on the population density on the ground.

The trajectory optimization model required three runs for three different cases in order to come to a satisfying conclusion. Optimizations are done for 3 ground segments (2 decision variables),

5 segments (5 decision variables) and 7 segments (8 decision variables). Expanding the ground track from 3 to 5 segments showed significant improvements in the number of awakenings. Expanding from 5 to 7 segments did not show significant improvement in the number of awakenings. The cost range for fuel consumptions remains unchanged for all three cases. Assuming that every additional decision variable increases the complexity of the optimization problem, it is concluded that an optimal number of 5 ground segments is required for the trajectory optimization model for this specific case scenario. Results of the sensitivity analysis can be found in appendix B.

A second sensitivity analysis is done to verify the added value of optimizing the vertical profile segments. Using the same settings, the trajectory is optimized a second time with additional decision variables that define the six segments of the vertical flight profile. The outcome is compared to the results of the first sensitivity analysis that included ground track parameters only. All cases show that including the profile parameters to the decision variables of the optimization results in additional savings of 200 awakenings on average, except for the case with three ground segments. This case shows even better improvements. The cost range for fuel consumptions remains unchanged. Plots of the optimal Pareto fronts for the second sensitivity analysis are included in appendix B as well.

As a result, the additional benefit of including optimization of the six vertical profile segments is proven to be ca. 200 awakenings, which equals to additional noise savings of 5% with respect to the optimization results for ground track segments only. It is concluded that the trajectory should be optimized for 11 decision variables: 5 variables defining the ground track and 6 variables defining the vertical profile.

6.2 Reference Scenario

To quantify the potential benefit of tailored SID and profile allocation for AAS, the outcome of the model is compared to the current situation. An actual flight schedule is used and the actual departure procedures are used to simulate the current situation by means of the developed models. The current situation is simulated after which it serves as reference data for the case study. By comparing the model output with the reference data the potential benefit of tailored SID and profile allocation is quantified.

6.2.1 Departure Flight Schedule

An actual flight schedule is provided by AAS and used for this case study. The flight schedule can be found in appendix C of this report. The schedule is filtered on departure flights only. Cargo flights are left out of the schedule as well as they are excluded from the project scope. Considering the runway departure fix combination for this case study, only departure flights with destinations in eastern Europe, the middle east, Australia and Asia are included. This selection is made according to figure 3.3 in chapter 3 of this report. Subsequently, every flight that is left

on the departure schedule is represented by one of the six flight categories that were introduced in this section. Additionally, the period of the day at which the operation takes place is also taken into account.[1] An overview of the entire operation for this case study is given by table 6.1.

Table 6.1: Number of flights per flight category, based on actual flight schedule from AAS

Cat.	Day	Evening	Night
B733-L	58	19	1
B733-M	13	3	4
B733-H	4	3	1
B744-L	1	2	0
B744-M	7	0	0
B744-H	9	5	1
Flights:			**131**

6.2.2 Current SID and Flight Procedures

The current situation serves as reference data for the case study and is simulated by following actual airport procedures. The SID used to simulate current departures is provided by the AIP and already discussed in section 3.2 of this report. According to the standard departure chart that can be found in appendix D outbound flights from runway 09 towards ARNEM end up at IVLUT way point after turns at EH055 and EH042. From IVLUT the aircraft change heading towards the alternative departure fix that is set at Barneveld for this case study. In general, the NADP-1 is used for vertical take-off procedures at AAS [1].

The trajectory model is used to simulate the current situation. By following current airport procedures, the departure trajectories can be defined by four straight legs and three fixed radius turns [39]. Subsequently, the trajectory model is used to simulate the current departure trajectories. This is done by providing fixed input parameters to the model. The parameters used to simulate the current trajectories are listed in table 6.2. Lengths L and fixed radius turns R are expressed in meters, $\Delta\chi$ is expressed in degrees and γ and η are percentages. An example of the simulated B733-M trajectory in its current state is shown by figure 6.3. The departure trajectories of all flight categories that are simulated according to current airport procedures are included in appendix E.
The trajectory model calculates corresponding cost values for fuel consumption and noise impact per xy-coordinate of the assessed grid. The cost values are used to calculate total fuel consumption and noise impact for the entire operation considered during this case study when making use of current SID and profile procedures. Use is made of the Microsoft EXCEL to calculate the cost values manually. Cost for the current situation are included in table 6.3.

[1] The allocation model makes use of the L_{den} metric which assigns extra noise penalties for operations during the evening and at night (chapter 5)

Table 6.2: Fixed input parameters used to simulate current departure trajectories

L_1	R_2	χ_2	L_3	R_4	χ_4	L_5	R_6	γ_1	γ_2	γ_3	η_3	γ_4	γ_5
7000	6000	23	4000	6000	7	21000	5000	1	1	.15	.98	.5	.15

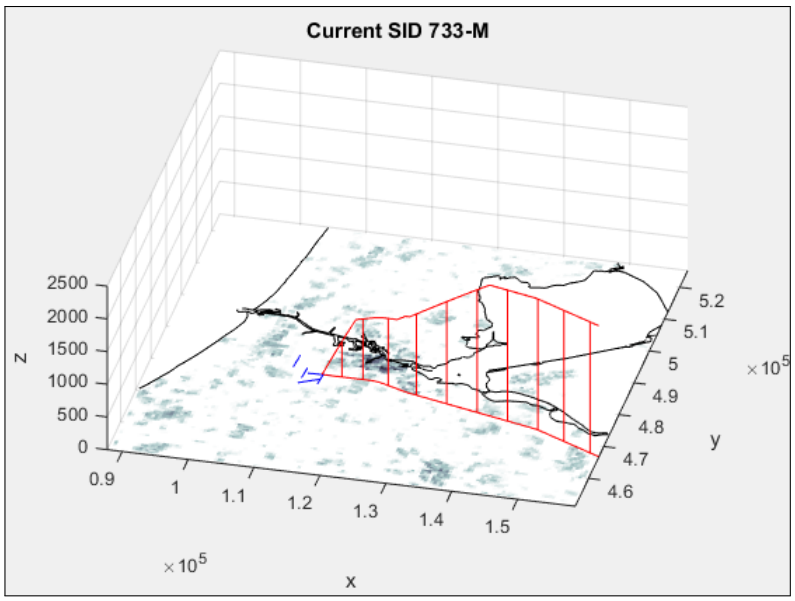

Figure 6.3: Simulated trajectory of the B733 medium take-off weight class

Table 6.3: Cost values for the reference scenario

Noise Limit [dB]	**Noise**	**Fuel [kg]**
58 L_{den}	5213 houses	118686
48 L_{den}	110700 people	118686
48 L_{night}	9013 houses	5954
40 L_{night}	110850 people	5954

6.3 Results

In this section the results of the case study are presented. First, a set of tailored trajectories is generated. The results of the trajectory optimization model and the final selection for the allocation model are discussed in the first subsection. Secondly, the selected trajectories are used by the allocation model to determine an optimal distribution of flights for fuel and noise. The second subsection elaborates on the outcome of the allocation model. Finally, results are compared to the reference scenario in the third subsection.

6.3.1 Trajectory Model

B733 Trajectories

Several simulation are done to compute tailored trajectories for the B737-300. The trajectory model optimized for three different take-off weight classes for two different flight procedures. For each flight category and flight procedure an optimal Pareto front is computed. After applying the selection method discussed in section 4.4 three tailored trajectories per flight category and profile procedure are chosen. An example of the optimal Pareto front for a B733 light take-off weight flying an NADP-2 procedure is given by figure 6.4. The selected trajectories corresponding to this Pareto front are shown in figure 6.5. The Pareto fronts and selected tailored trajectories of other weight classes and profile procedures of the B733 model can be found in appendix F.

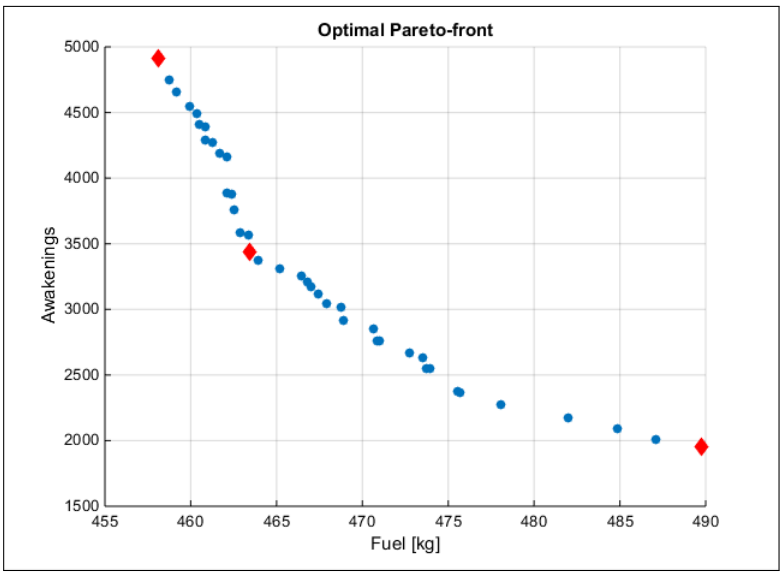

Figure 6.4: Optimal Pareto front solutions for the B733 light take-off weight class NADP-2 procedure. Selected solutions are indicated by red diamonds.

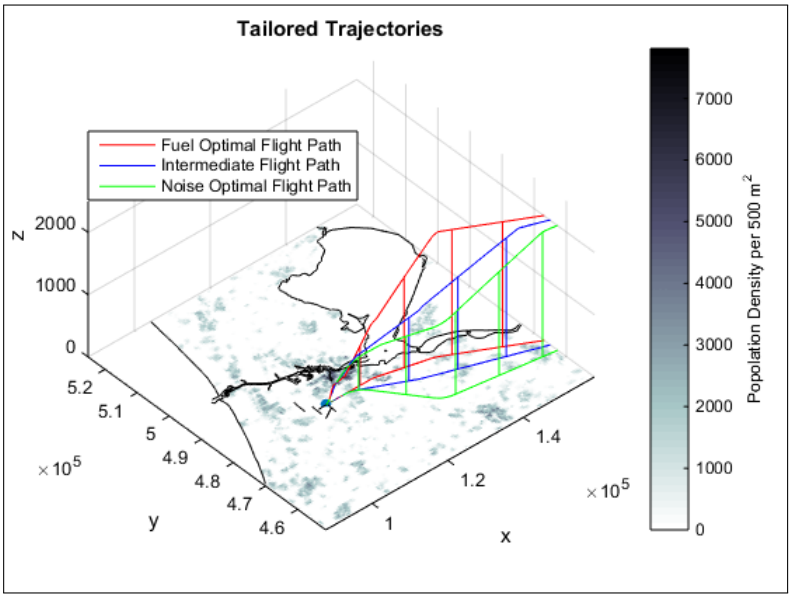

Figure 6.5: Selected tailored trajectories for the B733 light take-off weight class NADP-2 procedure.

The cost values of the selected trajectories for the different weight classes of the B733 are included in tables 6.4, 6.5 and 6.6 respectively.

Table 6.4: Cost values for selected tailored trajectories of a B737-300 light take-off weight class

	NADP-1		NADP-2	
Trajectory	**Fuel [kg]**	**Awakenings**	**Fuel [kg]**	**Awakenings**
Fuel Optimal	477,5	5665	458,1	4915
Intermediate	502,5	3065	463,42	3440
Noise Optimal	662,5	2351	489,74	1951

Table 6.5: Cost values for selected tailored trajectories of a B737-300 medium take-off weight class

	NADP-1		NADP-2	
Trajectory	**Fuel [kg]**	**Awakenings**	**Fuel [kg]**	**Awakenings**
Fuel Optimal	501,89	4367	475,84	5583
Intermediate	512,69	3652	483,9	2507
Noise Optimal	561,05	3161	503,08	1941

Table 6.6: Cost values for selected tailored trajectories of a B737-300 heavy take-off weight class

	NADP-1		NADP-2	
Trajectory	**Fuel [kg]**	**Awakenings**	**Fuel [kg]**	**Awakenings**
Fuel Optimal	541,67	6067	518,29	5529
Intermediate	548,94	4195	540,8	3031
Noise Optimal	576,51	3179	564,21	2449

B744 Trajectories

Several simulation are done to compute tailored trajectories for the B747-400. The trajectory model optimized for three different take-off weight classes for two different flight procedures. For each flight category and flight procedure an optimal Pareto front is computed. After applying the selection method discussed in section 4.4 three tailored trajectories per flight category and profile procedure are chosen. An example of the optimal Pareto front for a B744 light take-off weight flying the NADP-2 procedure is given by figure 6.6. The selected trajectories corresponding to this Pareto front are shown in figure 6.7. The Pareto fronts and selected tailored trajectories of other weight classes and profile procedures of the B744 model can be found in appendix F.

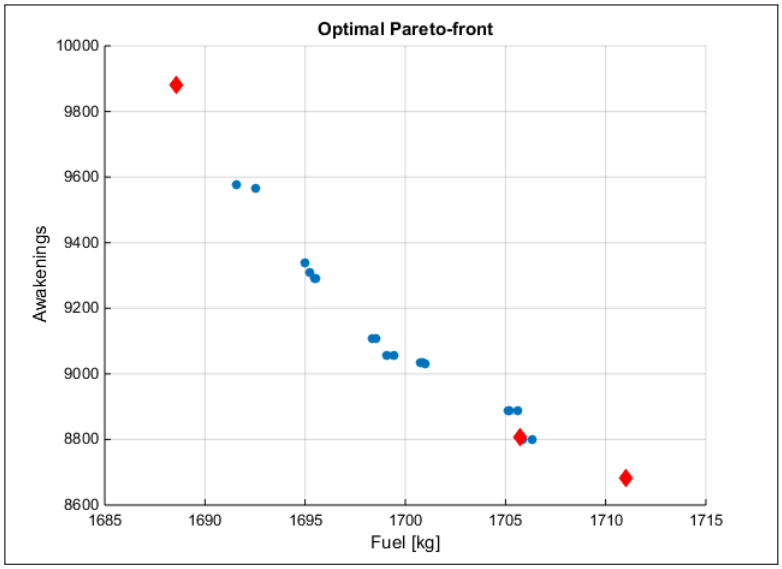

Figure 6.6: Optimal Pareto front solutions for the B744 light take-off weight class NADP-2 procedure. Selected solutions are indicated by red diamonds.

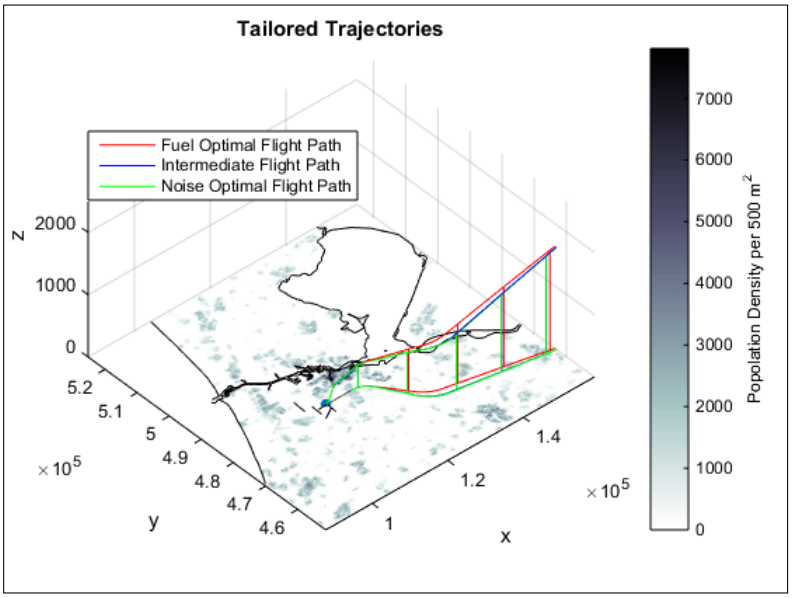

Figure 6.7: Selected tailored trajectories for the B744 light take-off weight class NADP-2 procedure.

The cost values of the selected trajectories for the different weight classes of the B747-400 are included in tables 6.7, 6.8 and 6.9 respectively.

Table 6.7: Cost values for selected tailored trajectories of a B747-400 light take-off weight class

	NADP-1		NADP-2	
Trajectory	**Fuel [kg]**	**Awakenings**	**Fuel [kg]**	**Awakenings**
Fuel Optimal	1864,33	10286	1688,56	9881
Intermediate	1941,96	8732	1705,7	8806
Noise Optimal	2120,01	7670	1711,01	8681

Table 6.8: Cost values for selected tailored trajectories of a B747-400 medium take-off weight class

	NADP-1		NADP-2	
Trajectory	**Fuel [kg]**	**Awakenings**	**Fuel [kg]**	**Awakenings**
Fuel Optimal	2297,67	12828	2138,75	12640
Intermediate	2487,22	11978	2154,04	12276
Noise Optimal	2525,09	11694	2561,24	11998

Table 6.9: Cost values for selected tailored trajectories of a B747-400 heavy take-off weight class

	NADP-1		NADP-2	
Trajectory	**Fuel [kg]**	**Awakenings**	**Fuel [kg]**	**Awakenings**
Fuel Optimal	2777,17	12164	2585,49	16763
Intermediate	2861,3	10463	2586,34	16220
Noise Optimal	3130,34	9782	2871,91	16138

Final Set of Tailored Trajectories

The results for the B733 aircraft show clear differences between the tailored trajectories of a specific flight category. For fuel optimal trajectories the optimization model computes trajectories that follow short routes towards the final departure-fix. Furthermore, these trajectories show large flight path angles of the optimized profile segments. For noise optimal trajectories the optimization model computes trajectories that avoid high populated areas as much as possible. Furthermore, these trajectories show smaller flight path angles of the optimized profile segments. The intermediate trajectories show characteristics that lie in between these two outliers. Looking at the cost values of different tailored trajectories, it becomes clear that for every take-off weight class of the B733 the NADP-2 procedures score better than the NADP-1 procedures. For every NADP-1 trajectory there is an NADP-2 trajectory available with better fuel and noise characteristics. Since the goal of this research is to quantify the potential benefit of this method for fuel and noise, it would not be beneficial for the outcome of the model to included trajectories with higher fuel and noise characteristics. For this reason, and to limit the input data of the trajectory allocation model, it is decided to eliminate all NADP-1 results for B733 aircraft from the final set of tailored trajectories.

The results for the B744 aircraft show less differences between the tailored trajectories of a specific flight category. After multiple runs for each flight category and profile procedure the three selected tailored trajectories show only minor differences in the ground track. The difference in fuel and noise characteristics mainly results from different flight path angles of the optimized profile segments. A possible explanation for this is that the trajectory optimization model converges to local optima. This problem is also experienced during the sensitivity analysis on the ground track segments of the B733 aircraft. The optimization model tends to converge to a local optimum when the number of decision variables is too low. Therefore, an additional sensitivity analysis for the B744 aircraft trajectory segments might possibly lead to an increased number of decision variables that define the ground track and allow the trajectory model to generate tailored trajectories that show more variety in ground track and vertical profile. Another reason for this behaviour could be the aircraft characteristics. In general, the B744 is known to be a bad climber and to show deviating behaviour with respect to other aircraft types when it comes to trajectory optimization studies. For now, the current results are used for the continuing process of this work. The B744 sensitivity analysis is included as a recommendation for future research in the final chapter of this report.

Looking at the fuel and noise characteristics of different tailored trajectories of the B744 flight categories, it becomes clear that only three trajectories score bad on both fuel and noise characteristics with respect to the other tailored trajectories. Therefore, it is decided to include both the NADP-1 and the NADP-2 results in the final set of tailored trajectories. This results in a final set of tailored trajectories with the following characteristics:

- For all B733 flight categories it holds that the allocation model has three options to assign the particular flight to
- For all B744 flight categories it holds that the allocation model has six options to assign the particular flight to

An overview of the final set of tailored trajectories is included in table F.1 in appendix F of this report.

6.3.2 Allocation Model

The allocation model uses the final set of tailored trajectories to compute the optimal allocation of flights for fuel, noise and different trade-off's between the two objectives. In doing this, the model evaluates four different criteria. These criteria are currently used by AAS and already discussed in chapter 3. Below, the results for all four criteria are discussed.

Criteria 1: 58 dB L_{den}

The first criteria involves the number of houses experiencing noise of 58 dB L_{den}. After determining the normalization factors for a noise limit of 58 dB L_{den} the optimal allocation for fuel and noise is computed by the model. Figure 6.8 shows the optimal allocation of flights for minimizing fuel consumptions. The bar plots give an overview of the allocation of flights per flight category and time of the day. The green bars mark NADP-1 procedures and the blue bars mark NADP-2 procedures. The difference between fuel efficient and noise efficient trajectories is indicated by a difference in contrast. It follows that all flights are allocated to the most fuel efficient trajectories. For all flight categories this is the NADP-2 trajectory optimized for fuel. Figure 6.9 shows the grid points that fall inside the noise contour as a result of optimizing the allocation for fuel.

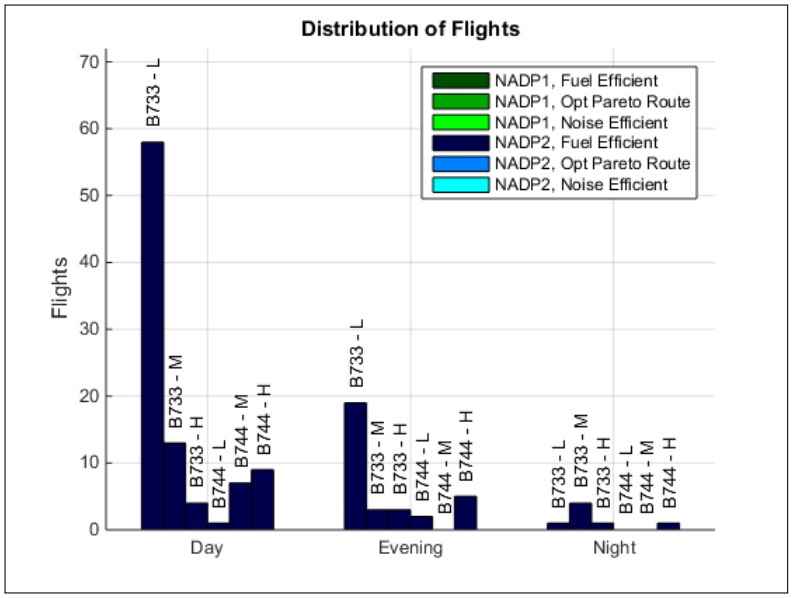

Figure 6.8: Allocation of flights when optimizing for fuel consumptions

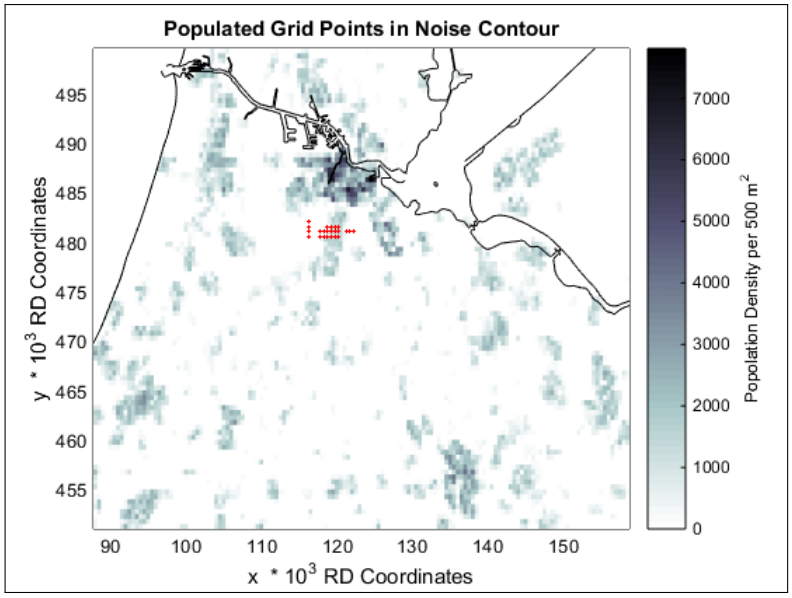

Figure 6.9: Grid points within the noise contour when optimizing for fuel

The potential benefit of the allocation when optimizing for fuel is quantified by comparing results with the reference scenario. This is shown by figure 6.10. It follows that an optimal allocation of the flight schedule results in maximum fuel savings of 8.8% with corresponding noise savings of -1.5%. Therefore, the results show that optimizing for fuel comes at the cost of producing more noise.

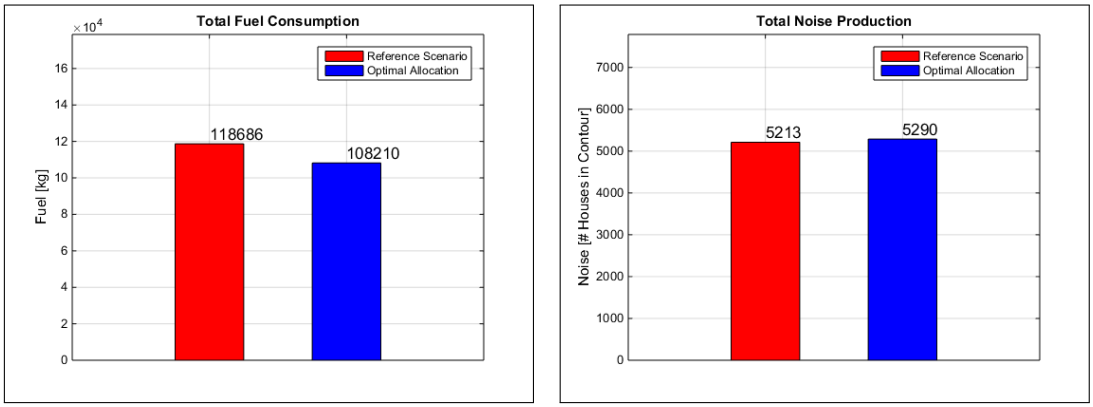

(a) Potential fuel savings of 8,8% **(b)** Corresponding noise savings of -1,5%

Figure 6.10: Potential benefit for criteria 1 when optimizing for fuel

Optimizing for noise leads to a different allocation of flights with different noise contours. Figure 6.11 shows the optimal allocation of flights. It follows that the flights are distributed over the trajectories that are available in order to keep noise to a minimum. Unlike the optimal allocation for fuel, not all flights are assigned to the most noise efficient trajectories. The corresponding grid points that fall inside the noise contour when minimizing for noise are shown by figure 6.12. Although the noise contour seems to reach further compared to the fuel optimal contour, it finds its way through less populated areas. In this way high populated grid points are exchanged for grid points with a low population density resulting in less noise for this criteria.

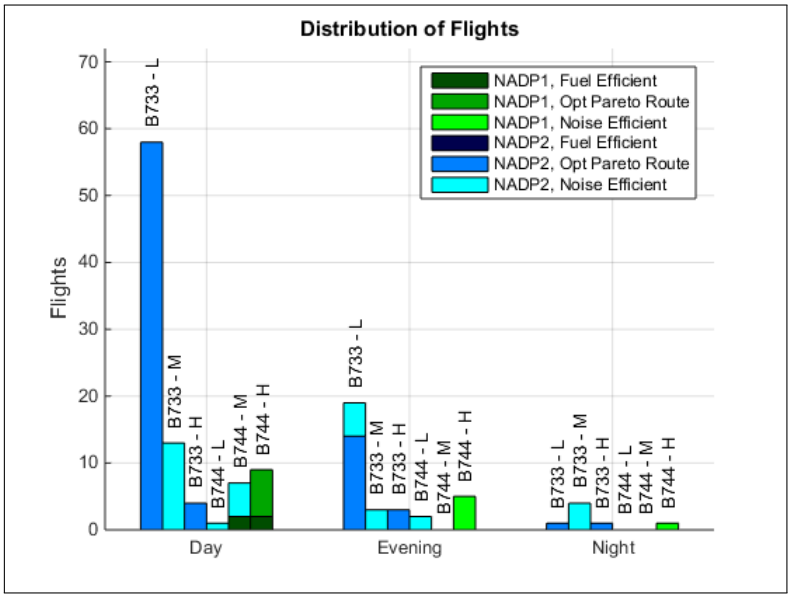

Figure 6.11: Allocation of flights when optimizing for noise

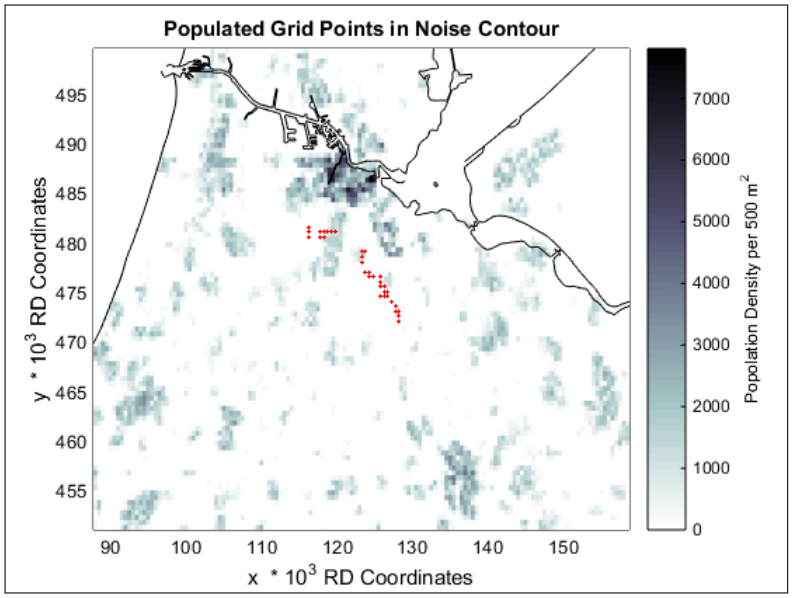

Figure 6.12: Grid points within the noise contour when optimizing for noise

The potential benefit of the allocation when optimizing for noise is quantified by comparing results with the reference scenario. This is shown by figure 6.13. It follows that an optimal allocation of the flight schedule results in maximum noise savings of 44.25% with corresponding fuel savings of 0.97%. Therefore, the results show that optimizing for noise comes with minimal savings for fuel as well.

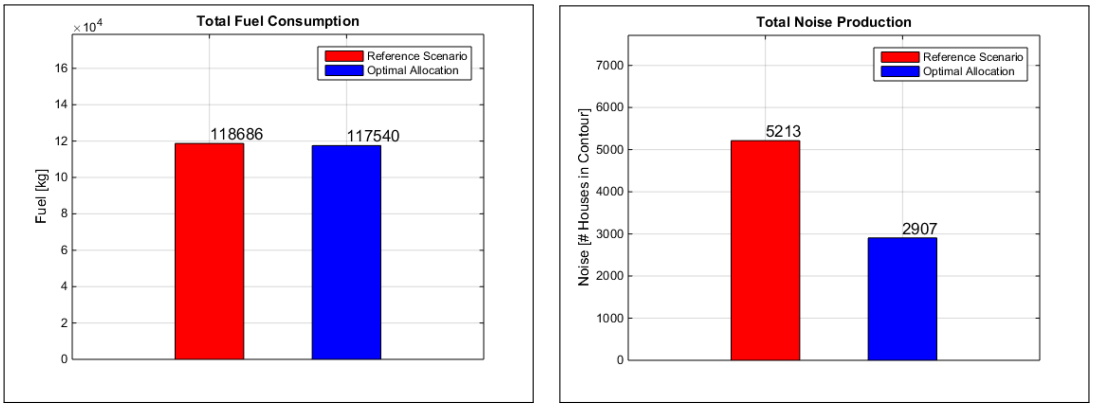

(a) Corresponding fuel savings of 0,97%

(b) Potential noise savings of 44,25%

Figure 6.13: Potential benefit for criteria 1 when optimizing for noise

Finally, different values for α are applied to the allocation model to vary the weightings on each objective. This allows for a trade-off between the two objectives. The resulting Pareto front with different optimal solutions is presented in figure 6.14. The values for α are selected by means of an iterative process. In this way, only the values for α that show a different allocation of flights

with respect to the other values for α are included in the Pareto front.

The reference scenario is indicated in red. In this way, all solutions are compared to the reference scenario. All solutions that lie above the horizontal dashed line and left of the reference scenario show potential savings for fuel only. All solutions that lie right of the vertical dashed line and below the reference scenario show potential savings for noise only. All solutions that lie in between the dashed lines show potential savings for both fuel and noise and are considered to be optimal solutions with respect to the reference scenario. An overview of the Pareto front solutions that are included in figure 6.14 is given by table 6.10. The results show that beneficial savings can be achieved for both objectives when $0 \leq \alpha \leq 0.9$.

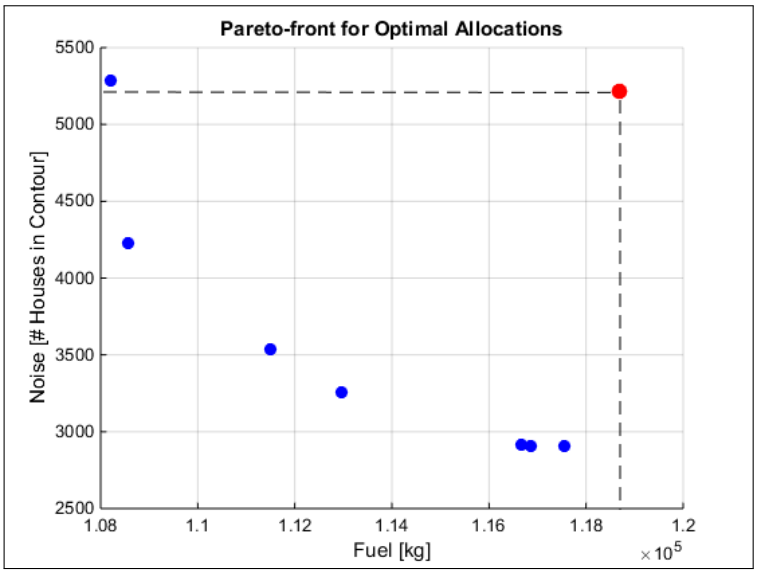

Figure 6.14: Optimal Pareto front solutions of the allocation model for different values of alpha

Table 6.10: Potential savings for Criteria 1 when applying different values of alpha

	Fuel [kg]	**Savings**	**Noise [Houses]**	**Savings**
Ref. Scenario	118686,47	0%	5213	0%
α				
1	108210	8.8%	5290	-1.5%
0.9	108560	8.5%	4230	18.9%
0.5	111490	6.1%	3540	32.1%
0.4	112970	4.8%	3253	37.6%
0.3	116670	1.7%	2917	44.1%
0.2	116860	1.5%	2910	44.2%
0	117540	0.97%	2907	44.3%

Criteria 2: 48 dB L_{den}

The second criteria involves the number of people seriously affected by noise of 48 dB L_{den} or more. It should be noted that the allocation model optimizes for the number of people living within the noise contour and not for the number of people that are seriously affected. After determining the normalization factors for a noise limit of 48 dB L_{den} the optimal allocation for fuel and noise is computed by the model. Optimizing the optimal allocation for fuel results in the fact that all flights are allocated to the most fuel efficient trajectories. Therefore the optimal allocation of flights is the same as for criteria 1, as shown by figure 6.8. Figure 6.15 shows the corresponding grid points that fall inside a noise contour of 48 dB L_{den}.

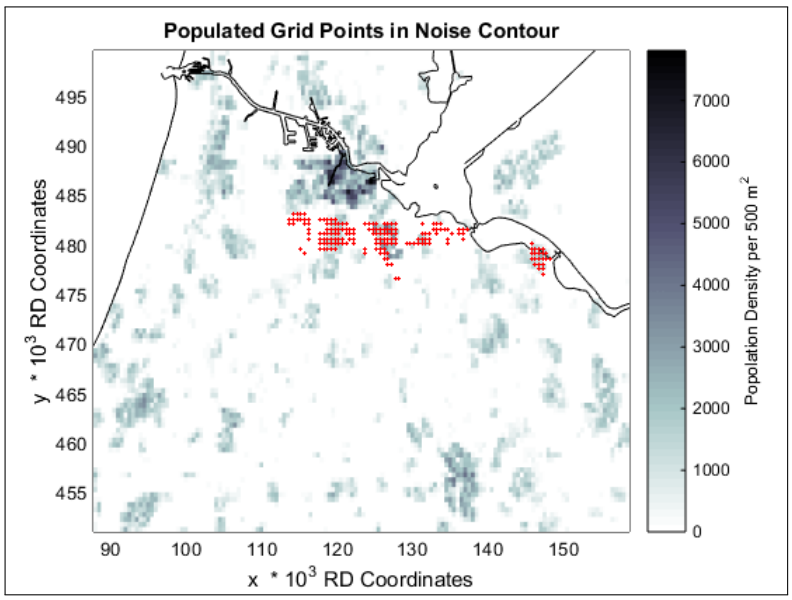

Figure 6.15: Grid points within the noise contour when optimizing for fuel

The potential benefit when optimizing for fuel is shown by figure 6.16. It follows that an optimal allocation of the flight schedule results in maximum fuel savings of 8.8% with corresponding noise savings of -35.7%. Therefore, the results show that optimizing for fuel comes at the cost of producing more noise.

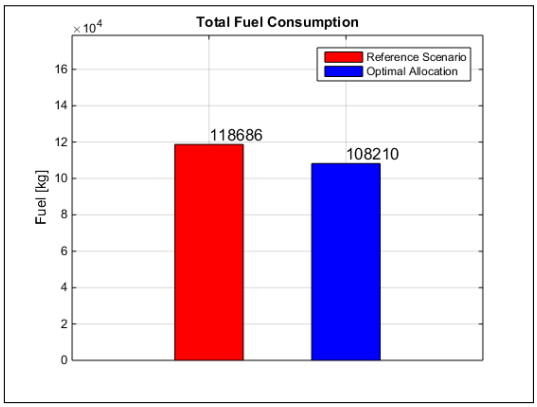

(a) Potential fuel savings of 8,8%

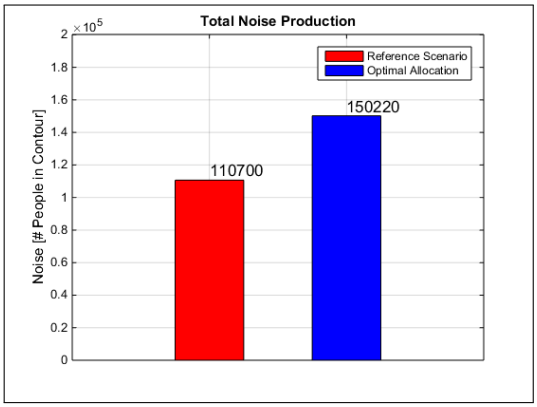

(b) Corresponding noise savings of -35.7%

Figure 6.16: Potential benefit for criteria 2 when optimizing for fuel

Optimizing for noise leads to a different allocation of flights with different noise contours. Figure 6.17 shows the optimal allocation of flights. It follows that the flights are distributed over the trajectories that are available in order to keep noise to a minimum. The results show similar behaviour as for criteria 1. The corresponding grid points that fall inside a noise contour of 48 dB L_{den} when minimizing for noise are shown by figure 6.18. Just like for criteria 1, high populated areas are avoided to minimize the number of people living within the noise contour.

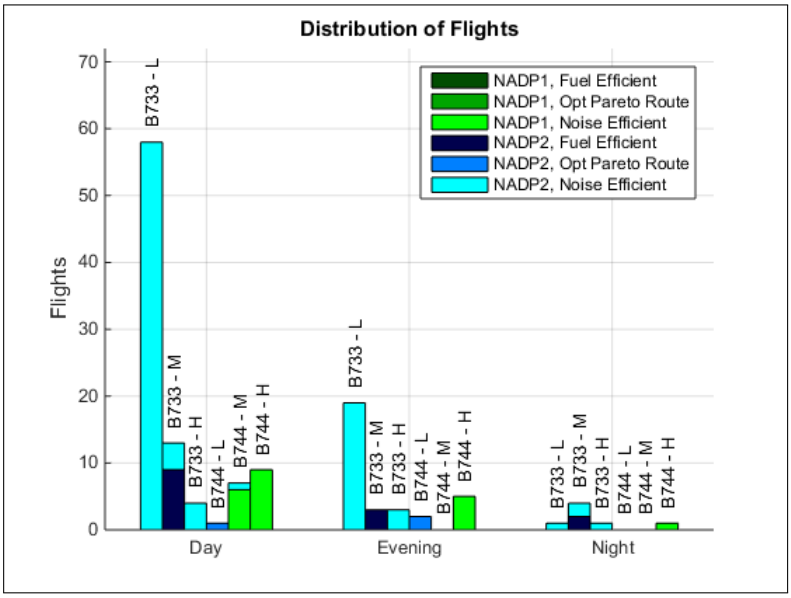

Figure 6.17: Allocation of flights when optimizing for noise

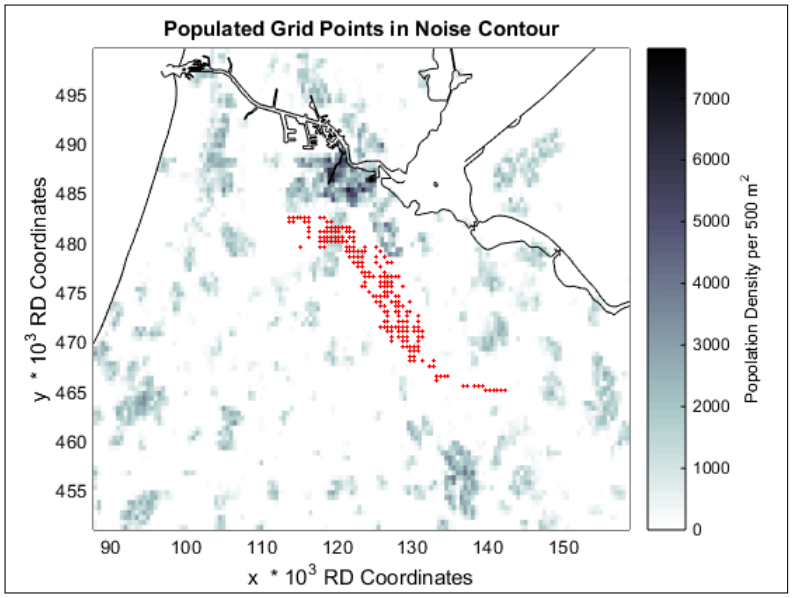

Figure 6.18: Grid points within the noise contour when optimizing for noise

The potential benefit when optimizing for noise is shown by figure 6.19. It follows that an optimal allocation of the flight schedule results in maximum noise savings of 48.8% with corresponding fuel savings of -2.9%. Therefore, the results show that optimizing for noise comes at the cost of higher fuel consumptions.

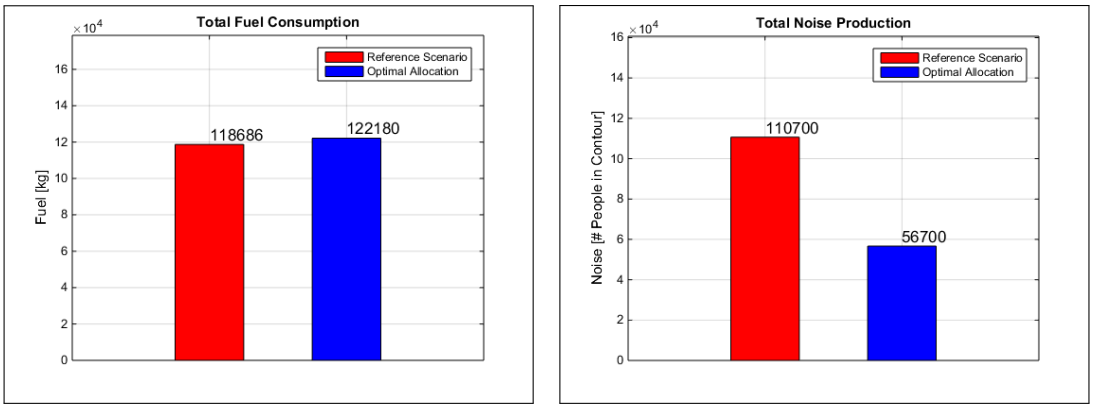

(a) Corresponding fuel savings of -2.9%

(b) Potential noise savings of 48.8%

Figure 6.19: Potential benefit for criteria 2 when optimizing for noise

Finally, different values for α are applied to the allocation model to vary the weightings on each objective. The resulting Pareto front with different optimal solutions is presented in figure 6.20. All solutions that lie in between the dashed lines show potential savings for both fuel and noise, and are considered to be optimal solutions with respect to the reference scenario. An overview

of the Pareto front solutions that are included in figure 6.20 is given by table 6.11. The results show that beneficial savings can be achieved for both objectives when $0.01 \leq \alpha \leq 0.66$.

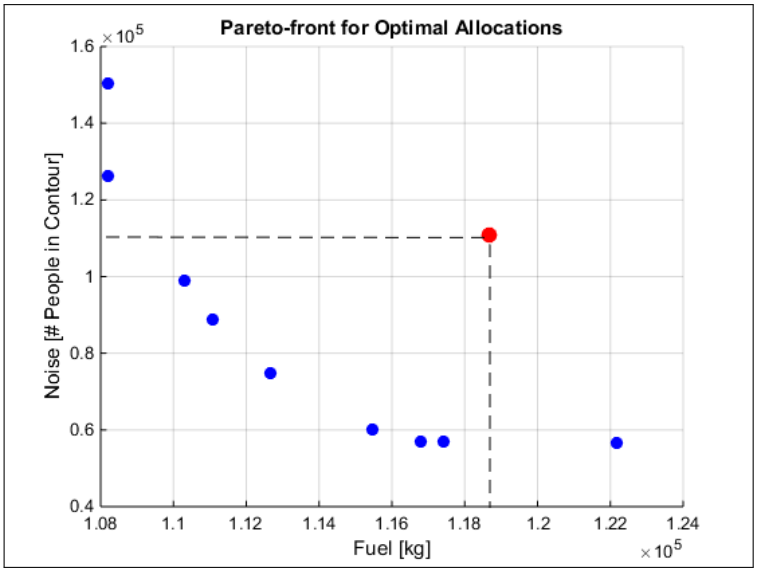

Figure 6.20: Optimal Pareto front solutions of the allocation model for different values of alpha

Table 6.11: Potential savings for Criteria 2 when applying different values of alpha

	Fuel [kg]	**Savings**	**Noise [People]**	**Savings**
Ref. Scenario	118686,47	0%	110700	0%
α				
1	108210	8.8%	150220	-35.7%
0.9	108220	8.8%	126090	-13.9%
0.66	110300	7.1%	99000	10.6%
0.6	111080	6.4%	88970	19.6%
0.5	112660	5.1%	74780	32.5%
0.4	115460	2.7%	60120	45.7%
0.2	116810	1.6%	57050	48.5%
0.01	117420	1.1%	56930	48.6%
0	122180	-2.9%	56700	48.8%

Criteria 3: 48 dB L_{night}

The third criteria involves the number of houses experiencing noise of 48 dB L_{night}. In order to evaluate this criteria only night flights are taken into account. Furthermore, the reference time period T_0 is set to 25200 seconds to account for L_{night} only. The penalties for different periods of the day are not necessary since only night flights are being considered. After determining the normalization factors for a noise limit of 48 dB L_{night} the optimal allocation for fuel and noise is computed by the model. Optimizing the optimal allocation for fuel results in an allocation to the most fuel efficient trajectories for all flights. Therefore the optimal allocation of flights is the same as for criteria 1 and 2, as shown by figure 6.8. Figure 6.21 shows the corresponding grid points that fall inside a noise contour of 48 dB L_{night}.

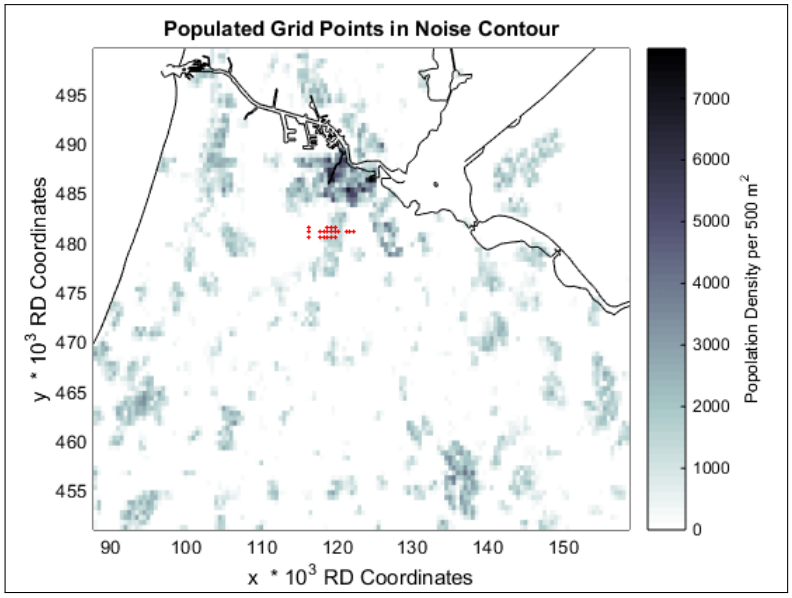

Figure 6.21: Grid points within the noise contour when optimizing for fuel

The potential benefit when optimizing for fuel is shown by figure 6.22. It follows that an optimal allocation of the flight schedule results in maximum fuel savings of 8.2% with corresponding noise savings of 53.3%. Therefore, the results show that optimizing for fuel leads to potential savings for noise as well.

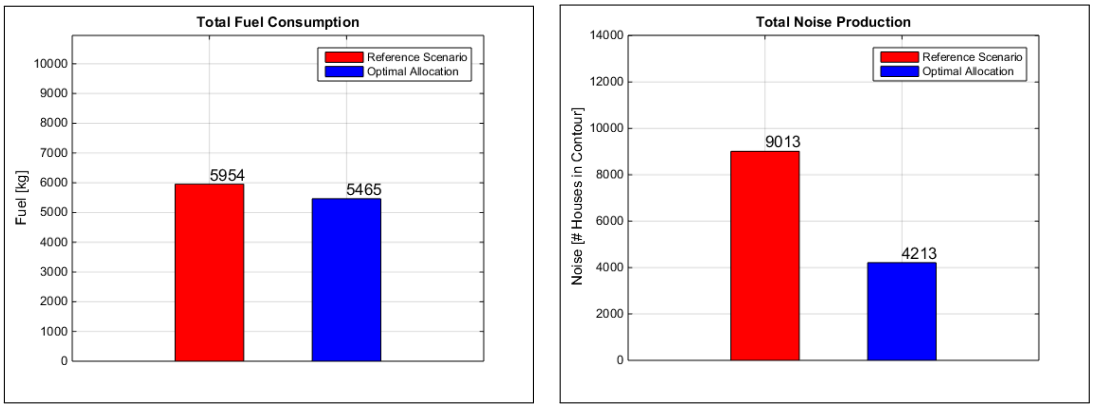

(a) Potential fuel savings of 8,2%

(b) Corresponding noise savings of 53.3%

Figure 6.22: Potential benefit for criteria 3 when optimizing for fuel

Optimizing for noise leads to a different allocation of flights with different noise contours. Figure 6.23 shows the optimal allocation of flights. The results show similar behaviour as for criteria 1 and 2. It follows that the flights are distributed over the trajectories that are available in order to keep noise to a minimum. The corresponding grid points that fall inside a noise contour of 48 dB L_{night} when optimizing for noise are shown by figure 6.24. Just like for criteria 1 and 2, high populated areas are avoided in order to minimize the number of people living within the noise contour.

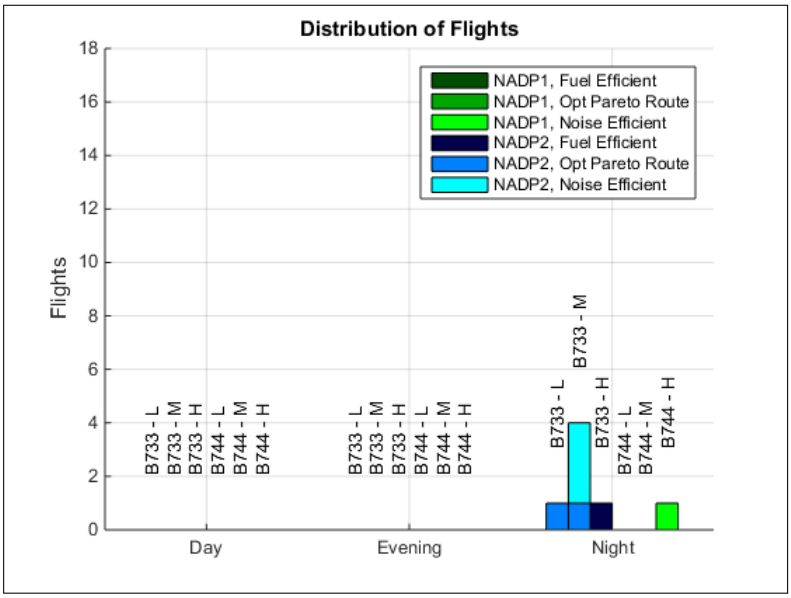

Figure 6.23: Allocation of flights when optimizing for noise

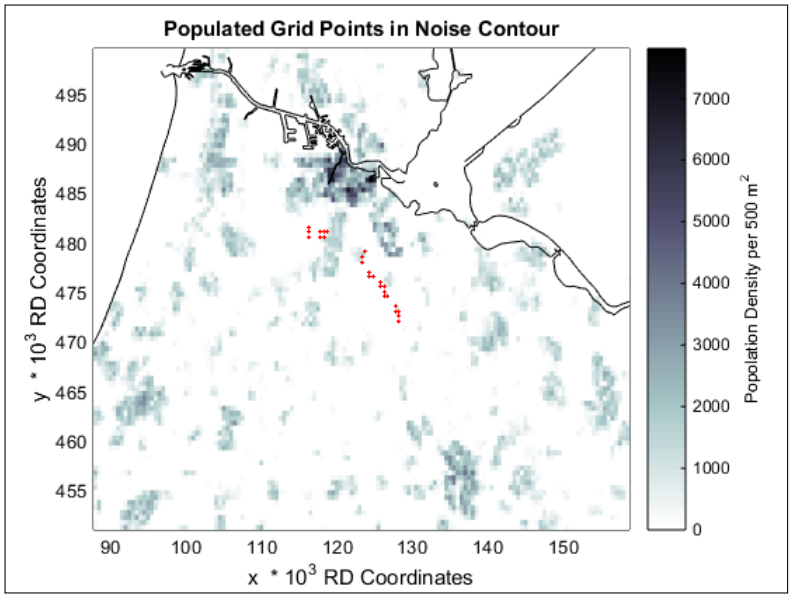

Figure 6.24: Grid points within the noise contour when optimizing for noise

The potential benefit when optimizing for noise is shown by figure 6.25. It follows that an optimal allocation of the flight schedule results in maximum noise savings of 78.8% with corresponding fuel savings of -2.5%. Therefore, the results show that optimizing for noise comes at the cost of higher fuel consumptions.

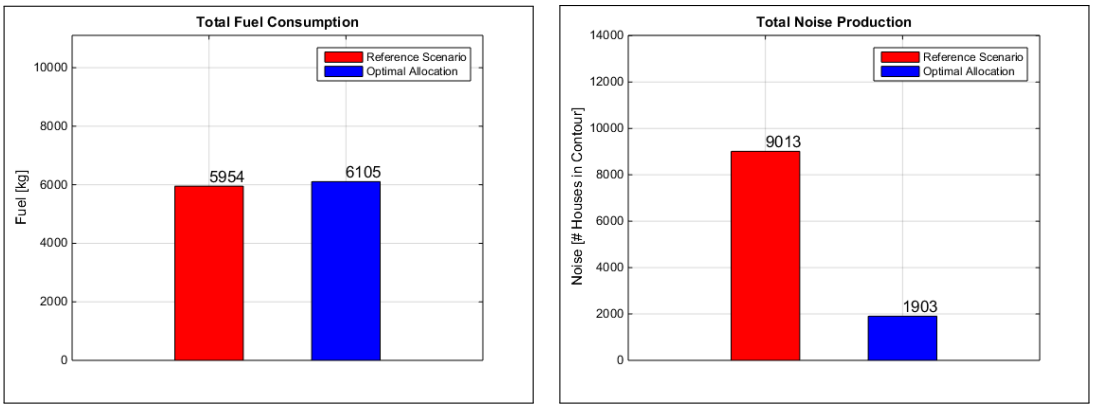

(a) Corresponding fuel savings of -2.5%

(b) Potential noise savings of 78.8%

Figure 6.25: Potential benefit for criteria 3 when optimizing for noise

Finally, different values for α are applied to the allocation model to vary the weightings on each objective. The resulting Pareto front with different optimal solutions is presented in figure 6.26. All solutions that lie in between the dashed lines show potential savings for both fuel and noise and are considered to be optimal solutions with respect to the reference scenario. An overview

of the Pareto front solutions that are included in figure 6.26 is given by table 6.12. The results show that beneficial savings can be achieved for both objectives when $0.13 < \alpha \leq 1$.

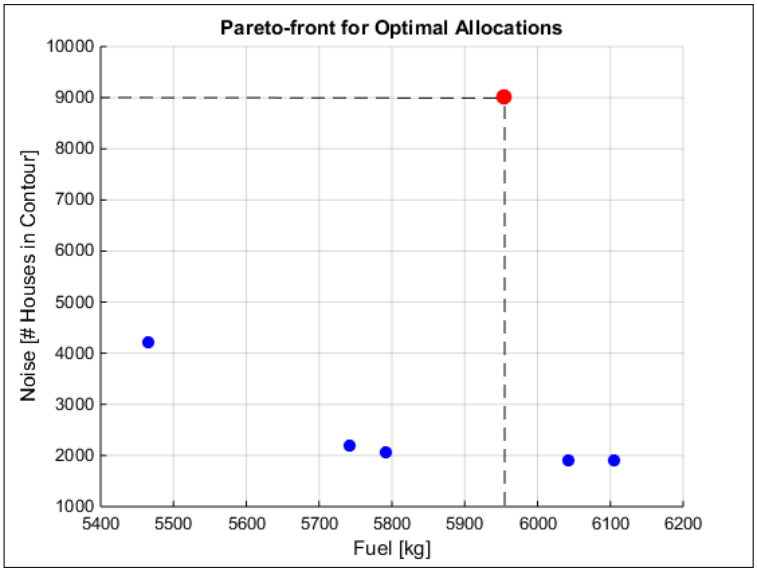

Figure 6.26: Optimal Pareto front solutions of the allocation model for different values of alpha

Table 6.12: Potential savings for Criteria 3 when applying different values of alpha

	Fuel [kg]	**Savings**	**Noise [Houses]**	**Savings**
Ref. Scenario	5954,23	0%	9013	0%
α				
1	5465	8.21%	4213	53.3%
0.6	5741	3.6%	2203	75.6%
0.4	5793	2.7%	2050	77.3%
0.13	6042	-1.5%	1903	78.8%
0	6102	-2.5%	1903	78.8%

Criteria 4: 40 dB L_{night}

The fourth criteria involves the number of awakenings because of noise of 40 dB L_{night} or more. It should be noted that the allocation model optimizes for the number of people living within the noise contour. In order to evaluate this criteria only night flights are taken into account. Furthermore, the same settings as for criteria 3 are used. After determining the normalization factors for a noise limit of 40 dB L_{night} the optimal allocation for fuel and noise is computed by the model. Optimizing the optimal allocation for fuel results in assigning all flights to the most fuel efficient trajectories. Therefore, the optimal allocation of flights is the same as for the other evaluated criteria, as shown by figure 6.8. Figure 6.27 shows the corresponding grid points that fall inside a noise contour of 40 dB L_{night}.

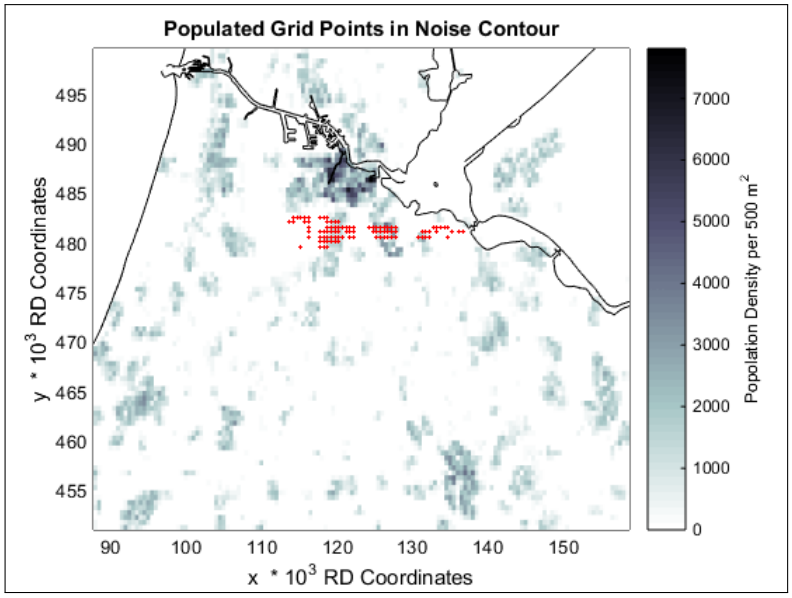

Figure 6.27: Grid points within the noise contour when optimizing for fuel

The potential benefit when optimizing for fuel is shown by figure 6.28. It follows that an optimal allocation of the flight schedule results in maximum fuel savings of 8.2% with corresponding noise savings of 29.5%. Therefore, the results show that optimizing for fuel leads to potential savings for noise as well.

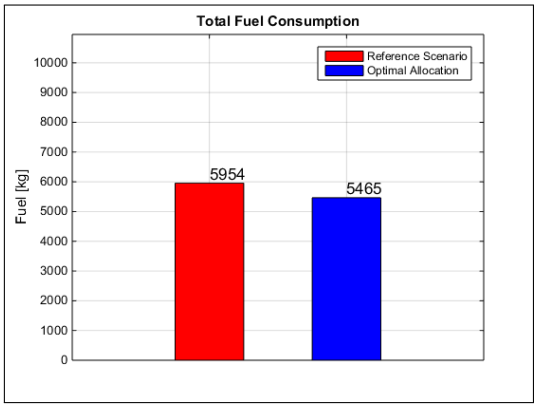

(a) Potential fuel savings of 8,2%

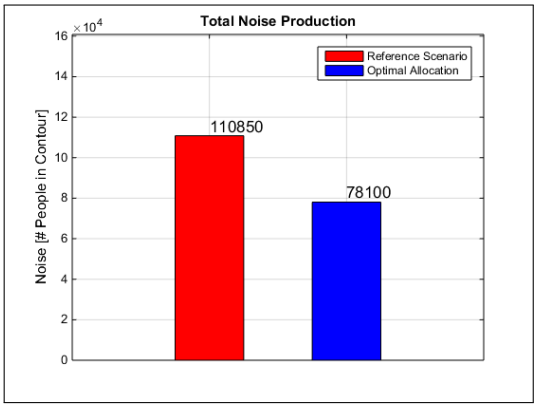

(b) Corresponding noise savings of 29.5%

Figure 6.28: Potential benefit for criteria 4 when optimizing for fuel

Optimizing for noise leads to a different allocation of flights with different noise contours. Figure 6.29 shows the optimal allocation of flights. The results show similar behaviour as for the other evaluated criteria. It follows that the flights are distributed over the trajectories that are available in order to keep noise to a minimum. The corresponding grid points that fall inside a noise contour of 40 dB L_{night} when optimizing for noise are shown by figure 6.30. Just like for the other evaluated criteria, high populated areas are avoided to minimize the number of people living within the noise contour.

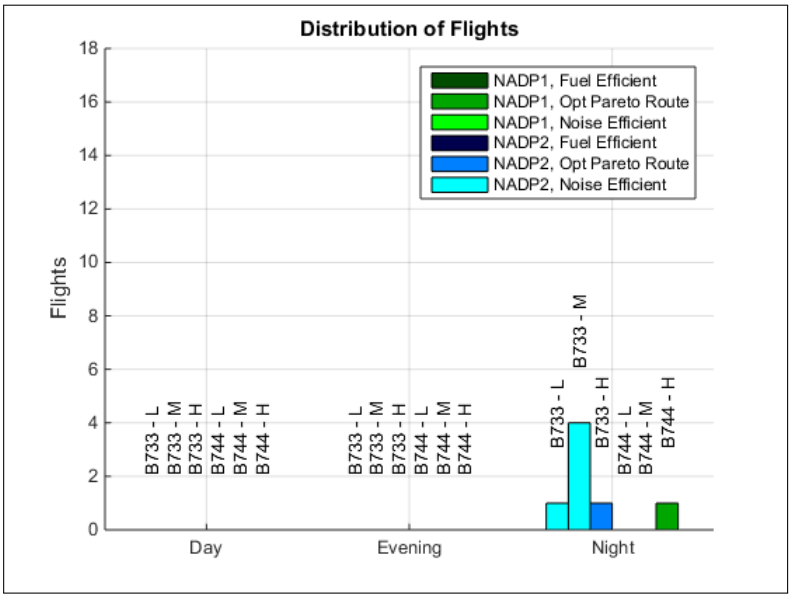

Figure 6.29: Allocation of flights when optimizing for noise

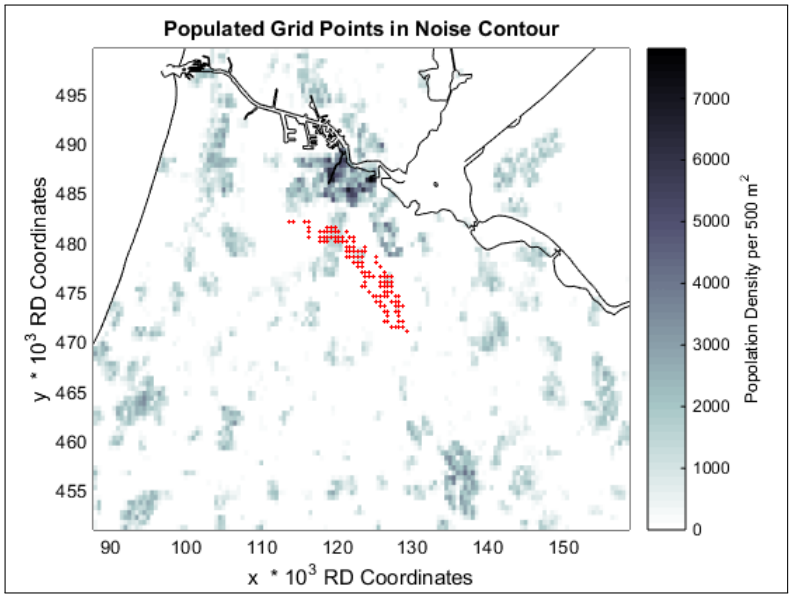

Figure 6.30: Grid points within the noise contour when optimizing for noise

The potential benefit when optimizing for noise is shown by figure 6.31. It follows that an optimal allocation of the flight schedule results in maximum noise savings of 64.9% with corresponding fuel savings of 0.84%. Therefore, the results show that optimizing for noise results in minor savings for fuel consumptions as well.

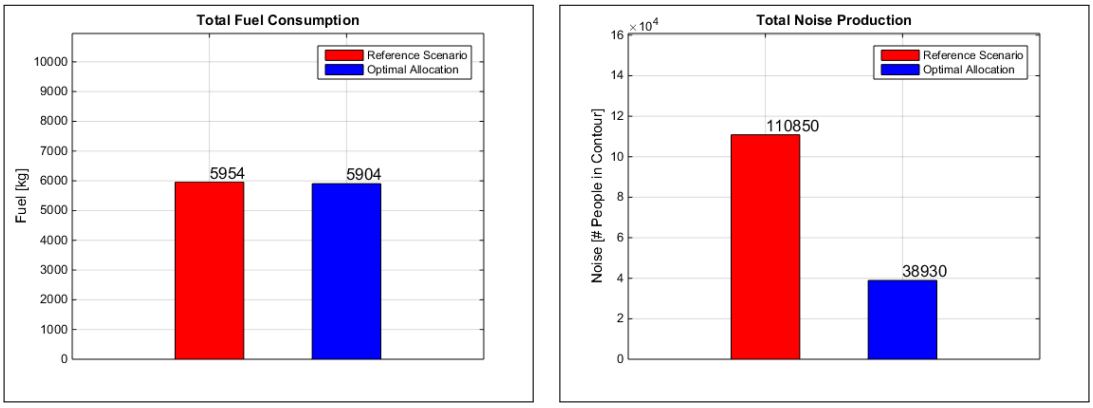

(a) Corresponding fuel savings of 0.84%

(b) Potential noise savings of 64.9%

Figure 6.31: Potential benefit for criteria 4 when optimizing for noise

Finally, different values for α are applied to the allocation model to vary the weightings on each objective. The resulting Pareto front with different optimal solutions is presented in figure 6.32. All solutions in between the dashed lines show potential savings for both fuel and noise, and are considered to be optimal solutions with respect to the reference scenario. An overview of the Pareto front solutions that are included in figure 6.32 is given by table 6.13. The results show

that beneficial savings can be achieved for all values of α.

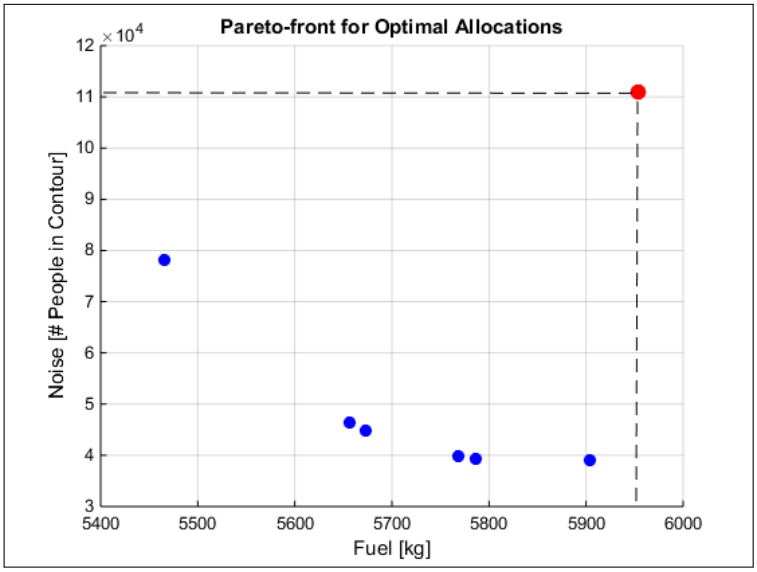

Figure 6.32: Optimal Pareto front solutions of the allocation model for different values of alpha

Table 6.13: Potential savings for Criteria 4 when applying different values of alpha

	Fuel [kg]	**Savings**	**Noise [People]**	**Savings**
Ref. Scenario	5954,23	0%	110850	0%
α				
1	5465	8.2%	78100	29.5%
0.6	5657	5%	46510	58%
0.4	5673	4.7%	44810	59.6%
0.3	5768	3.1%	39730	64.2%
0.1	5787	2.8%	39210	64.6%
0	5904	0.8%	38930	64.9%

6.3.3 Case Study Results

Combining the outcome of the allocation model for all four criteria leads to the final result of this case study. Looking at the optimal Pareto fronts of all four criteria it can be observed that the allocation model provides satisfying results for both fuel and noise criteria for a specific range in values of α. Combining the lower and upper bounds of all criteria results in a final optimum range for α, as shown by equation 6.2. It holds that positive results are achieved for all four criteria when applying values for α that are within the optimal range.

$$\alpha_{lb} \leq \alpha \leq \alpha_{ub} \qquad \text{, where} \quad \begin{aligned} \alpha_{lb} &= 0.14 \\ \alpha_{ub} &= 0.66 \end{aligned} \tag{6.2}$$

The optimal range for α has its effect on each criteria. The potential benefit of tailored SID and profile allocations that can be achieved by means of this method is now limited due to the lower and upper bound of the optimal range. An overview of maximum savings per evaluated criteria as a result of the optimal range for α is provided by table 6.14.

Table 6.14: Maximum savings on fuel and noise as a result of the optimal range for α

	Max Savings	
Criteria	**Fuel:** $\alpha = .66$	**Noise:** $\alpha = .14$
1	6.1%	44.2%
2	7.1%	48.5%
3	3.6%	78.8%
4	5%	64.2%

Looking at the final results the question rises why the trajectories developed by the model are not used in real practice when the potential benefit of tailored SID and profile allocation has proven to be so significantly high, especially for noise.

First of all, it should be noted that part of the extreme outcome can be declared by the behaviour of the allocation model. In order to compute the optimal allocation of flights the model will try to keep as much grid points as possible just below the noise limit. Therefore, at some point, other trajectories than the most noise efficient trajectories are selected by the model as well. It is likely that some of the grid points reach cumulative noise levels that are very close, but just below the opposed noise limits. Therefore, according to the model the corresponding population remains outside the noise contour although in real practice the experienced noise levels are almost similar as the opposed noise limits.

Secondly, it should be noted that the case scenario is chosen because its noisy characteristics provide a suitable extreme for the case study. Furthermore, the B744 aircraft model is used to represent all wide body aircraft, which is dominant in terms of noise. Subsequently, the reference data is simulated by assuming that all flights follow the same SID crossing areas with high population densities. Compared to the tailored SID, which are optimized for noise, it is likely that

the extreme results for noise can partly be declared by the extreme scenario that is evaluated for this case study.

Nevertheless, the potential benefit of tailored SID and profile allocation is still proven to be significantly high. When trying to answer the question why tailored trajectories are not yet used in real practice, one enters a political discussion with many stakeholders involved. It requires a lot of effort to find compromises between the different stakeholders in order to change the current state of airport operations at AAS. All stakeholders have their own interests. It often comes down to the fact that economical interest is given priority. Unless the outcome of scientific research is expected to realize economical growth and guarantee that main stakeholders can profit directly, it is less likely that those stakeholders will invest in the implementation of novel technologies like tailored SID and profile allocation. Although, for this research it seems to be the case that many stakeholders would benefit from the developed trajectories, it might still not be the right time for implementation in order to gain full profit of the potential that tailored departure trajectories have for AAS.

7

Verification and Validation

In the process of doing this research two models are developed to investigate the potential benefit of tailored SID and profile allocation. In this chapter the verification and validation of the models is discussed. Section 7.1 explains what methods are used to verify the models. Subsequently, the validation of the models is discussed in section 7.2.

7.1 Verification

By means of verification it is checked whether the predefined design requirements are met and if the model shows desired behaviour. Verification of the model is done by checking the individual building blocks of each model separately. For the trajectory optimization model this means that the trajectory simulation block and noise impact model are checked on desired behaviour before applying the multi-objective optimization algorithm. The behaviour and outcome of the trajectory model is checked for different input parameters, consisting of a variety in aircraft type, take-off weight and flight profile procedures. Subsequently, the optimization algorithm is applied. The outcome of the trajectory optimization model is checked on sufficient variety between the trajectory parameters of different optimal solutions.

The same strategy is applied to the trajectory allocation model. Individual blocks of the allocation model are verified separately. Expected outcomes for noise and fuel are calculated manually and compared to the results of the model. Additionally, a concept case is performed to test the behaviour of the two models combined. The concept case is performed in order to test the working principle of the overall model and decide whether developed method is sufficient in achieving the overall research objective of the MSc. thesis research. For the concept case two tailored trajectories are developed. One noise optimal trajectory that avoids a centralized population

area and one fuel optimal trajectory that crosses the centralized population area. Subsequently, the allocation model computed the optimal allocation of flights for one aircraft type with fixed take-off weight. In this way, the main objectives and requirements of the model are verified. Details of the concept case can be found in appendix G of this report.

Finally, an extra verification is done by means of the case study discussed in chapter 6. Just like with the concept case, the case study provides another possibility to check whether the predefined design requirements are met and if the model shows desired behaviour. By comparing the case study results to the reference data, it is verified whether the developed model leads to positive results for this research. In this way, it is verified if the main objective of the developed model is achieved.

7.2 Validation

By means of validation it is verified whether outcomes of the model correspond to actual data. Validation is done to check if the model generates realistic results. This gives an indication of the feasibility of the developed model. In order to validate the allocation model noise levels are compared with measurements of an official measurement system of AAS. This are the 'handhavingspunten' around AAS. By means of the 'handhavingspunten' actual noise levels as a result of the aircraft movements are measured to give an indication of the actual noise impact on the environment [40]. Since a specific scenario is considered for the case study, only a limited number of 'handhavingspunten' is selected for the validation. From the 35 measurment points only five (points 19-23) are located in the vicinity of the Buitenveldert runway and on track of the 09 departure trajectory. The exact location of all 'handhavingspunten' can be found in appendix H together with a table that includes the noise limit values and actual measured noise values corresponding to each 'handhavingspunt'.

In table 7.1 actual data of the selected 'handhavingspunten' is compared to the outcome of the model. The table shows that results are within a reasonable range from the actual data. Positive results are found for points 19 and 22 where the outcome of the model shows noise levels that are lower than the actual data. For the other three locations the simulated noise levels exceed the reference data. This deviation can be declared due to the fact that the noise values from the 'handhavingspunten' are based on average yearly movements. On the other hand, the model takes a specific scenario into account for a 24 hours day only. Assuming that other days can compensate for current results, outliers are allowed as long as they stay within a reasonable range from the reference data. Furthermore, all wide body aircraft are represented by a B744 model, which is one of the noisiest and worst climbers of the entire fleet operating at AAS. This can be the cause of higher noise levels measured at locations close to the departure track.

The validation method of the 'handhavingspunten' proved to be not completely satisfying. The fact that result are based on a different scenario with respect to the reference data results in

Table 7.1: Validation of noise levels in the vicinity of runway 09

Location	**Limit** [L_{den}]	**Measured Value** [L_{den}]	**Simulated Value** [L_{den}]
19	54.57	53.54	51.05
20	59.56	59.29	63.17
21	58.39	56.92	60.34
22	58.32	55.41	53.14
23	57.72	56.16	62.10

some deviation which is assumed to be declarable. Another way to validate model outcome is by validation of the trajectory optimization model. Realistic values of the single tailored trajectories should result in realistic outcome of the allocation model as well. Fuel values of the trajectory model are checked with BADA and compared to results of other optimization studies evaluating the same aircraft types [4] [12]. The same strategy is used to validate noise levels of the trajectory optimization model. Validation of the single tailored trajectories is done for both aircraft types individually. Knowledge of experts in the field of trajectory optimization is used as an extra validation measure.

Additionally, several experts in the field of noise and climate effects or trajectory optimization have been consulted to discuss the results of the model. Their advice contributed to the validation of the model and achieve improvements on the model outcome. Among these experts were people from the ATO section of the aerospace faculty in Delft and people from Schiphol Group.

8

Conclusions & Recommendations

This research investigates the potential benefit of tailored SID and profile allocation. The main driver for this research is to achieve significant noise reduction and fuel savings for AAS. Where research on tailored arrivals already lead to the practical implementation of CDA's, the potential benefit of tailored departures has been left relatively undiscovered. An optimal allocation of tailored aircraft departures potentially decreases the number of people annoyed by noise and result in fuel savings for the airlines. The research is executed after formulating the following research objective statement:

Quantify the potential benefit of tailored SID and profile allocation for Amsterdam Airport Schiphol by developing a model that is capable of simulating departure trajectories per runway departure fix and optimize the overall allocation of departing aircraft for noise and fuel consumption.

For this purpose two models are developed after which results have been compared with results of a simulated real case scenario from AAS. In this chapter the conclusions of the research are presented. Subsequently, the main limitations of the model are discussed. This allows to think of any improvements to be made for further development of the models and formulate recommendations for future research on this topic. This chapter will start with presenting the conclusions in section 8.1. In section 8.2 the main limitations of the model are discussed. Finally, recommendations for future research are done in section 8.3.

8.1 Conclusions

The most important conclusion for this research is that the potential benefit of tailored SID and profile allocation can now be quantified by means of the proposed method. This method includes

the development of two optimization models. The first model is capable of simulating tailored departure trajectories dependent on aircraft type and take-off weight. By running the model for different combinations of aircraft type and take-off weight a final set of tailored trajectories is generated, which serve as input for the second model. The second model is capable of computing the optimal allocation of flights to the tailored trajectories and calculate corresponding cost for fuel and noise.

A second important conclusion is that the potential benefit of tailored SID and profile allocation has proven to be significant for both fuel consumption and noise abatement purposes. The concept of tailored SID and profile allocation is tested by applying the models to a real case scenario and evaluate the results for four different noise criteria. It should be noted that the outcomes of this research correspond to the initial phase of departure flights only. This includes the moment of take-off until a specified departure fix is reached. According to the hypothesis stated in chapter 3 of this report a potential benefit of 5% fuel savings with respect to current departure operations was expected. The case study results showed potential fuel savings that range from 3.6% to 7.1%, as shown by table 8.1. For three of the four noise criteria the case study results either confirmed or exceed expectations that were done in the hypothesis. It can be concluded that the potential benefit of tailored SID and profile allocation for fuel consumptions exceeds expectations and is therefore considered to be a positive outcome of this research.

According to the hypothesis done in chapter 3 of this report a potential benefit of 10% noise savings with respect to current departure operations was expected. The case study results showed potential noise savings that range from 44.2% to 78.8%, as shown by table 8.1. For all four noise criteria the case study results exceed expectations that were done in the hypothesis and are rather extreme. The main reason for this is that the B744 aircraft model is used to represent all wide body aircraft, which is dominant in terms of noise. Furthermore, the reference case scenario is simulated by assuming that all flights follow one fixed SID and profile which crosses areas with high population densities compared to the tailored SID, which are optimized for noise. In combination with the fact that a noise dominant aircraft type is used for the case study, it is assumed that this causes the extreme results for noise.

Table 8.1: Maximum savings on fuel and noise as a result of the optimal range for α

	Max Savings	
Criteria	**Fuel:** $\alpha = .66$	**Noise:** $\alpha = .14$
1	6.1%	44.2%
2	7.1%	48.5%
3	3.6%	78.8%
4	5%	64.2%

A second reason is the fact that noise contours of the current situation are simulated and located in populated areas, whereas the allocation model tries to relocate noise contours to less populated

areas. The latter will be explained in more detail later on in this section. Nevertheless, it is expected that for a wider range of aircraft types, the case study will still show positive results for noise but to a lesser extend. It should be noted that a noise sensitive area in combination with a noise dominant aircraft has been used for the case study. It is assumed that this has its effect on the extreme outcome of noise abatement results. Overall, it can be concluded that the potential benefit of tailored SID and profile allocation for noise exceeds expectations and is therefore considered to be a positive outcome of this research.

Now that the main conclusions are discussed, several conclusions with respect to the process of aircraft trajectory modelling can be made. The tailored trajectories are developed by performing a multi objective optimization of a single event for different flight categories. Firstly, it can be concluded that noise optimal trajectories come at the cost of fuel and vice versa. This is confirmed by the outcome of the trajectory optimization model. Results of the multi objective genetic optimization algorithm are presented by means of optimal Pareto fronts which illustrates the trade-off to be made between two objectives. Looking at the results for the B733 aircraft model it can be concluded that fuel optimal routes follow the shortest route towards the departure fix and use a NADP-2 profile procedure. Noise optimal routes tend to avoid populated areas and use a NADP-2 procedure as well.

Furthermore, it can be concluded that the number of ground track segments requires an additional sensitivity analysis per aircraft type taken into account for the case study. The sensitivity analysis is performed to determine the number of ground track segments required for satisfying results of the trajectory optimization model. For the case study a sensitivity analysis is done for the B733 only. Subsequently, the same number of ground segments is used for the development of the B744 tailored trajectories. Final results for the B744 trajectories tend to originate from a local optimum in the optimization problem. This follows from the fact that the different tailored trajectories show only minor differences in ground track parameters.

To conclude this section, several conclusions with respect to the allocation model are discussed as well. The allocation model computes the optimal allocation for a cumulative set of events with respect to noise, fuel or a trade-off between these two objectives. It can be concluded that when optimizing the allocation for fuel all flights are assigned to the most fuel efficient trajectories available for the specific flight categories from the assessed flight schedule.

When optimizing the overall allocation for noise it can be concluded that flights from the assessed flight schedule are distributed over the different tailored trajectories available. It follows that not all flights are assigned to the most noise efficient trajectories available. The reason for this is that, when optimizing for noise, the model allocates flights to a tailored trajectory until the noise limit at the corresponding grid points is almost reached. In order to optimize for noise other alternative trajectories are considered as well before cumulative noise levels of the corresponding grid points pass the threshold. Secondly, when the noise contour increases as a

result of additional departures, the model assigns the flights in such a way that the grid points with the lowest population densities are included in the noise contour.

This results in the fact that the possibility exists that part of the flights is assigned to trajectories other than the most noise efficient trajectories. It is important to realize that optimization of single events is not necessarily determined for optimization of cumulative events. Although it is unlikely that the allocation model will assign flights to the B733 trajectories with a NADP-1 flight procedure, it can be concluded that it might have been premature to ignore them for the allocation problem.

8.2 Limitations

In this section several limitations of the model are discussed. It is important to be aware of the model's limitations. This allows to formulate clear recommendations for future research on the topic of tailored SID and profile allocation, which will be discussed in the next section. In this section the main limitations of the overall research, the trajectory optimization model and the allocation model are discussed separately.

The Main Research

The current outcome of the model is limited to a specific case scenario and only considers one runway departure fix combination. Applying the model to other scenario's would require some adjustments to the trajectory model in terms of geometric calculations of the departure trajectory. Scaling up the problem is expected to be time consuming.

The model outcome is not directly feasible for practical use. In order to investigate the practical feasibility of tailored SID and profile allocation the basic concept should be expanded first and include all possible runway departure fix combinations of AAS.

It should be noted that this method does not take the practical burden of living within the noise contour into account. Once a specific point falls inside the contour the model tends to allocate flights to trajectories crossing this point because it already falls inside the noise contour. In this way, the model avoids that other grid points fall inside the contour as well. Relating this to real life it might be concluded that it is unfair to leave people with an increased flight intensity while they already experience significant noise levels.

On the other hand, the model will try to keep as much grid points as possible just below the noise limit. Therefore, at some point, other trajectories than the most noise efficient trajectories are selected by the model as well. It is likely that some of the grid points reach cumulative noise levels that are very close, but just below the opposed noise limits. Therefore, according to the model the corresponding population remains outside the noise contour although in real practice

the experienced noise levels are almost similar as the opposed noise limits.

Trajectory Model

Currently, one of the main limitations of the trajectory model involves the fact that many steps need to be executed manually. The main steps are listed below.

- Changing input parameters for aircraft type, take-off weight and departure profile.
- Adjust take-off speed, V_2 and flap setting retraction schedule as a result of different flight category.
- After running the optimization, the derivative method is used to make a selection of optimal solutions that are candidate solutions for the third tailored trajectory. The final selection of this third point is done manually.

Furthermore, final results for noise levels seem to be higher than expected. This can have several causes. First of all, it should be noted that the low diversity between the B744 ground tracks has large impact on the noise contours of the allocation model. Furthermore, it is generally known that the B744 is a bad climber. Only 50% of the wide body aircraft from the departure schedule is actually a B744. The other 50% consists of other wide body aircraft types that are presented by this noise dominant B744. This probably causes higher noise levels with respect to actual noise data.

Expanding the number of aircraft types will be time consuming. The number of parameters required to assure enough flexibility of the ground track might differ with respect to other aircraft types. It is likely that a new sensitivity analysis is required for every single aircraft type added to the fleet when scaling up the number of aircraft types.

Allocation Model

It is not possible to optimize for the dose-response relations due to their non-linear characteristics. Currently, optimizations for noise are based on the number of people or houses per grid point.

Secondly, normalization factors need to be determined for every individual criteria evaluated by the allocation model.

8.3 Recommendations

After discussing the limitations of this research, this section provides any suggestions for further improvements of the developed model. Secondly, recommendations for future research on the topic of tailored trajectory and profile allocation are done. The recommendations are discussed below.

First of all, most potential can be found in scaling up the research case. The proposed method of this research proved to be a valid way of quantifying the potential benefit of tailored SID and profile allocation for an individual case scenario. Scaling up the research would allow to evaluate the potential benefit for yearly operations at AAS. Since it is expected that this process will be rather time consuming the following step by step approach is recommended:

- First, apply the model to other departure fixes. This allows for assessing a full departure schedule since all five departure fixes are taken into account. It should be noted that in this case it is still assumed that all flights depart from the 09 runway.
- Secondly, expand the number of aircraft types. This will positively influence the case study since flights from the actual flight schedule can be represented by the right combination of aircraft type and take-off weights. Just like for this research, this can be done by integrating aircraft performance models of other aircraft types into the trajectory optimization model. Another way to expand the number of aircraft types is by considering several sub classes. Aircraft types that show similar performance characteristics can make use of already generated tailored trajectories. This makes trajectory optimization unnecessary and only requires to calculate the cost coefficients for fuel and noise of the different sub classes.
- Thirdly, take an extra runway into account and combine this with all five departure fix combinations. In this way a real case scenario can be simulated with respect to runway configuration which allows to evaluate peak and off-peak hours.
- Finally, it is desirable to take all runway departure fix combinations into account. This would allow for evaluating different airport runway configuration scenario's and challenge the current preference list.

In case future research results in clear insights to the potential benefit of tailored SID and profile allocation for AAS as a whole, new opportunities arise. Positive results could be combined with research into optimal allocation of aircraft arrivals. This would allow for investigating the potential benefit of runway allocation for AAS taking both tailored arrivals and tailored departures into account.

The main requirement for applying the allocation model to other runway configuration scenario's is the availability of data on tailored trajectories. This is experienced to be the main challenge and most time consuming process of the research. Future research on this topic not only includes application of the trajectory model to other airport scenario's, but also involves expanding the number of aircraft types taken into account. In order to keep future projects within realistic time bounds, one should look for efficient ways to generate the required data on tailored trajectories. In order to do so, several suggestions are done below:

- The use of already existing trajectory optimization models is highly recommended. The models should be able to optimize trajectories for different aircraft types and take-off weights. In order to use the data for the allocation model it is important that the outcome

of these models include cost values for fuel and noise values (SEL) per grid point of the to be evaluated grid.

- Tailored trajectories can be defined by doing reasonable assumptions, based on data files from programmes like BADA, INM, etc. By making use of aircraft grouping, thrust-to-weight ratio's reasonable assumptions can be made as well.
- As a final option, it would be possible to simply assume departure trajectories and use a program like INM to calculate the noise impact per grid point. The downside of this approach, is that the term 'tailored' is not applicable any more since the potential benefit of a specific aircraft type take off weight combination is not incorporated by a trajectory model.

Looking at the developed trajectory optimization model several suggestions can be done for further improvement of the model. Currently, many steps need to be executed manually in order to generate a set of tailored trajectories for one specific flight category. It is recommended to investigate the possibilities to make the current process more efficient. For instance, this could be done by adding a post-processor to the trajectory model. By means of the post-processor the process of selecting the final solutions from the optimal Pareto-front could be optimized.

Furthermore, an additional study could be carried out on how many tailored trajectories actually are necessary to significantly improve noise abatement. For this study only three trajectories were selected per flight category. The result showed that for a noise optimal allocation the model tends to divide flights over multiple trajectories in order to keep the noise contour to a minimum. A sensitivity analysis on the number of tailored trajectories required would say something about the limits of this research.

Looking at the developed allocation model several suggestions can be done for further improvement of the model. The current model optimizes for the number of people or houses within the noise contour. It evaluates whether the cumulative noise level of a grid point is below or above the threshold and therefore, if the corresponding population falls within or outside the noise contour. After optimization the cumulative noise level per grid point is known. This allows for calculating the dose-response relations per grid point after the optimization is done and display the values in the Pareto front. In this way, the model outcomes can be compared to the real noise criteria of AAS. It should be noted that for this case study the model still optimizes for the number of people within a certain noise contour and not for the number of people seriously hindered!

Bibliography

[1] Schiphol Group. Gebruiksprognose Amsterdam Airport Schiphol 2015. Technical report, 2014.

[2] Schipol Group. Annual Report 2011. Technical report, 2011.

[3] International Civil Aviation Organization (ICAO). Procedures for Air Navigation Services - Aircraft Operations (PANS - OPS). Technical Report fifth edition, 2006.

[4] S. Hartjes and H.G. Visser. Efficient trajectory parameterization for environmental optimization of departure flight paths using a genetic algorithm. *Journal of Aerospace Engineering*, Part G, 2016.

[5] S.A. de Araujo, K.C. Poldi, and J. Smith. A Genetic Algorithm for the One-Dimensional Cutting Stock Problem With Setups. *Pesquisa Operacional*, 34(2), 2014.

[6] Air Traffic Control The Netherlands (LvNL). Integrated Aeronautical Information Package Netherlands (AIP), 2015.

[7] R. White. World Airport Traffic Report 2014, 2015.

[8] International Air Transport Association (IATA). Economic performance of the airline industry. Technical report, 2014.

[9] Dutch Ministry of Infrastructure and the Environment. International Benchmark of Airport Capacaties. Technical report, 2009.

[10] Schiphol Group. Annual Report 2015. Technical report, 2016.

[11] K. Chircop, M. Xuereb, D. Zammit-Mangion, and E. Cachia. A generic framework for multi-parameter optimization of flight trajectories. In *Proceedings of the 27th Congress of the International Council of the Aeronautical Sciences (ICAS)*, Nice, France, 2010.

[12] S.J. Hebly and H.G. Visser. Advanced noise abatement departure procedures: custom optimized departure profiles. *The Aeronautical Journal*, 119(1215):647–661, 2015.

[13] S. Hartjes. INMTM v3 Noise Calculation Tool Specification. Technical report, 2010.

[14] J.G. Delsen. *Flexible Arrival & Departure Runway Allocation.* PhD thesis, Faculty of Aerospace Engineering, Delft University of Technology, 2016.

[15] T.R. Meerburg, R.J. Boucherie, and M. van Kraaij. Noise Load Management at Amsterdam Airport Schiphol. *Airline Group of the International Federation of Operations Research Societies (AGIFORS)*, pages 1–21, 2007.

[16] Advisory Circular - Federal Aviation Administration. Noise Abatement departure Profiles. Technical report, 1993.

[17] B. Kim, B. Manning, B. Sharp, J.P. Clarke, I. Robeson, J. Brooks, and D. Senzig. Environmental Optimization of Aircraft Departures: Fuel Burn, Emissions, and Noise. Technical report, 2013.

[18] S. Hartjes, H.G. Visser, and S. Hebly. Optimization of RNAV Noise and Emission Abatement Departure Procedures. *Aeronautical Journal*, 114(1162):757–767, 2009.

[19] Omgevingsraad Schiphol. Instellingsdocument. Technical report, 2015.

[20] European Civil Aviation Conference. Doc 29. In *Report on Standard Method of Computing Noise Contours around Civil Airports*, volume 1, pages 7—-46, 2005.

[21] H.M.E. Miedema and H. Vos. Exposure-response relationships for transportation noise. *The Journal of the Acoustical Society of America*, 104(6):3432–3445, 1998.

[22] T. Coleman, M.A. Branch, and A. Grace. Optimization Toolbox For Use with MATLAB. Technical report, 1999.

[23] E.R. Boeker, E. Dinges, B. He, G. Fleming, C.J. Roof, P.J. Gerbi, A.S. Rapoza, and J. Hemann. Integrated Noise Model (INM) Version 7.0 Technical Manual. Technical report, 2008.

[24] Z. Ugray, L. Lasdon, J. Plummer, F. Glover, J. Kelly, and R. Marti. Scatter Search and Local NLP Solvers : A Multistart Framework for Global Optimization. *INFORMS Journal on Computing*, 19(3):328–340, 2002.

[25] L.I.N. Song. NGPM – A NSGA-II Program in Matlab. Technical report, 2011.

[26] J. Branke. Multi-Objective Evolutionary Algorithms and MCDA. *Euro Working Group on Multicriteria Decision Aiding (EWG-MCDA)*, 25(3):1–3, 2012.

[27] H.G. Visser and R.A.A. Wijnen. Optimization of Noise Abatement Departure Trajectories. *Journal of Aircraft*, 38(4):620–627, July 2001.

[28] Y. Rabinovich and A. Wigderson. Techniques for bounding the convergence rate of genetic algorithms. *Random Structures and Algorithms*, 14(2):111–138, 1999.

[29] P.S. Oliveto, J. He, and X. Yao. Time complexity of evolutionary algorithms for combinatorial optimization: A decade of results. *International Journal of Automation and Computing*, 4(3):281–293, 2007.

[30] P.M. Chaudhari, R.V. VDharaskar, and V.M. Thakare. Computing the Most Significant Solution from Pareto Front obtained in Multi-objective Evolutionary. *International Journal of Advanced Computer Science and Applications (IJACSA)*, 1(4):63–68, 2010.

[31] E. Zio and R. Bazzo. A Comparison of Methods for Sleceting Preferred Solutions in Multi0objective Decision Making. *Atlantis Computational Intelligence Systems*, 6(1):23–43, 2012.

[32] J. Wang. *Encyclopedia of Business Analytics and Optimization*. Business Science Reference (an imprint of IGI Global), 3 edition, 2014.

[33] K.G. Murty. *Operations Research and Management Science Handbook*. Taylor and Francis Group, 2009.

[34] H. Mausser. Normalization and Other Topics in Multi Objective Optimization. In *Fields-MITACS Industrial Problems Workshop*, pages 89–101, 2006.

[35] W. Jakob and C. Blume. Pareto optimization or cascaded weighted sum: A comparison of concepts. *MDPI - Open Access Algorithms*, 7:166–185, 2014.

[36] R.M. Karp. *Complexity of Computer Computations*. Springer US, Berkeley, 1972.

[37] Delft Universit of Technology. Model Boeing 737-300. Technical report.

[38] M. Teengs. Model of the Boeing 747-400. Technical report, 2006.

[39] Air Traffic Control The Netherlands (LvNL). Integrated Aeronautical Information Package Netherlands (AIP), 2015.

[40] Inspectie Leefomgeving en Transport. Handhavingsrapportage Schiphol. Technical report, Ministerie van Infrastructuur en Milieu, 2015.

Appendices

A

Research Methodology

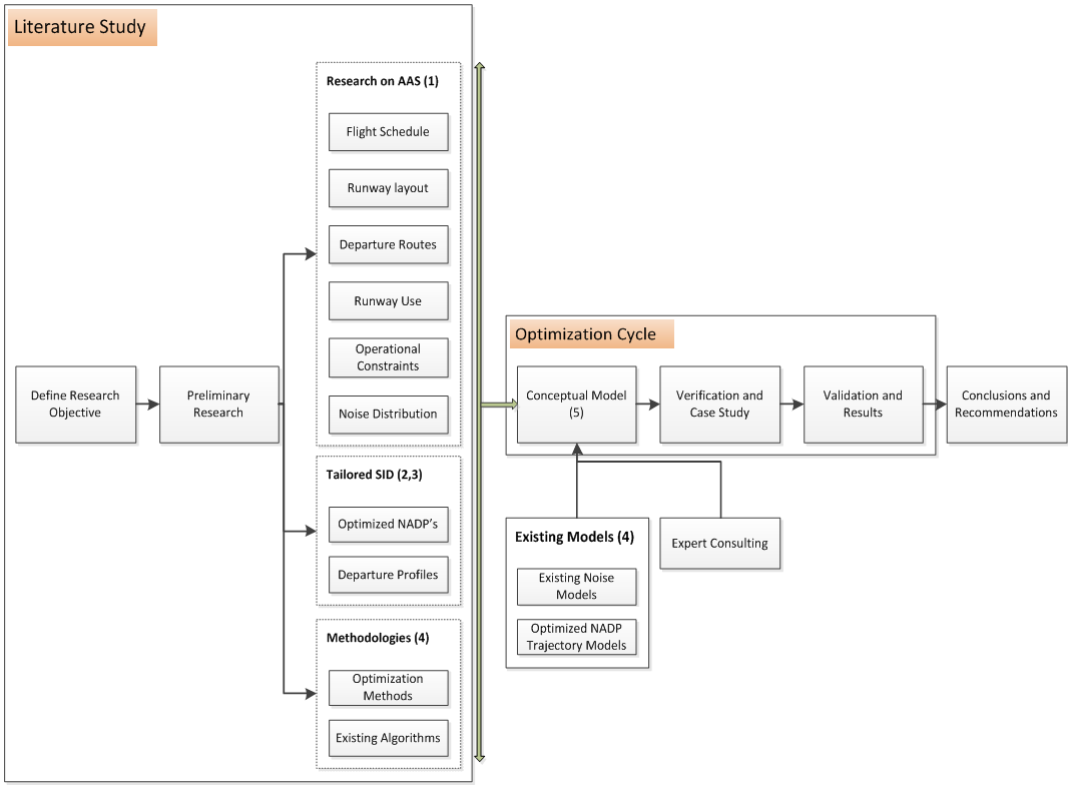

Figure A.1: Schematic representation of the research methodology used for this MSc thesis

B

Sensitivity Analysis

B.1 Overview of the Sensitivity Analysis

	Cases					
	Ground Track Only			Profile Segments Included		
	3 segments	5 segments	7 segments	3 segments	5 segments	7 segments
L1	DV	DV	DV	DV	DV	DV
R2	DV	DV	DV	DV	DV	DV
Δχ2	-	DV	DV	-	DV	DV
L3	-	DV	DV	-	DV	DV
R4	-	DV	DV	-	DV	DV
Δχ4	-	-	DV	-	-	DV
L5	-	-	DV	-	-	DV
R6	-	-	DV	-	-	DV
Υ1	-	-	-	DV	DV	DV
Υ2	-	-	-	DV	DV	DV
Υ3	-	-	-	DV	DV	DV
η3	-	-	-	DV	DV	DV
Υ4	-	-	-	DV	DV	DV
Υ5	-	-	-	DV	DV	DV
Total DV's	2	5	8	8	11	14
Min Fuel [kg]	476	472.4	472.6	479	478.9	476
Min Noise [Aw]	4246	1978	2176	3583	1788	1827

Figure B.1: An overview of the different cases and their results, as being evaluated during the sensitivity analysis

B.2 Sensitivity Analysis on Ground Track Only

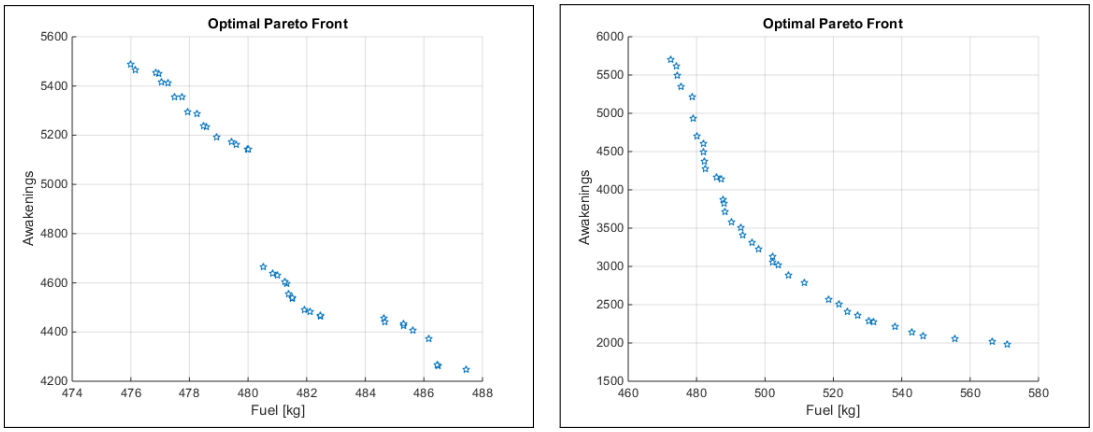

Figure B.2: Optimal Pareto-front solutions for optimization with 3 (left) and 5 (right) ground segments

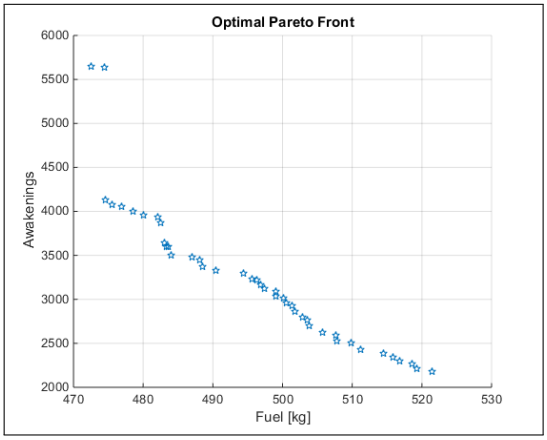

Figure B.3: Optimal Pareto-front solutions for optimization with 7 ground segments

B.3 Sensitivity Analysis with Vertical Profile Segments Included

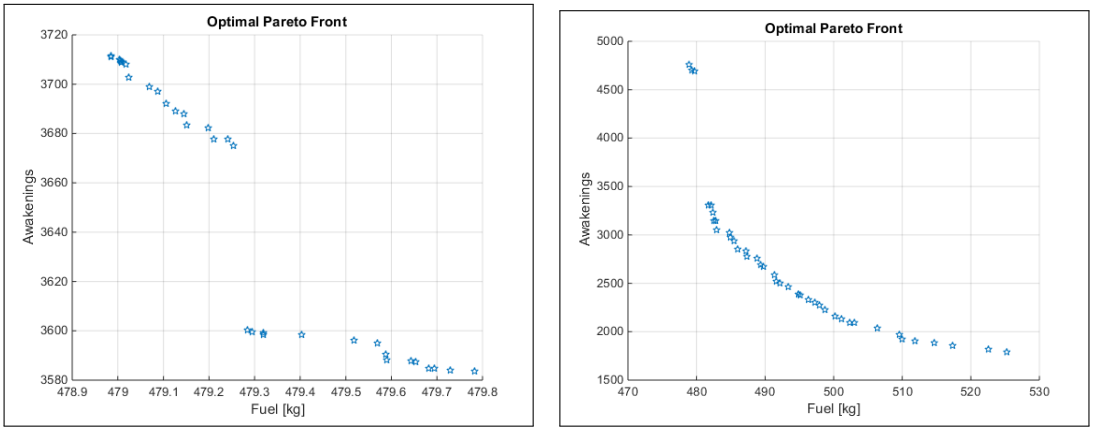

Figure B.4: Optimal Pareto-front solutions for optimization with 3 (left) and 5 (right) ground segments, including vertical profile segments

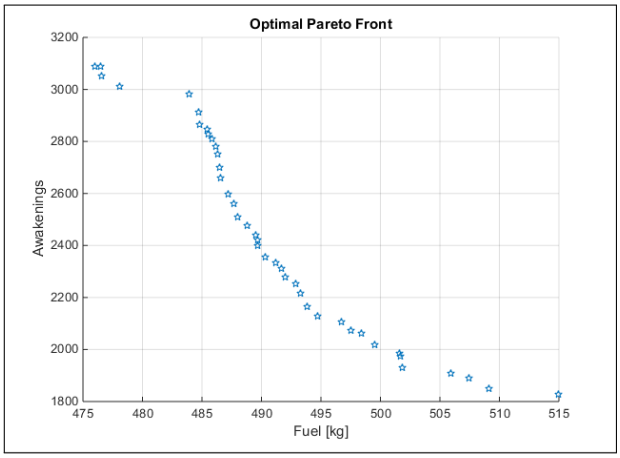

Figure B.5: Optimal Pareto-front solutions for optimization with 7 ground segments, including vertical profile segments

C

AAS Flight Schedule

Table C.1: Actual flight schedule provided by AAS. All flights that are outside the scope of this research are removed from the flight schedule.

ID	STime	DepArr	Origin	Destination	ACType	Pax	FLType	AirlineCode	Freight
19	16:30	Dep	Airport	AGP	B737700	119	NAT	HV	0
20	07:40	Dep	Airport	AGP	B737700	119	NAT	HV	0
21	14:15	Dep	Airport	ALA	B767200	176	INT	KL	35.200000762939503
24	14:00	Dep	Airport	AMM	A320	112	INT	RJ	3.5
26	04:30	Dep	Airport	AOK	B737800	149	NAT	HV	0
36	07:30	Dep	Airport	ASR	A300	238	INT	F2	11.300000190734901
37	10:05	Dep	Airport	ATH	B737700	98	NAT	KL	0
38	20:00	Dep	Airport	ATH	B737700	98	NAT	KL	0
39	12:40	Dep	Airport	ATH	B737400	117	NAT	OA	1.79999995231628
40	06:00	Dep	Airport	ATH	B737800	149	NAT	HV	0
46	20:30	Dep	Airport	AYT	B757PW	175	INT	F2	5.5
48	14:25	Dep	Airport	BAH	B767200	176	INT	KL	35.200000762939503
62	19:35	Dep	Airport	BEY	B737700	98	INT	KL	0
67	19:20	Dep	Airport	BGY	B737700	119	NAT	HV	0
68	06:55	Dep	Airport	BGY	B737700	119	NAT	HV	0
69	09:50	Dep	Airport	BHX	B737300	118	NAT	WW	0
70	18:05	Dep	Airport	BHX	B737300	118	NAT	WW	0
71	16:15	Dep	Airport	BHX	FK100	81	NAT	KL	4.6999998092651403
72	21:00	Dep	Airport	BHX	B737700	98	NAT	KL	0
73	13:55	Dep	Airport	BHX	B737700	98	NAT	KL	0
74	18:35	Dep	Airport	BHX	FK70	64	NAT	KL	5.9000000953674299
75	07:15	Dep	Airport	BHX	FK70	64	NAT	KL	5.9000000953674299
76	09:45	Dep	Airport	BHX	B737700	98	NAT	KL	0
77	20:00	Dep	Airport	BKK	B747200	216	INT	KL	40.900001525878899
78	14:25	Dep	Airport	BKK	B747400	318	INT	CI	14.8999996185303
79	12:35	Dep	Airport	BKK	B747400	218	INT	BR	54.5
91	10:25	Dep	Airport	BOM	DC1030	216	INT	NW	13.5
114	10:30	Dep	Airport	BTS	B737500	106	NAT	NE	3.4000000953674299
115	16:15	Dep	Airport	BUD	B737700	98	NAT	MA	0
116	14:15	Dep	Airport	BUD	B737700	98	NAT	MA	0
117	20:30	Dep	Airport	BUD	B737700	98	NAT	MA	0
118	10:00	Dep	Airport	BUD	B737700	98	NAT	MA	0
119	10:15	Dep	Airport	BUD	B737500	106	NAT	5P	3.4000000953674299
120	20:40	Dep	Airport	BUD	B737500	106	NAT	5P	3.4000000953674299
121	13:25	Dep	Airport	BUD	B737700	98	NAT	KL	0
122	20:10	Dep	Airport	CAI	MD11	226	INT	KL	46.099998474121101
123	16:00	Dep	Airport	CAI	A320	116	INT	MS	0
141	10:25	Dep	Airport	CGN	FK50	40	NAT	KL	3.5
142	19:35	Dep	Airport	CGN	FK50	40	NAT	KL	3.5
143	16:05	Dep	Airport	CGN	FK50	40	NAT	KL	3.5
167	12:00	Dep	Airport	DAM	A320	122	INT	RB	0
168	19:25	Dep	Airport	DAM	B737700	98	INT	KL	0
169	11:25	Dep	Airport	DEL	MD11	226	INT	KL	46.099998474121101
170	12:40	Dep	Airport	DMM	B767200	176	INT	KL	35.200000762939503
188	14:35	Dep	Airport	DXB	B777200	229	INT	KL	22
204	21:15	Dep	Airport	ESB	A300	238	INT	F2	11.300000190734901
205	23:30	Dep	Airport	ESB	B737800	124	INT	TK	0
222	14:40	Dep	Airport	FRA	B737500	82	NAT	LH	1.70000004768372
223	10:30	Dep	Airport	FRA	B737500	82	NAT	LH	1.70000004768372
224	12:15	Dep	Airport	FRA	B737500	82	NAT	LH	1.70000004768372
225	20:20	Dep	Airport	FRA	B737500	82	NAT	LH	1.70000004768372
226	15:55	Dep	Airport	FRA	B737500	82	NAT	LH	1.70000004768372
227	19:40	Dep	Airport	FRA	B737500	82	NAT	LH	1.70000004768372
228	20:50	Dep	Airport	FRA	A310	147	NAT	PK	12.8999996185303
229	07:00	Dep	Airport	FRA	BAE146200	64	NAT	LH	0
230	18:25	Dep	Airport	FRA	A320	115	NAT	LH	1.5
231	12:55	Dep	Airport	FRA	B757PW	154	NAT	4L	5.5
232	16:15	Dep	Airport	FRA	FK70	64	NAT	KL	5.9000000953674299
233	13:55	Dep	Airport	FRA	FK70	64	NAT	KL	5.9000000953674299
234	19:05	Dep	Airport	FRA	FK70	64	NAT	KL	5.9000000953674299
235	08:50	Dep	Airport	FRA	FK100	81	NAT	KL	4.6999998092651403
236	09:45	Dep	Airport	FRA	B737300	98	NAT	LH	2.4000000953674299
255	09:50	Dep	Airport	HAJ	FK70	64	NAT	KL	5.9000000953674299
256	19:20	Dep	Airport	HAJ	FK70	64	NAT	KL	5.9000000953674299
257	15:50	Dep	Airport	HAJ	FK70	64	NAT	KL	5.9000000953674299
258	12:30	Dep	Airport	HAJ	FK50	40	NAT	KL	3.5
273	06:00	Dep	Airport	HER	B737800	149	NAT	HV	0
287	11:35	Dep	Airport	IST	B737800	124	INT	TK	0

ID	STime	DepArr	Origin	Destination	ACType	Pax	FLType	AirlineCode	Freight
288	07:20	Dep	Airport	IST	B737800	124	INT	TK	0
289	17:30	Dep	Airport	IST	B737800	124	INT	TK	0
290	10:10	Dep	Airport	IST	B737700	98	INT	F2	0
291	10:00	Dep	Airport	IST	B737700	98	INT	KL	0
292	19:30	Dep	Airport	IST	B737700	98	INT	KL	0
300	10:05	Dep	Airport	KBP	B737700	98	NAT	PS	0
301	11:15	Dep	Airport	KBP	B737700	98	NAT	KL	0
304	12:45	Dep	Airport	KIV	A320	115	NAT	9U	0
315	14:50	Dep	Airport	LCA	B737800	149	INT	HV	0
372	10:15	Dep	Airport	LJU	CRJ200	38	NAT	JP	0.40000000596046398
422	20:30	Dep	Airport	MNL	B777200	229	INT	KL	22
434	17:05	Dep	Airport	MUC	CRJ100	40	NAT	LH	0.69999998807907104
435	08:45	Dep	Airport	MUC	CRJ100	40	NAT	LH	0.69999998807907104
436	06:55	Dep	Airport	MUC	CRJ100	40	NAT	LH	0.69999998807907104
437	21:10	Dep	Airport	MUC	CRJ100	40	NAT	LH	0.69999998807907104
438	19:05	Dep	Airport	MUC	CRJ700	56	NAT	LH	0
439	20:30	Dep	Airport	MUC	B737700	98	NAT	KL	0
440	11:20	Dep	Airport	MUC	FK70	64	NAT	KL	5.9000000953674299
441	14:05	Dep	Airport	MUC	B737700	98	NAT	KL	0
442	08:00	Dep	Airport	MUC	B737700	98	NAT	KL	0
443	17:50	Dep	Airport	MUC	FK70	64	NAT	KL	5.9000000953674299
444	13:00	Dep	Airport	MUC	CRJ100	40	NAT	LH	0.69999998807907104
470	14:20	Dep	Airport	NUE	FK70	64	NAT	KL	5.9000000953674299
471	19:05	Dep	Airport	NUE	FK70	64	NAT	KL	5.9000000953674299
472	09:30	Dep	Airport	NUE	FK70	64	NAT	KL	5.9000000953674299
491	10:40	Dep	Airport	OTP	B737700	98	NAT	KL	0
492	08:55	Dep	Airport	OTP	B737700	98	NAT	KL	0
493	19:30	Dep	Airport	OTP	B737700	98	NAT	KL	0
497	13:40	Dep	Airport	PFO	A330300	236	INT	CY	9
501	09:25	Dep	Airport	PRG	B737500	85	NAT	QS	3.4000000953674299
502	16:20	Dep	Airport	PRG	B737500	83	NAT	OK	1
503	10:05	Dep	Airport	PRG	B737400	112	NAT	OK	1.20000004768372
504	08:55	Dep	Airport	PRG	B737700	98	NAT	KL	0
505	14:10	Dep	Airport	PRG	B737700	98	NAT	KL	0
506	19:25	Dep	Airport	PRG	A320	120	NAT	OK	1
518	11:50	Dep	Airport	SIN	B777200	258	INT	SQ	48.099998474121101
519	20:45	Dep	Airport	SIN	B747200	216	INT	KL	40.900001525878899
521	05:25	Dep	Airport	SMI	B737800	149	NAT	HV	0
522	10:00	Dep	Airport	SOF	B737300	109	NAT	FB	0
547	16:20	Dep	Airport	THR	B767200	176	INT	KL	35.200000762939503
555	19:50	Dep	Airport	TLV	B737700	98	INT	KL	0
556	10:25	Dep	Airport	TLV	B767200	165	INT	LY	10.800000190734901
562	08:10	Dep	Airport	TXL	B737700	115	NAT	AB	0
563	09:35	Dep	Airport	TXL	B737700	98	NAT	KL	0
564	19:20	Dep	Airport	TXL	B737700	98	NAT	KL	0
565	07:10	Dep	Airport	TXL	FK70	64	NAT	KL	5.9000000953674299
566	16:05	Dep	Airport	TXL	FK100	81	NAT	KL	4.6999998092651403
567	14:05	Dep	Airport	TXL	FK100	81	NAT	KL	4.6999998092651403
571	20:05	Dep	Airport	VIE	A319	101	NAT	OS	0
572	16:45	Dep	Airport	VIE	FK70	64	NAT	KL	5.9000000953674299
573	20:00	Dep	Airport	VIE	B737700	98	NAT	KL	0
574	08:10	Dep	Airport	VIE	FK100	81	NAT	KL	4.6999998092651403
575	13:45	Dep	Airport	VIE	B737700	98	NAT	KL	0
576	07:45	Dep	Airport	VIE	A319	101	NAT	OS	0
577	10:45	Dep	Airport	VIE	A319	101	NAT	OS	0
578	16:35	Dep	Airport	VIE	CRJ200	40	NAT	OS	0
582	19:50	Dep	Airport	WAW	B737700	98	NAT	KL	0
583	10:10	Dep	Airport	WAW	B737700	98	NAT	KL	0
584	13:35	Dep	Airport	WAW	B737700	98	NAT	KL	0
585	07:45	Dep	Airport	WAW	EMB145	38	NAT	LO	4.3000001907348597
586	10:35	Dep	Airport	WAW	EMB145	38	NAT	LO	4.3000001907348597
587	19:45	Dep	Airport	WAW	EMB170	56	NAT	LO	7.4000000953674299
594	17:40	Dep	Airport	ZAG	A319	106	NAT	OU	6.6999998092651403
595	11:20	Dep	Airport	ZAG	A319	106	NAT	OU	6.6999998092651403

D

Schiphol Runway 09 Standard Instrument Departure Chart

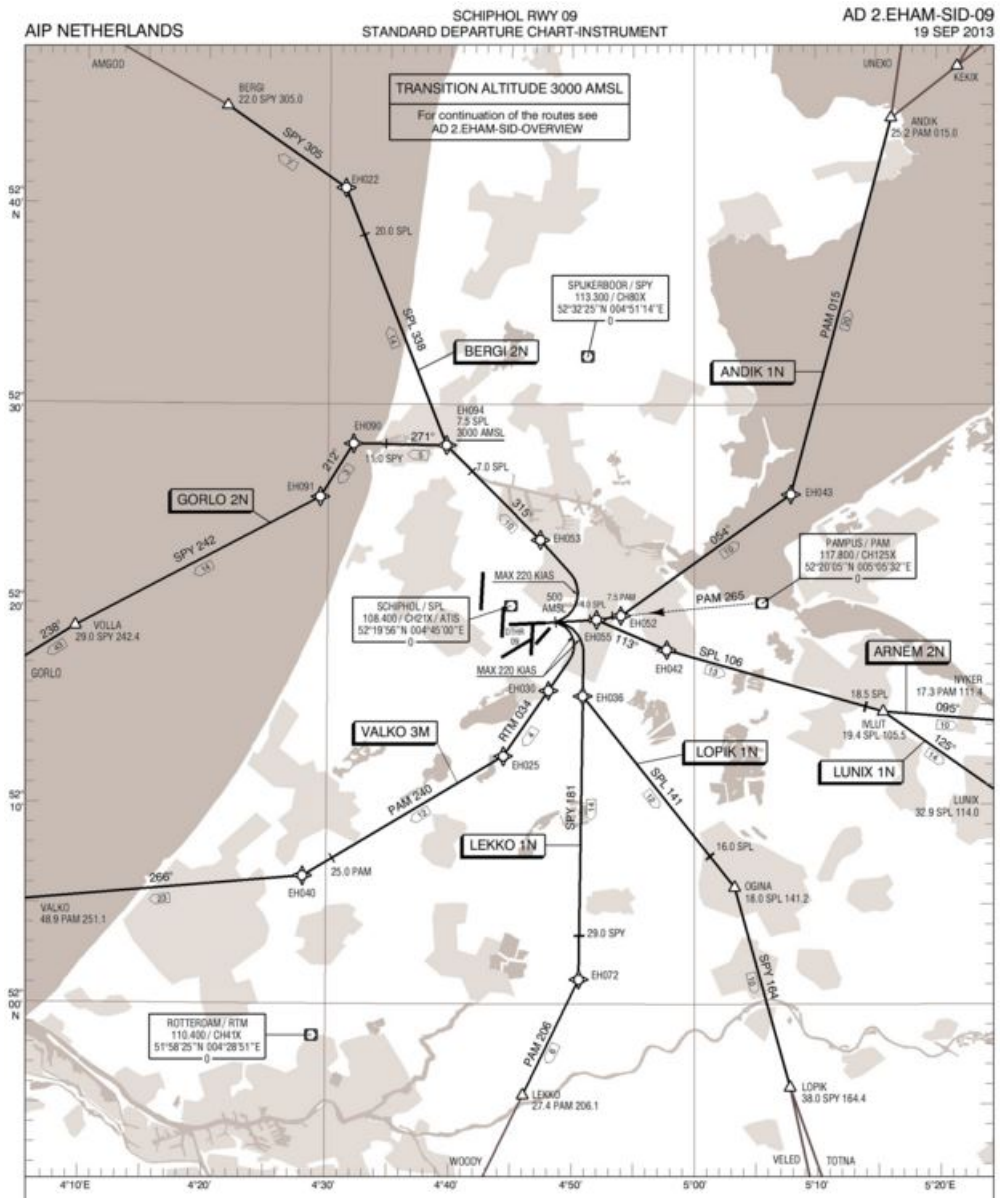

Figure D.1: Standard Instrument Departures from runway 09 at AAS [6]

E

Reference Case Trajectories

This appendix includes the simulated trajectories of the reference case. The trajectories are simulated by the developed trajectory model. Use is made of fixed input parameters that follow from actual airport operations. The parameters are presented in chapter 6 of this report. Trajectories of the B737-300 and B747-400 of the light, medium and heavy take-off weight class are shown by figure E.1, E.2 and E.3 respectively.

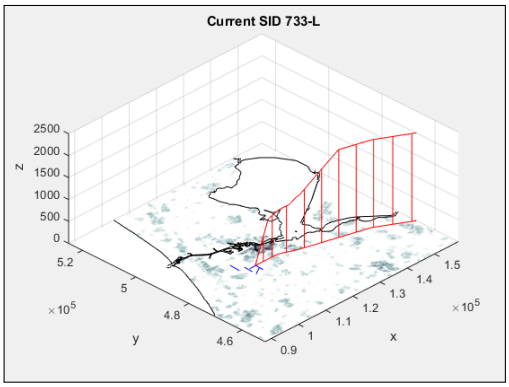

(a) Current trajectory of the B733 low take-off weight

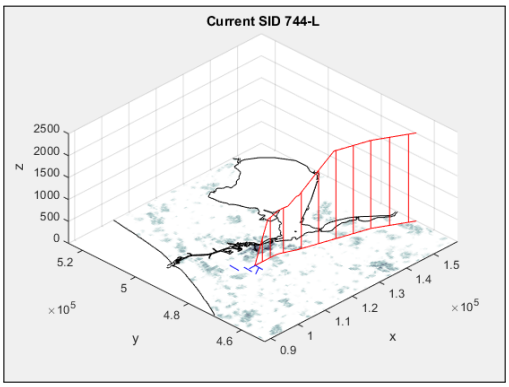

(b) Current trajectory of the B744 low take-off weight

Figure E.1: Current trajectories of light weight class from 09 runway ARNEM departure fix

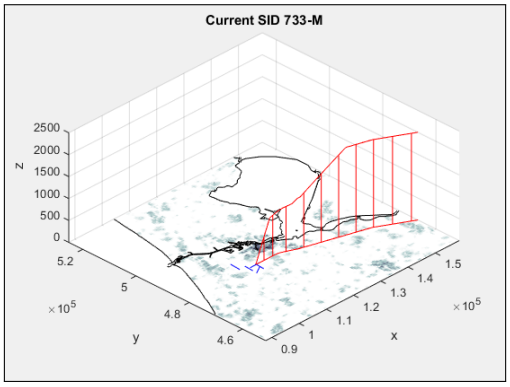

(a) Current trajectory of the B733 medium take-off weight

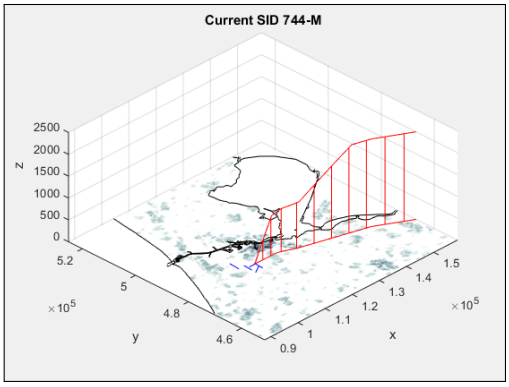

(b) Current trajectory of the B744 medium take-off weight

Figure E.2: Current trajectories of medium weight class from 09 runway ARNEM departure fix

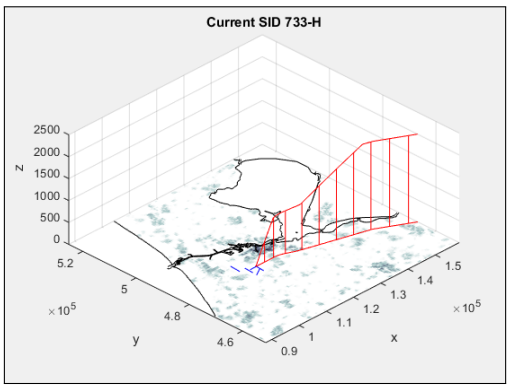

(a) Current trajectory of the B733 heavy take-off weight

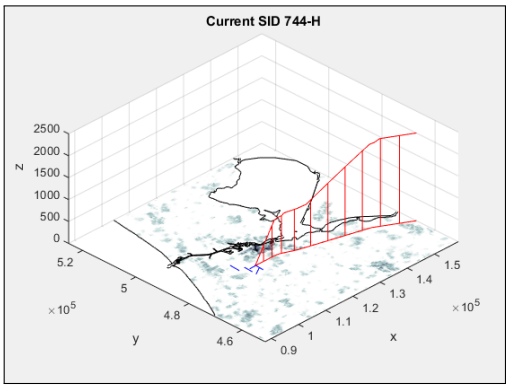

(b) Current trajectory of the B744 heavy take-off weight

Figure E.3: Current trajectories of heavy weight class from 09 runway ARNEM departure fix

F

Results Case Study

Table F.1: Final set of tailored trajectories that serves as input for the allocation model

	NADP-1		NADP-2	
Flight Cat.	**Fuel [kg]**	**Awakenings**	**Fuel [kg]**	**Awakenings**
	-	-	458,1	4915
B733-L	-	-	463,42	3440
	-	-	589,74	1951
	-	-	475,84	5583
B733-M	-	-	483,9	2507
	-	-	503,08	1941
	-	-	518,29	5529
B733-H	-	-	540,8	3031
	-	-	564,21	2449
	1864,33	10286	1688,56	9881
B744-L	1941,96	8732	1705,7	8806
	2120,01	7670	1711,01	8681
	2297,67	12828	2138,75	12640
B744-M	2487,22	11978	2154,04	12276
	2525,09	11694	2561,24	11998
	2777,17	12164	2585,49	16763
B744-H	2861,3	10463	2586,34	16220
	3130,34	9782	2871,91	16138

F.1 Results Trajectory Optimization Model

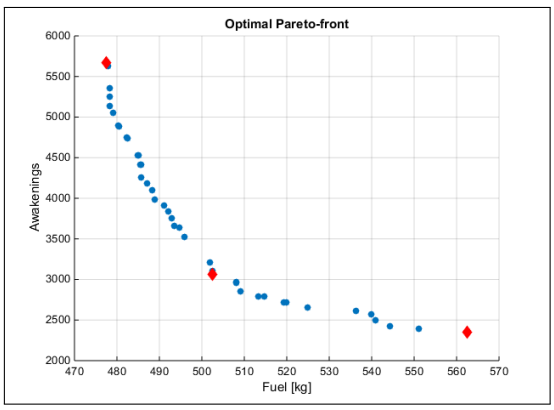

(a) Pareto-front of optimal solutions. The red diamonds mark the selected solutions

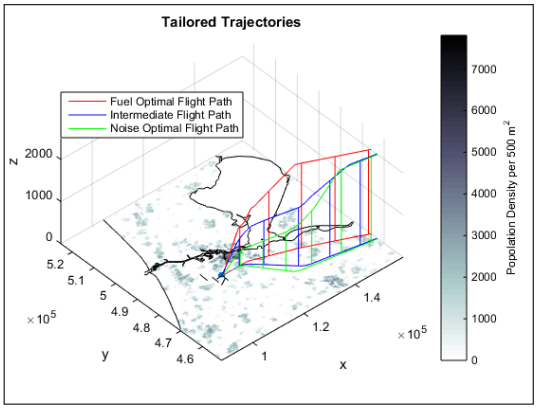

(b) Selected tailored trajectories -

Figure F.1: B737-300 light take-off weight and NADP-1 flight procedure

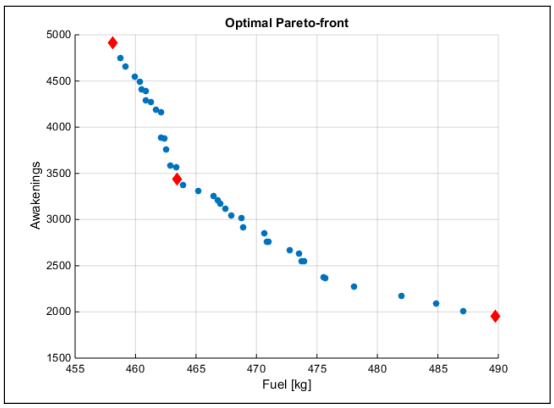

(a) Pareto-front of optimal solutions. The red diamonds mark the selected solutions

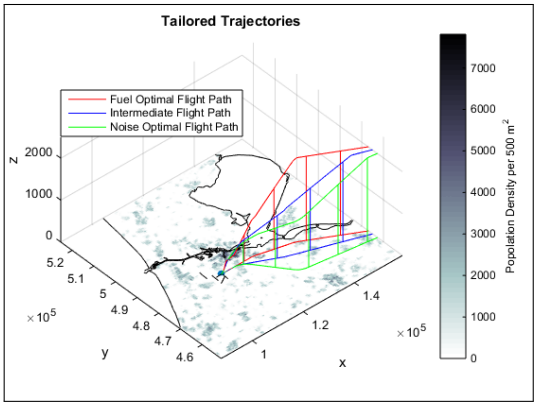

(b) Selected tailored trajectories -

Figure F.2: B737-300 light take-off weight and NADP-2 flight procedure

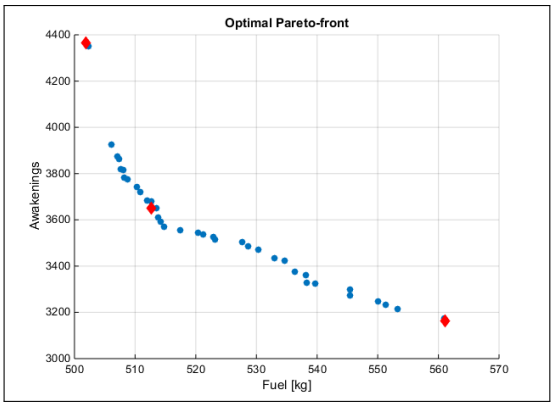

(a) Pareto-front of optimal solutions. The red diamonds mark the selected solutions

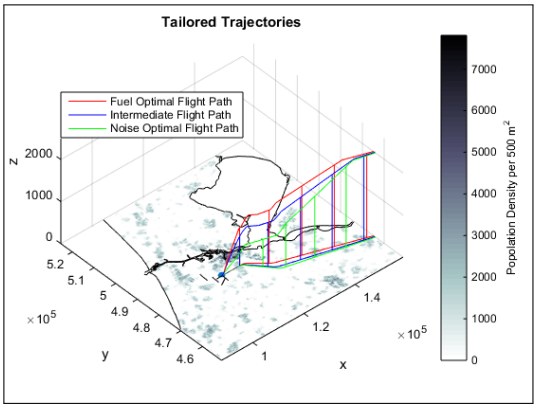

(b) Selected tailored trajectories -

Figure F.3: B737-300 medium take-off weight and NADP-1 flight procedure

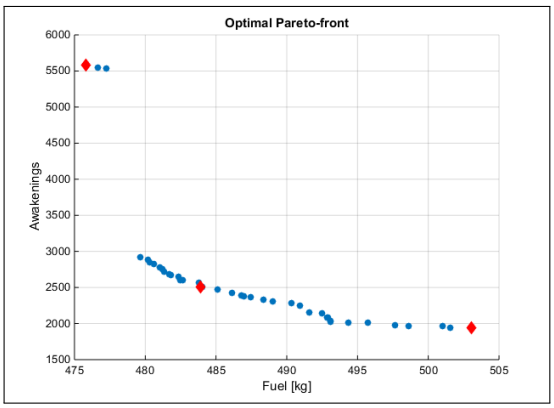

(a) Pareto-front of optimal solutions. The red diamonds mark the selected solutions

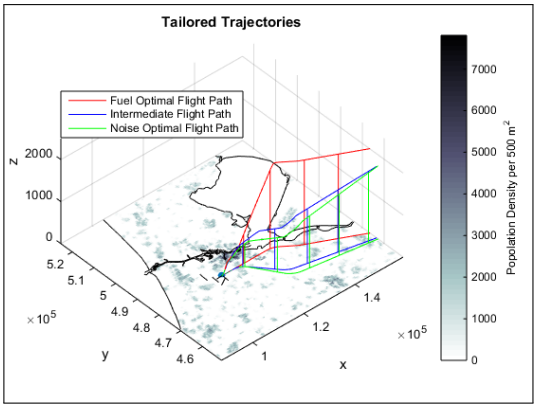

(b) Selected tailored trajectories -

Figure F.4: B737-300 medium take-off weight and NADP-2 flight procedure

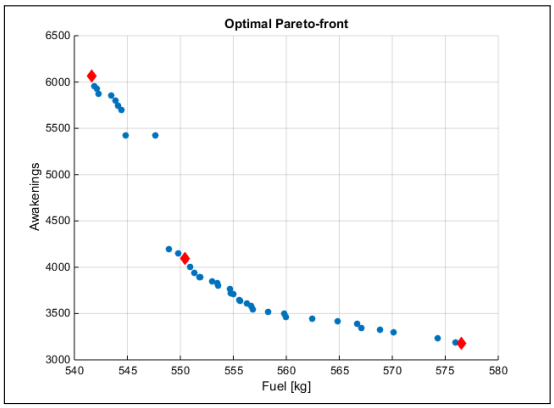

(a) Pareto-front of optimal solutions. The red diamonds mark the selected solutions

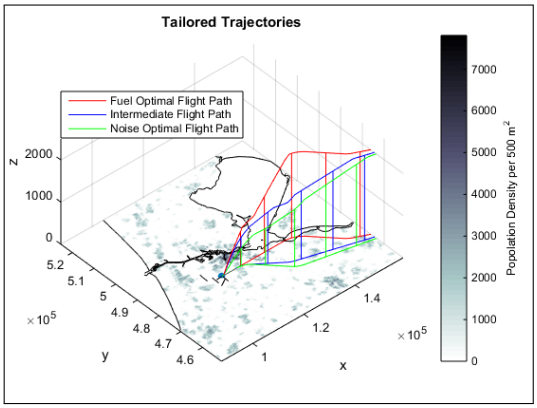

(b) Selected tailored trajectories -

Figure F.5: B737-300 heavy take-off weight and NADP-1 flight procedure

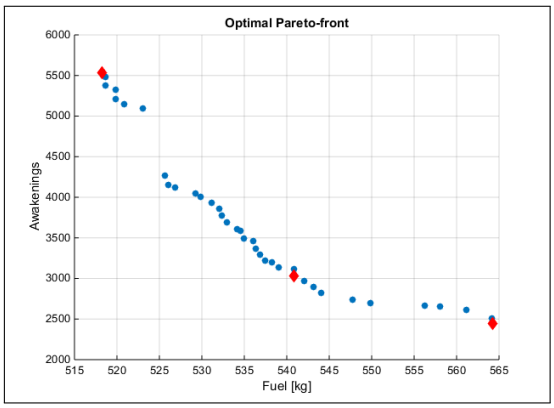

(a) Pareto-front of optimal solutions. The red diamonds mark the selected solutions

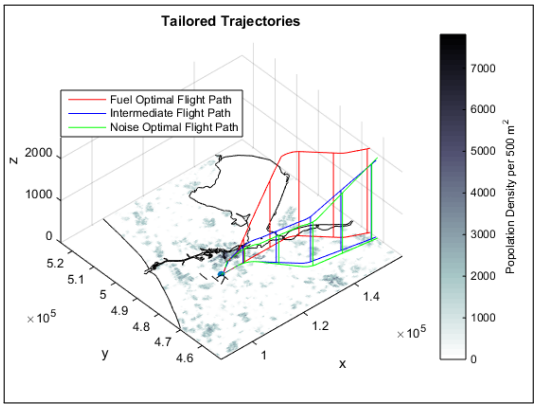

(b) Selected tailored trajectories -

Figure F.6: B737-300 heavy take-off weight and NADP-2 flight procedure

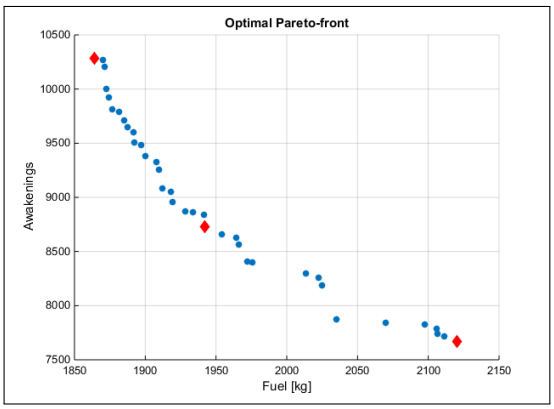

(a) Pareto-front of optimal solutions. The red diamonds mark the selected solutions

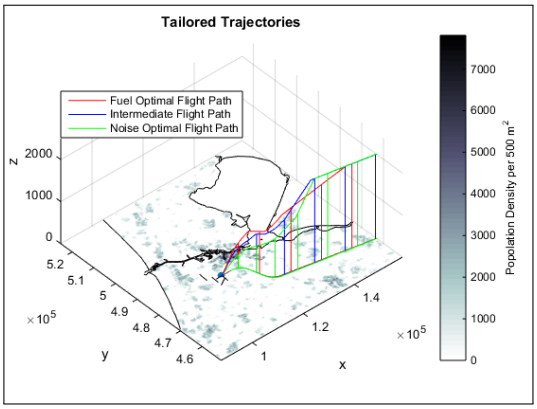

(b) Selected tailored trajectories -

Figure F.7: B747-400 light take-off weight and NADP-1 flight procedure

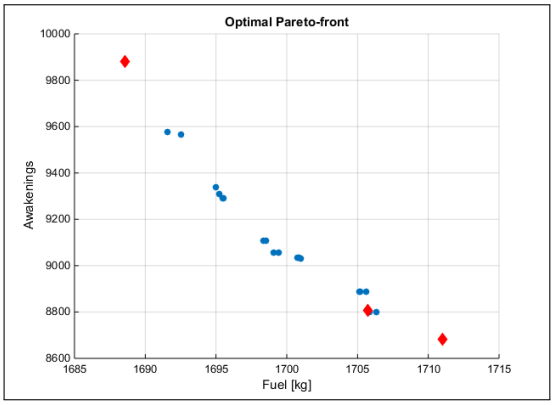

(a) Pareto-front of optimal solutions. The red diamonds mark the selected solutions

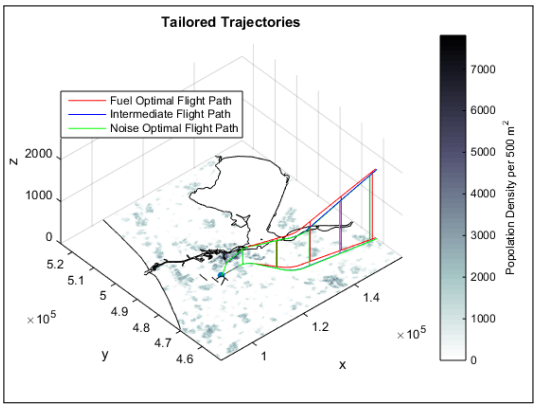

(b) Selected tailored trajectories -

Figure F.8: B747-400 light take-off weight and NADP-2 flight procedure

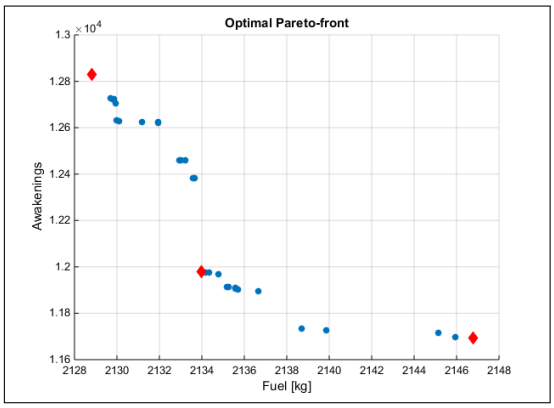

(a) Pareto-front of optimal solutions. The red diamonds mark the selected solutions

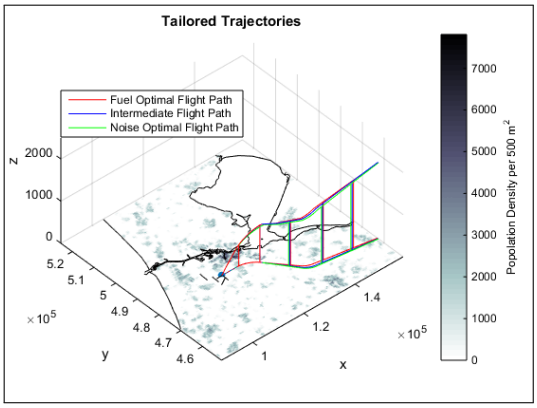

(b) Selected tailored trajectories

-

Figure F.9: B747-400 medium take-off weight and NADP-1 flight procedure

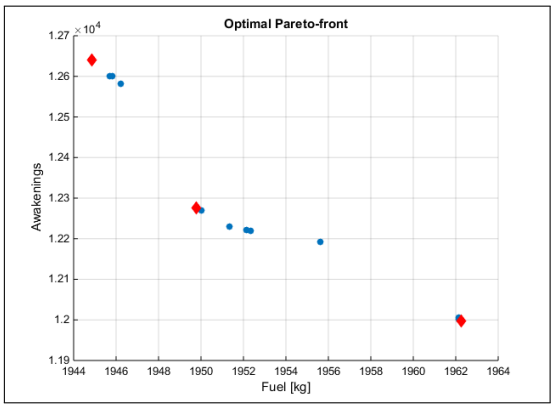

(a) Pareto-front of optimal solutions. The red diamonds mark the selected solutions

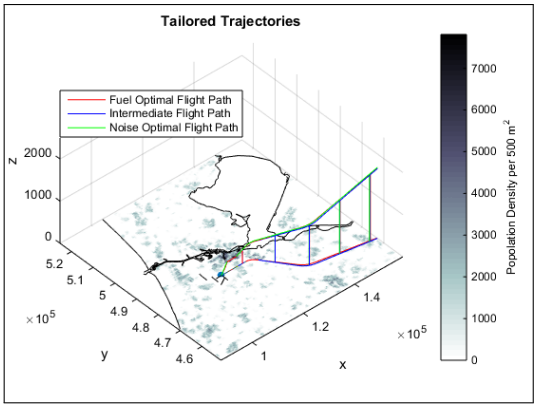

(b) Selected tailored trajectories

-

Figure F.10: B747-400 medium take-off weight and NADP-2 flight procedure

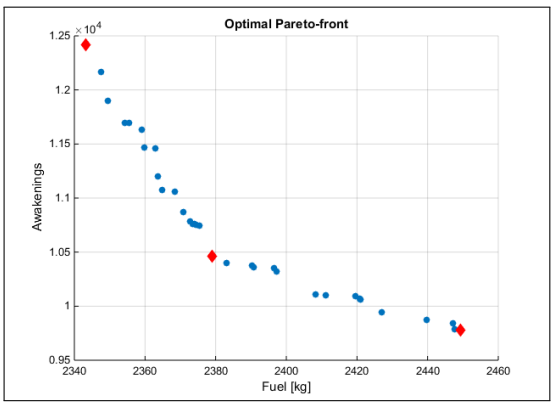

(a) Pareto-front of optimal solutions. The red diamonds mark the selected solutions

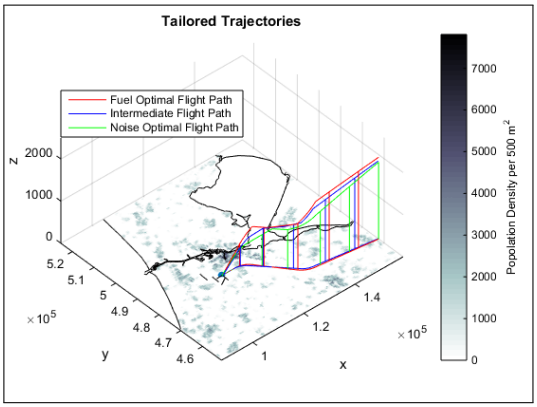

(b) Selected tailored trajectories

Figure F.11: B747-400 heavy take-off weight and NADP-1 flight procedure

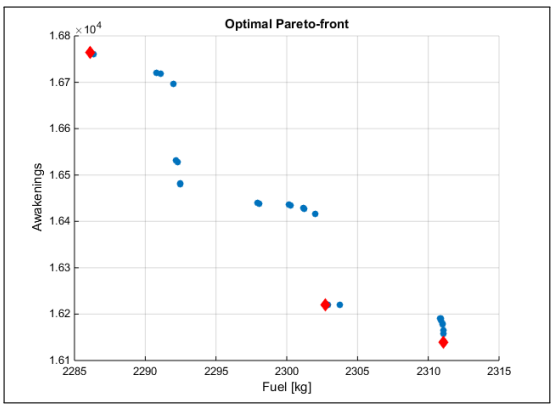

(a) Pareto-front of optimal solutions. The red diamonds mark the selected solutions

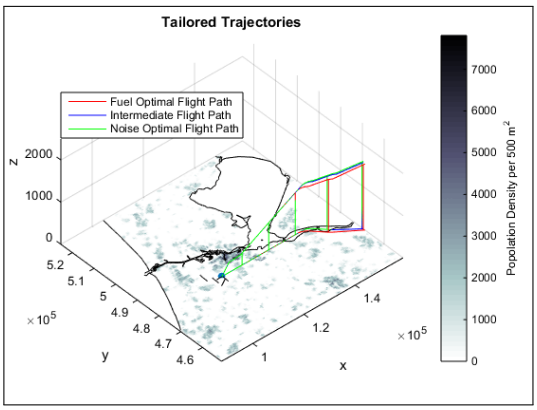

(b) Selected tailored trajectories

Figure F.12: B747-400 heavy take-off weight with NADP-2 flight procedure

G

Verification: Conceptual Model

This appendix provides an overview of the concept case used to verify the two models. The concept case is performed in order to test the working principle of the overall model and decide whether developed method is sufficient in achieving the overall research objective of the MSc. thesis research. For the concept case two tailored trajectories are developed. One noise optimal trajectory that avoids a centralized population area and one fuel optimal trajectory that crosses the centralized population area. Subsequently, the allocation model computed the optimal allocation of flights for one aircraft type with fixed take-off weight.

G.1 Experimental Set-Up

Scenario

- Only one aircraft type is being considered
- Only one departure weight is being considered
- The departure schedule is predefined and spread throughout a 24 hrs day
- Two different SID are being considered
- For both SID two different profiles are being considered (NADP-1 & NADP-2)
- Only one runway is being considered
- All departure tracks lead to the same departure fix
- Populated areas in the vicinity of the airport are centralized

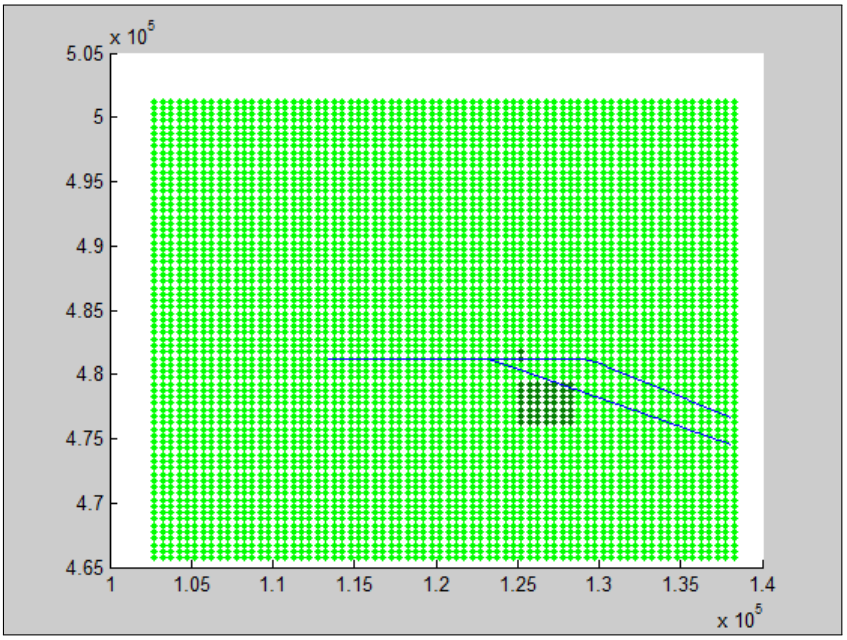

Figure G.1: Graphical representation of the concept scenario in grid form [rijkscoordinates]

Table G.1: Departure trajectory characteristics for the concept case: showing fuel consumption [kg]and noise impact [Awakenings] per trajectory

	SID 1	**SID 2**
NADP-1	477 kg, 796 Aw	550 kg, 319 Aw
NADP-2	661 kg, 1109 Aw	665 kg, 223 Aw

G.2 Conceptual Model

The analytical content of the model for the experimental set-up is written below.

Sets and indices

- F_f = 3 (set of flight categories)
- A_a = 1 (set of aircraft types)
- W_w = 1 (set of aircraft departure weights)
- D_d = 3 (set of different periods of the day)
- P_P = 2 (set of profiles)
- R_r = 2 (set of routes)

Cost functions

The cost of the tailored trajectories for the concept case are included in table G.1.

Equality Constraints

$$\sum_{p \in P} \sum_{r \in R} x_{1,1,1,p,r} = 500 \tag{G.1}$$

$$\sum_{p \in P} \sum_{r \in R} x_{1,1,2,p,r} = 150 \tag{G.2}$$

$$\sum_{p \in P} \sum_{r \in R} x_{1,1,3,p,r} = 10 \tag{G.3}$$

Inequality Constraints

The noise limit N_{limit} and the penalty factor M are set by the user. $C^N_{a,w,d,p,r}$ is computed by the trajectory simulation model and given as an input to the allocation model.

H

Validation: Handhavingspunten

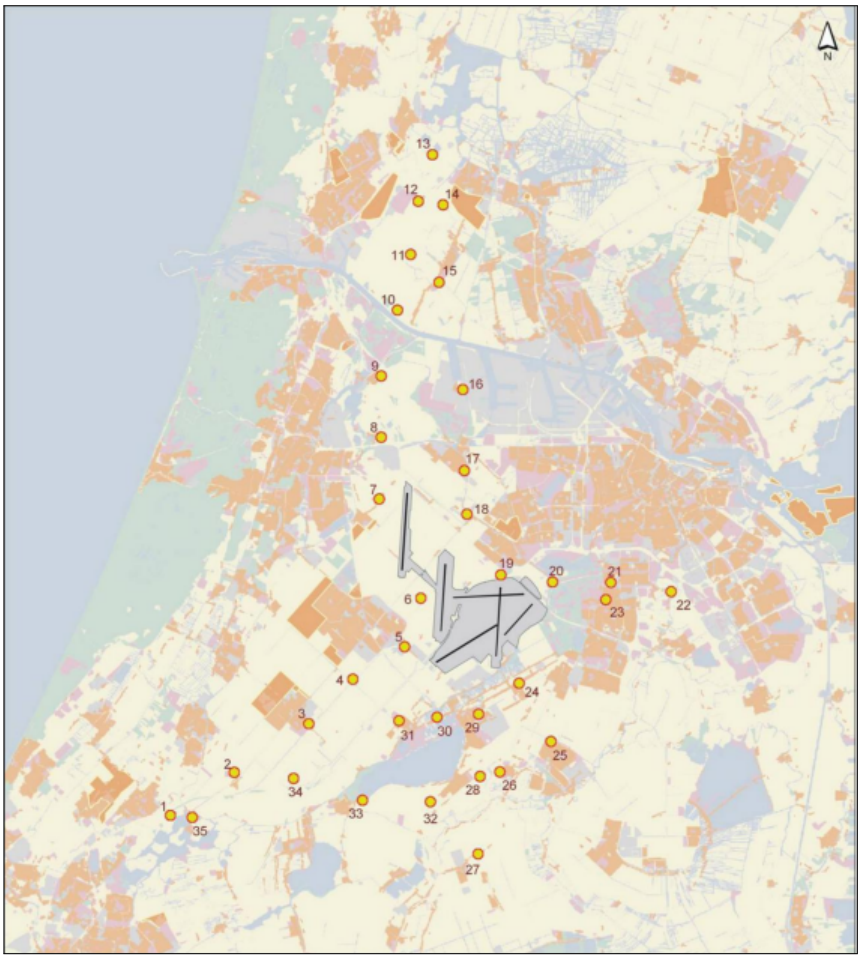

Figure H.1: Handhavingspunten at AAS

Grenswaarden en geluidbelasting handhavingspunten etmaal L_{den} [dB(A)]				
Punt Nr.	X-coördinaat	Y-coördinaat	Grenswaarde	Geluidbelasting
1	97.325	470.400	55,90	53,58
2	100.475	472.525	57,60	55,02
3	104.150	474.925	58,67	56,04
4	106.325	477.125	58,14	57,58
5	108.875	478.725	57,88	56,94
6	109.675	481.125	61,42	53,52
7	107.625	486.025	57,52	55,11
8	107.725	489.075	58,47	55,86
9	107.725	492.100	56,93	54,04
10	108.525	495.350	59,00	57,22
11	109.175	498.100	58,54	57,34
12	109.550	500.725	58,18	57,46
13	110.250	503.025	57,22	57,08
14	110.775	500.550	56,63	55,58
15	110.575	496.725	57,77	56,53
16	111.750	491.425	57,04	55,15
17	111.825	487.425	57,37	54,45
18	111.950	485.275	61,63	58,54
19	113.625	482.275	54,57	53,54
20	116.175	481.925	59,56	59,29
21	119.050	481.900	58,39	56,92
22	122.025	481.450	58,32	55,41
23	118.800	481.050	57,72	56,16
24	114.525	476.925	57,18	56,87
25	116.100	474.050	57,56	57,80
26	113.575	472.550	55,21	54,39
27	112.500	468.500	56,21	55,79
28	112.600	472.325	55,37	53,33
29	112.525	475.400	56,71	56,16
30	110.475	475.250	57,98	56,31
31	108.600	475.075	58,82	58,17
32	110.150	471.075	57,18	56,40
33	106.800	471.150	56,82	57,63
34	103.400	472.225	57,19	55,46
35	98.400	470.300	57,10	54,59

Figure H.2: Noise limits and measured values per measurement point